THE EFFECT OF DENSITY AND IONISATION RING PARAMETER ON THE PERFORMANCE OF TAYLOR CONE CHARACTERISTICS BASED ON ELECTROSPRAY TECHNIQUE

NURFADZILAH BINTI MOHD SANI

MASTER OF SCIENCE IN MECHANICAL ENGINEERING

2025

Faculty of Mechanical Technology and Engineering

THE EFFECT OF DENSITY AND IONISATION RING PARAMETER ON THE PERFORMANCE OF TAYLOR CONE CHARACTERISTICS BASED ON ELECTROSPRAY TECHNIQUE

NURFADZILAH BINTI MOHD SANI

Master of Science in Mechanical Engineering

2025

THE EFFECT OF DENSITY AND IONISATION RING PARAMETER ON THE PERFORMANCE OF TAYLOR CONE CHARACTERISTICS BASED ON ELECTROSPRAY TECHNIQUE

NURFADZILAH BINIT MOHD SANI

A thesis submitted
in fulfillment of the requirements for the degree of
Master of Science in Mechanical Engineering

Faculty of Mechanical Technology and Engineering

UNIVERSITI TEKNIKAL MALAYSIA MELAKA

2025

DECLARATION

I declare that this thesis entitled "The Effect of Density and Ionisation Ring Parameter on The Performance of Taylor Cone Characteristics Based on Electrospray Technique " is the result of my own research except as cited in the references. The thesis has not been accepted for any degree and is not concurrently submitted in candidature of any other degree.

Signature :..

Name :Nurfadzilah Binti Mohd Sani

Date :15 October 2025

APPROVAL

I hereby declare that I have read this thesis and in my opinion this thesis is sufficient in terms of scope and quality for the award of Master of Science in Mechanical Engineering.

Signature :..

Supervisor Name : Ir. Ts. Dr. Abdul Rafeq Bin Saleman

Date :..

DEDICATION

This thesis is dedicated to the most important people in my life, whose support and encouragement have been invaluable throughout my journey. To my family, for their unwavering love and belief in me, to my mom, Siti Maimunah, whose endless sacrifices and prayers have been my greatest source of strength, and to the memory of my late dad, Mohd Sani, whose guidance and wisdom continue to inspire me every day. I also extend my heartfelt gratitude to my siblings Norfairuzliyana, Norfadzlin and Mohd Fikri for their constant support and understanding. I would like to dedicate this dissertation to my special Muhamad Azry Che Ariff who supported me at my lowest, through thick and thin and stood up for me during the process. My deepest appreciation goes to my supervisor, Ir Ts Dr. Abdul Rafeq Saleman, for his insightful guidance, patience, and encouragement, and to my co-supervisor, Dr. Ridhwan Jumaidin, for his invaluable advice and assistance. I am also grateful to my past main supervisor, Ir Dr. Fudhail Abdul Munir, for his foundational support and direction. Lastly, to my friend, Tan Kim Loong, Faiq Aiman, Nur Al Aswad, Muhammad As Shakirin, Ahmad Muhajer, Fathiah and my bestfriend Khairunnisa for always being there to help me through the challenges and celebrate the successes of this journey. Thank you all for your unwavering support and encouragement. I dedicate this work to all the researchers who came before me, paving the way for my exploration in this field. May this contribute to the collective pursuit of knowledge.

ABSTRACT

This study investigates the influence of fluid density and ionisation ring parameters on the formation and stability of the Taylor cone in electrospray systems that are utilised in precision combustion, biomedical, and microfabrication applications. Despite the intense research on electrospray, achieving a consistent Taylor cone remains a challenge due to the complex interplay between electrostatic forces and fluid dynamics. To overcome the problem, this work aims to optimise electrospray parameters, including ionisation ring diameter (IDIR), ionisation ring (IR) positioning or nozzle-to-target distance, and applied voltage. In addition, the effects of electrospray settings on the density of liquid and Taylor cone formation are comprehensively investigated. An experimental approach was taken to examine the influences of fluid densities using ethanol and n-heptane mixtures and ionisation ring configuration effects on cone angle, jet length, and droplet dispersion. Key parameters evaluated include applied voltage (2–10 kV), ionisation ring inner diameters, and axial distances from the nozzle (10.3 mm, 15.3 mm, and 21.2 mm), under controlled flow rates using a precision syringe pump. Imaging was employed to observe transitions between dripping, spindle, cone-jet, and multijet modes. Results reveal that lower-density fluids, like ethanol, require less voltage for cone-jet initiation but exhibit greater instability at higher voltages, while denser fluids, such as water, demand higher voltages and closer ionisation ring proximity for stable operation. The combination of low-density fluid and optimised ionisation ring positioning yielded the most uniform spray and droplet sizes. Furthermore, the study identifies significant synergistic effects between fluid density and electric field shaping via the ionisation ring, with field concentration found to strongly dictate cone formation quality. In conclusion, the results suggest that a larger IDIR requires a higher voltage to initiate the formation of the Taylor cone but provides a wider range of stable cone-jet operation. In contrast, low-density liquids require a lower voltage to generate the Taylor cone; however, they are more susceptible to transitioning into a spray or flying current at higher voltages.

KESAN KETUMPATAN DAN PARAMETER GELANG PENGIONAN TERHADAP PRESTASI CIRI KON TAYLOR BERDASARKAN TEKNIK ELEKTROSEMBURAN

ABSTRAK

Kajian ini meneliti pengaruh ketumpatan bendalir dan parameter gelang pengion terhadap pembentukan serta kestabilan kon Taylor dalam sistem semburan elektrik (electrospray) yang digunakan dalam aplikasi pembakaran berketepatan tinggi, bioperubatan, dan fabrikasi mikro. Walaupun penyelidikan mengenai teknik semburan elektrik telah dijalankan secara meluas, pencapaian pembentukan kon Taylor yang konsisten masih menjadi cabaran disebabkan oleh interaksi kompleks antara daya elektrostatik dan dinamik bendalir. Bagi mengatasi isu ini, kajian ini bertujuan mengoptimumkan parameter operasi terhadap semburan elektrik ini, termasuk diameter gelang pengion (IDIR), kedudukan gelang pengion atau jarak muncung ke sasaran, serta voltan yang dikenakan. Selain itu, kajian ini juga meneliti secara menyeluruh kesan tetapan daripada teknik semburan terhadap ketumpatan cecair dan pembentukan kon Taylor. Pendekatan eksperimen digunakan bagi mengkaji pengaruh ketumpatan bendalir dengan menggunakan campuran etanol dan n-heptana, serta menilai kesan konfigurasi gelang pengion terhadap sudut kon, panjang jet, dan penyebaran titisan. Parameter utama yang diuji termasuk voltan operasi antara 2–10 kV, diameter dalam gelang pengion, dan jarak paksi dari muncung (10.3 mm, 15.3 mm, dan 21.2 mm), di bawah kadar aliran terkawal menggunakan pam picagari berketepatan tinggi. Teknik pengimejan digunakan untuk memerhati peralihan antara mod titisan (dripping), gelendong (spindle), kon-jet, dan multi-jet. Hasil kajian menunjukkan bahawa bendalir berkepadatan rendah, seperti etanol, memerlukan voltan yang lebih rendah untuk memulakan mod cone-jet namun menunjukkan ketidakstabilan yang lebih tinggi pada voltan yang besar. Sebaliknya, bendalir berketumpatan tinggi seperti air, memerlukan voltan yang lebih tinggi dan kedudukan gelang pengion yang lebih hampir bagi mencapai operasi yang stabil. Gabungan bendalir berkepadatan rendah dengan kedudukan gelang pengion yang dioptimumkan menghasilkan semburan dan taburan saiz titisan yang paling seragam. Kajian ini turut mengenal pasti kesan sinergistik yang signifikan antara ketumpatan bendalir dan pembentukan medan elektrik melalui gelang pengion, di mana kepekatan medan elektrik didapati memainkan peranan penting dalam menentukan kualiti pembentukan kon. Kesimpulannya, dapatan kajian mencadangkan bahawa gelang pengion dengan IDIR yang lebih besar memerlukan voltan permulaan yang lebih tinggi untuk membentuk kon Taylor, namun menyediakan julat operasi kon-jet yang stabil dengan lebih luas. Sebaliknya, bendalir berkepadatan rendah memerlukan voltan yang lebih rendah untuk menjana kon Taylor, namun lebih terdedah kepada peralihan kepada mod semburan atau arus terbang pada voltan yang lebih tinggi.

ACKNOWLEDGEMENT

In the Name of Allah, the Most Gracious, the Most Merciful.

First, gratefulness of thanks to our creator, Allah the Almighty, for his continuous blessing which makes this work completed smoothly. Secondly, I would like to extend my appreciation to Universiti Teknikal Malaysia Melaka (UTeM) for providing the research platform and providing the funding for this project.

Secondly, I would like to thank my supervisor, Ir. Ts. Dr. Abdul Rafeq Bin Saleman for his continuous patience and guidance in completing this thesis. Without his insights and support involvements in the process of conducting this project, this thesis would be extremely difficult to accomplish. I would like to express my highest gratitude for your helpful advice and support for the period of this project. The knowledge and tips given are valuable to my future career. Also, I wish to give my thanks to my co-supervisor, Dr. Ridhwan Jumaidin who gave me a much deeper awareness about my project with his support, inspiration and understanding. I am thankful for the chance he gave to me during the progress of the project. Thank you to my past main supervisor Ir. Dr. Fudhail Bin Abdul Munir that very dedicated in helping me throughout his service at UTeM.

My sincere thanks to my fellow friends, for their constant support and helpfulness during the initial stage of research and experimental developments. During the hard times where we were unfortunately faced with pandemic rampaging, they had kindly assisted me with their knowledge and compassion during the progress of this thesis.

TABLE OF CONTENTS

LIST OF TABLES

LIST OF FIGURES

LIST OF ABBREVIATIONS

CC	-	Constant current
CJ	-	Taylor cone or jet bead (cone)
DM	-	Dripping mode
Djet	-	Cone jet diameter
Dring	-	Diameter nozzle tips
FC	-	Flaying current
Fps	-	Frame per second
G	-	Gauge
ID	-	Inner diameter
IDIR	-	Inner diameter of ionisation ring
IR	-	Ionisation ring
Ljet	-	Jet length
MT	-	Multi-jet mode
OD	-	Outer diameter
SM	-	Spindle Mode
TJ	-	Tilted jet mode
UTeM	-	Universiti Teknikal Malaysia Melaka
Vring	-	Ionisation ring

LIST OF SYMBOLS

%	-	Percentage
°	-	Degree (angle)
℃	-	Degree Celsius
cm^3	-	Cubic centimeter
kg	-	Kilogram
kg/m^3	-	Kilograms per cubic meter
lux	-	Lumen per square meter
mL/hr	-	Milliliters per hour
mL/min	-	Milliliters per minute
mm	-	Millimeters
MPa	-	Megapascal
ppm/°C	-	Parts per million per degree Celsius
ρ	-	Fluid density
θcone	-	Cone angle
V	-	Voltage
μL/hr	-	Microliters per hour

LIST OF APPENDICES

LIST OF PUBLICATIONS

The followings are the list of publications related to the work on this thesis:

Nurfadzilah Mohd Sani, Abdul Rafeq Saleman, Fudhail Abdul Munir, Muhammad Hasrul Rosli, Ridhwan Jumaidin, Mohd Shukri Yob, Herman Saputro, 2024. Electrospray Dynamics: Investigating the Impact of Voltage and Ionisation Ring Parameters on Taylor Cone Characteristics. Journal of Advanced Research Micro and Nano Engineering (ARMNE)., vol. 25, pp. 52–65, 2024. (SCOPUS indexed)

Nurfadzilah Mohd Sani, Fudhail Abdul Munir, Abdul Rafeq Saleman, Ridwan Jumaidin, 2024. Generating Droplets Using Small Scale Electrospray for Micropower Generation. 3rd Internasional Conference on Applied Science, Engineering, Advance Technology, and Social Science in Conjunction with Effective Article Writing Workshop for High Impact Journal Publication.

Abdul Munir F, Jumaidin R, Mohd Sani N, Saleman A, Sapotro H, Yop M, 2024. Evaluation of Droplet Generated from Small-Scale Electrospray for Micro Power
Generation Utilization., 258, ICEM 2024 - International Conference on E-Mobility

The 6th Postgraduate Research Symposium on mechanical Engineering (PRiSME 2024) Program

CHAPTER 1

INTRODUCTION

1.1 Background

Electrospray is an electrohydrodynamic (EHD) process where liquid subjected to a high electric field disperses into fine, charged droplets. This technique relies on the delicate balance between electrostatic forces and surface tension, where an applied voltage deforms the liquid meniscus into a conical shape known as a Taylor cone, from which a thin jet emerges and breaks into droplets.

William Gilbert, the first to see and document the effects of an electric field on a liquid surface, made significant contributions to EHD. His main work, "The Magnete," published in 1600, provided crucial insights into how electric fields influence the behaviour of liquid droplets. Gilbert's pioneering discoveries established the framework for further research on electrospray phenomena (Bošković and Bugarski, 2018). The phenomenon was first mathematically described by Geoffrey Taylor (1964), with later breakthroughs by Fenn et al. (1989) demonstrating its application in mass spectrometry, ultimately leading to Nobel Prize-winning work on electrospray ionisation (ESI) in 2002. Due to these findings, ESI has been found in vast applications, such as multi-particulate medication delivery (Alfatama et al., 2024), food processing (Yang et al., 2024), plant nutrition (Pejman Sereshkeh et al., 2024), surface coatings (Rafeq Saleman et al., 2022a, 2022b; Saleman et al., 2019), and many more.

In 2005, Yeo *et al*. conducted a rigorous examination of the impacts of electric fields on droplet size, distribution, and charge, shedding light on the complex link between electric fields and droplet characteristics (Yeo et al., 2005). Furthermore, in 2017, Ondimu *et al*.

conducted a comprehensive study that corroborated and built on Gilbert's findings, underlining its long-term importance in current electrospray research (Ondimu et al., 2017; Wu et al., 2020). Their discoveries highlighted the dynamic nature of the electrospray behaviour of droplets during electrospraying changes based on the properties of the applied electric field, resulting in different electrospray modes such as dripping, spindle, pre-break-up, and cone-jet mode.

Based on past findings, it is understood that the voltage applied has a noticeable effect on the production and behaviour of the Taylor cone (Zhao et al., 2019). It controls the strength of the electric field, which influences the creation of the Taylor cone and subsequent jets (Naderi et al., 2019). Lower voltages produce bigger liquid droplets because the electric force may be insufficient to maintain a continuous jet formation (Wang et al., 2020). As the voltage increases, the jet becomes steadier and produces smaller, more uniform droplets.

Another crucial component is the ionisation ring (IR), which influences spatial distribution and droplet size (Camelot et al., 2018). The position and size of the IR can have a substantial impact on the electric field distribution surrounding the jet, impacting Taylor cone breakage and creation (Crotti et al., 2011). Hartman *et al.* provide the physical numerical model that properly calculates the geometry of the liquid cone and jet, as well as the current and surface charge distribution (Hartman et al., 2000). EHD atomisation in the cone-jet mode produces a size distribution that varies based on the jet's diameter and droplet formation (Wang et al., 2022).

A stable cone-jet mode requires a minimum flow rate for each liquid; where at this minimum flow rate, the jet breaks apart due to axisymmetric instabilities, which are also known as varicose instabilities(Hartman et al., 1999). Jet breakup above a particular surface charge and can be affected by lateral or azimuthal instabilities. These instabilities are also known as kink instabilities; during the kink instabilities, the size distribution of major droplets widens (Bruins, 1998). Consequently, the transition between varicose- and kink-dominated regimes critically governs resultant droplet populations, with EHD atomisation in cone-jet mode yielding size distributions inherently dependent on jet diameter, charge density, and the dynamic interplay of these instabilities ultimately determining spray uniformity and application efficacy.

Although there have been vast numbers of researchers and findings in the past related to EHD, the inability to accurately regulate the Taylor cone is always an issue that often leads to inadequate system performance, evident in irregular droplet consistency, spray instability, or ineffective material deposition. Thus, this research is driven by the need to enhance electrospray precision by addressing the critical gaps in understanding fluid density and IR parameters that independently and synergistically influence the Taylor cone stability and droplet characteristics. By systematically investigating these factors, this study aims to establish fundamental design principles, enabling more reliable and efficient electrospray systems for advanced applications. The findings will provide a deeper understanding of the interplay between fluid properties and electrostatic parameters, enabling better control over electrospray performance. Ultimately, this work seeks to establish practical guidelines for selecting optimal operating conditions, improving reliability in both industrial and scientific electrospray applications.

1.2 Problem Statement

Electrospray technology has become indispensable across diverse fields ranging from mass spectrometry to additive manufacturing. However, despite its widespread adoption, achieving precise control over Taylor cone characteristics and resultant droplet properties remains a significant challenge due to the complex interplay of multiple physical and electrical parameters. While previous research has extensively investigated the roles of electrical conductivity, viscosity, and surface tension in electrospray processes, critical gaps persist in these fundamental understandings of two key factors, which are fluid density and the position of the ionisation ring parameters. Thus, this study elucidates the electrospray parameters that affect the characteristics of the spray pattern, namely the inner diameter of the ring ionisation (IR), the positioning of the IR, the distance from the nozzle to the target of the IR, and the applied voltage to the system.

1.3 Research Question

i). This study seeks to address four fundamental research questions that systematically investigate the effects of fluid density and ionisation ring parameters on electrospray performance:

ii). What is the quantitative impact of adjusting the voltage applied to an ionisation ring (or other key parameters like its distance from the nozzle, flow rates of liquid, and diameter of ionisation ring) on the Taylor cone form, jet breakup behaviour, and resultant spray pattern?

iii). How does systematic variation in the density of the working fluid influence the Taylor cone angle, jet initiation stability, and droplet morphology in a controlled electrospray system?

iv). Is there a statistically significant interaction effect between fluid density and the ionisation ring parameter on the observed Taylor cone characteristics and electrospray performance?

v). What are the underlying physical mechanisms (e.g., changes in electric field distribution, fluid inertia, and charge transport) that explain the observed effects of density and ionisation ring parameters on the Taylor cone and jet?

1.4 Research Objectives

The main aim of this research is to achieve the following objectives through systematic experimental investigation:

i). To investigate the effect of electrospray parameters, namely IDIR size, position of IR, and voltage, on cone jet characteristics.

ii). To establish the fundamental relationship between working fluid density and Taylor cone characteristics.

1.5 Scope of Research

The study will comprehensively examine the impact of ionisation ring parameters. The primary focus will be on the applied voltage to the ionisation ring (Vring), which will be systematically varied over a range from 0 kV to 10 kV, relative to a common electrical ground. This range has been chosen to encompass both field-enhancing and field-shielding effects on the Taylor cone. To ensure clear attribution of the observed phenomena, the axial distance of the ionisation ring from the nozzle tip (Dring) will be maintained at a variance value of 10.3 mm, 15.3 mm, and 21.2 mm throughout the experiments. Furthermore, a single, precisely defined ionisation ring form, including its inner diameter, outer diameter, and thickness, will be employed consistently across all experimental runs, thereby eliminating the variations of surrounding factors as confounding factors. Secondly, fluid density (ρ) will be varied across a controlled and experimentally relevant range, specifically from approximately 0.01 mL/cm3 to 0.60 mL/cm3. This will be achieved through the preparation of solutions utilising water, ethanol, and n-heptane as the primary medium. High-resolution imaging techniques will be primarily employed to measure the Taylor cone angle (θ cone), providing insight into the equilibrium shape of the meniscus. The stability and morphology of the emanating jet will be evaluated through measurements of the jet diameter (Djet) at a consistent point downstream from the cone apex and the stable jet length (Ljet) before the onset of instability or breakup. The scope is specifically delimited to the stable cone-jet mode of electrospray, as it is the most relevant for applications demanding precise control over droplet formation.

1.6 Significance of Study

At a foundational level, this study is designed to offer novel insights into the intricate interplay of fluid dynamics and EHD in the electrospray process. This research explores the knowledge gaps within the existing literature by systematically isolating and investigating the influence of fluid density and by meticulously examining the role of electrode parameters specifically, including ionisation ring position, diameter, and the distance between collector and nozzle. While numerous studies have explored the impact of electrical properties and rheological characteristics, a comprehensive understanding of how fluid density directly modulates Taylor cone formation and stability, particularly in conjunction with controlled external electric fields, remains a grey area and thus requires deeper empirical elucidation. Consequently, the findings will enrich the theoretical framework of electrospray, contributing to a more complete and subtle picture of its underlying physical principles. Furthermore, this investigation aims to provide a granular understanding of the mechanistic pathways through which these specific parameters dictate the precise configuration and stability of the Taylor cone, thereby enhancing our predictive capabilities concerning jetting behaviour and ultimate droplet characteristics.

From an applied perspective, the results of this research hold significant promise for the advancement and optimisation of electrospray-based technologies. The findings will be invaluable for the design and fine-tuning of electrospray systems, fostering enhanced control over critical performance attributes such as droplet size uniformity, spray pattern, and deposition precision. Such refined control is indispensable for high-demand applications where consistency and accuracy are crucial. Moreover, the robust experimental data generated will serve as a benchmark for the validation and iterative refinement of computational models simulating the electrospray process. This capability for data-driven model improvement is crucial for developing more accurate predictive tools, which can significantly reduce the empirical optimisation cycles typically associated with electrospray system development. By fostering a clearer understanding of the parameter-performance relationships, this study will also facilitate the expansion of electrospray into novel and emerging applications that necessitate stringent control over specific droplet characteristics or highly localised material deposition, including, but not limited to, advanced functional coatings, precision bio-printing, and high-resolution patterning techniques. Ultimately, these insights are expected to translate into the development of more robust, predictable, and economically scalable electrospray processes, benefiting industries such as pharmaceuticals, electronics manufacturing, and advanced materials engineering.

1.7 Thesis Outline

Based on the objectives previously presented and on the approach proposed before, this thesis is made up of five (5) chapters. The contents are summarised as follows:

- Chapter 1. Introduction: This chapter provides the background, problem statement, research questions, objectives, significance, and scope of the study.
- Chapter 2. Literature review: This chapter presents a comprehensive review of existing knowledge on electrospray, fluid properties, auxiliary electrode influences, and performance metrics, identifying the research gap.
- Chapter 3. Methodology: This chapter details the experimental setup, materials, experimental design, data acquisition protocols, and analytical techniques used.

- Chapter 4. Result and Discussion: This chapter presents the experimental findings, analyses the data, interprets the results in the context of theoretical understanding, and compares them with existing literature.
- Chapter 5. Conclusion and Recommendations for Future Research: This chapter summarises the key findings, states the contributions of the research, discusses practical implications, and suggests directions for future work.

CHAPTER 2

LITERATURE REVIEW

2.1 Introduction

In electrospray technology has emerged as a pivotal technique in various applications, including mass spectrometry (Chang and Urban, 2024), nanotechnology (Zakaria et al., 2020), and thin-film deposition (Tang et al., 2021), due to its ability to generate fine, charged droplets. A critical aspect of this process is the formation of the Taylor cone, a conical liquid meniscus that forms under the influence of an electric field. The stability and characteristics of the Taylor cone significantly influence the efficiency and quality of electrospray performance (Zhou and Biswas, 2021).

Two key factors affecting Taylor cone formation and its subsequent behaviour are liquid density and ionisation ring parameters. The density of the working fluid determines its inertial and viscous properties, influencing droplet formation and jet stability (Gamero-Castaño and Cisquella-Serra, 2021; Johari et al., 2022; Panahi et al., 2020). Meanwhile, the ionisation ring typically serving as a counter electrode are plays a crucial role in shaping the electric field distribution, thereby affecting the cone-jet mode transition and spray uniformity (Di Natale et al., 2023; Yang et al., 2022).

Despite extensive research on electrospray dynamics, the combined effect of density and the ionisation ring parameters such as voltage, geometry, and positioning on Taylor cone characteristics remains insufficiently explored. Previous studies have largely focused on either fluid properties or electric field configurations in isolation, leaving a gap in understanding their synergistic influence (Saputro et al., 2022; Z. Wang et al., 2024; Wu et al., 2020). This literature review aims to consolidate existing knowledge on the subject, analyze key findings, and identify research gaps to provide a foundation for further investigation.

By examining theoretical models, experimental studies, and numerical simulations, this review will evaluate how variations in density and ionisation ring settings impact Taylor cone stability, jet formation, and droplet size distribution. The insights gained will contribute to optimizing electrospray systems for enhanced performance in industrial and scientific applications.

2.2 Literature Survey

In recent years, the electrospray method, which uses electric fields to break up liquids into tiny droplets, has become more popular because it could be used in combustion, drug delivery, inkjet printing, and microfabrication. To make sure that the spray is consistent and controlled, a stable Taylor cone must be formed. This is a cone-shaped structure of liquid that forms when there is electrostatic stress.

2.2.1 Fundamentals of Electrospray and Taylor Cone Formation

In 1964, Taylor became the first to write about the concept of creating cone-jet. Taylor elucidated that when the electrostatic force exceeds the surface tension at the interface of the liquid and air, a conical structure known as the Taylor cone is generated. This result in charged droplets softly detaching (Geoffrey Taylor, 1964). Since that time, scientists have examined several factors that may alter this tendency. The parameters include voltage, flow rate, and the liquids properties such as viscosity, conductivity and density (Gañán-Calvo and Montanero, 2009; Jaworek and Krupa, 1999).

The Taylor cone is a key part of electrospray that changes how the charged droplets act (Di Natale et al., 2023). A stable Taylor cone is important for getting droplets to spread out evenly, which affects how stable the combustion is. The electrospray process is affected by many things, such as the voltage used, the shape of the electrodes, the properties of the liquid, and the flow rate (Bošković and Bugarski, 2018). If you know these things, you can figure out how electrospray settings affect the properties of the spray.

2.2.2 Influence of Applied Voltage on Electrospray Characteristics

The characteristics of the liquid, including surface tension, viscosity, and electrical conductivity, substantially affect the efficacy of an electrospray. These qualities influence the pressures exerted on the liquid meniscus and its response to the electric field. Density influences the overall mass flow rate and the inertial dynamics in the spray process; nevertheless, it has not been examined as extensively in isolation as surface tension or conductivity (Panahi et al., 2020). A denser liquid may need a more robust electrostatic force to accelerate and establish a steady jet. This may alter the onset voltage and stability range of the Taylor cone. While it is generally acknowledged that specific liquid properties, such as density, influence electrospray, the interaction of density with particular ionisation ring parameters (IDIR and position) concerning Taylor cone formation and spray characteristics, especially for combustion-relevant fuels, remains poorly understood (Chang and Urban, 2024). Research often focuses on model liquids or specific fuel types, and the relationship between liquid properties and electrode design is complex.

The fluid's density significantly influences the stability and starting voltage required for electrospray. Ethanol is a low-density, low-viscosity liquid that has been extensively researched because of its ease of ionisation and ability to form cones at reduced voltages (Loo et al., 1989). Conversely, denser fluids such as water need higher voltages to form stable cones due to the greater strength of surface tension forces. Recent studies have investigated the use of mixed fuels, such as ethanol and n-heptane, to amalgamate the optimal characteristics of both for enhanced atomization and combustion (Cao et al., 2022; Pielecha et al., 2021).

These mixtures enable the alteration of density and conductivity, which directly influence the spray angle, cone stability, and transitions between jet modes. The density and surface tension of the working fluid are crucial in the formation of the Taylor cone. Research by Cloupeau and Prunet-Foch (1994) indicated that low-viscosity liquids, including ethanol, need lower critical voltages to initiate cone-jet mode compared to water (Cloupeau and Prunet-Foch, 1994). Gafian-Calvo *et al.* (1997) similarly found that fluid conductivity and permittivity influence droplet size distribution, thereby decreasing combustion efficiency (Gafian-Calvo et al., 1997).

2.2.3 Role of Electrode Geometry and Ionisation Ring Parameters

The accurate positioning of the electrodes significantly influences the distribution of the electric field, particularly the ionisation ring diameter (IDIR) and its relationship with the spray needle. Research indicates that reduced IDIR values enhance the electric field strength, resulting in sharper cone angles and increased jet production. In contrast, elevated IDIR levels result in broader and more stable spray patterns (Kim et al., 2022). The position of the ionisation ring either in upstream or downstream of the needle tip influences the stability of the cone jet and the transition between electrospray modes, such as spindle mode, jet beads, and multijet (Lee et al., 2018). The configuration and geometry of the electrodes, particularly the counter electrode sometimes referred to as the ionisation ring or extractor, are essential for modifying the electric field and enhancing the efficacy of the electrospray process. The ionisation ring (IDIR) significantly influences the strength and uniformity of the electric field around the Taylor cone (Yang et al., 2022; Zuo et al., 2022).

Researchers have investigated several configurations of electrodes to enhance the stability of the spray and improve the quality of the droplets. To maintain a constant electric field intensity, a greater voltage is often required as the distance between the capillary and the extractor electrode is increased (Magnusson et al., 2020; Si et al., 2024). The trajectory and dispersion of the droplets alter as the separation between the capillary and extractor electrodes is augmented (Jaworek and Krupa, 1999) The dimensions of the ionisation ring (IR) are critical as they alter the field lines around the Taylor cone. This impacts the stability of the cone and the spray angle. The electric field may be more intense with an increased ring diameter. These parameters may alter the containment efficacy of the spray and the stability of the cone at elevated voltages (López-Herrera et al., 2005). A comprehensive investigation is required to ascertain how certain IDIR values, their geographical distribution, and factors such as liquid density influence the characteristics of the Taylor cone and the stability of the spray.

2.2.4 Effect of Liquid Properties, with a Focus on Density

The characteristics of the liquid, including surface tension, viscosity, and electrical conductivity, substantially affect the efficacy of an electrospray. These qualities influence the pressures exerted on the liquid meniscus and its response to the electric field. Density influences the overall mass flow rate and the inertial dynamics in the spray process; nevertheless, it has not been examined as extensively in isolation as surface tension or conductivity (Panahi et al., 2020). A denser liquid may need a more robust electrostatic force to accelerate and establish a steady jet. This may alter the onset voltage and stability range of the Taylor cone (Chen et al., 2022; Park et al., 2022; Zhang et al., 2021). While it is generally acknowledged that specific liquid properties, such as density, influence electrospray, the interaction of density with particular ionisation ring parameters (IDIR and position) concerning Taylor cone formation and spray characteristics, especially for combustion-relevant fuels, remains poorly understood (Chang and Urban, 2024). Research often focuses on model liquids or specific fuel types, and the relationship between liquid properties and electrode design is complex.

The fluid's density significantly influences the stability and starting voltage required for electrospray. Ethanol is a low-density, low-viscosity liquid that has been extensively researched because of its ease of ionisation and ability to form cones at reduced voltages (Loo et al., 1989). Conversely, denser fluids such as water need higher voltages to form stable cones due to the greater strength of surface tension forces. Recent studies have investigated the use of mixed fuels, such as ethanol and n-heptane, to amalgamate the optimal characteristics of both for enhanced atomization and combustion (Cao et al., 2022; Pielecha et al., 2021).

These mixtures enable the alteration of density and conductivity, which directly influence the spray angle, cone stability, and transitions between jet modes. The density and surface tension of the working fluid are crucial in the formation of the Taylor cone. Research by Cloupeau and Prunet-Foch (1994) indicated that low-viscosity liquids, including ethanol, need lower critical voltages to initiate cone-jet mode compared to water (Cloupeau and Prunet-Foch, 1994). Gafian-Calvo et al. (1997) similarly found that fluid conductivity and permittivity influence droplet size distribution, thereby decreasing combustion efficiency (Gafian-Calvo et al., 1997).

2.3 Research, Ideology and Concept from the Previous Project

2.3.1 Early Foundation of Electrospray Research Until Current Research

The electrospray technique, a process whereby a liquid is atomized into fine charged droplets using electrostatic forces, has its conceptual foundation dating back to the early 20th century. The pioneering work of Zeleny (1917) marked one of the first documented observations of the phenomenon where he investigated the behavior of liquid menisci under high electric fields (John Zeleny, 1917). This foundational study laid the groundwork for understanding the dynamics of liquid jets and their subsequent breakup under electrostatic forces.

A significant theoretical breakthrough came in the 1960s with the work of Sir Geoffrey Taylor, who mathematically described the shape of the conical meniscus that forms at the tip of a charged liquid jet (Geoffrey Taylor, 1964). This structure, later termed the "Taylor cone", became a critical concept in electrospray research. Taylor (1964) demonstrated that under the balance of surface tension and electrostatic pressure, a cone with a half-angle of approximately 49.3° forms, and this shape is integral for the stable emission of charged droplets.

By the 1980s and 1990s, electrospray technology experienced substantial advancement, particularly with the development of electrospray ionisation (ESI) as a powerful technique in mass spectrometry. Fenn *et al*. (1989) revolutionized analytical chemistry by introducing ESI-MS, enabling the analysis of large biomolecules such as proteins and peptides without fragmentation, a development that ultimately earned them the Nobel Prize in Chemistry in 2002 (Fenn et al., 1989). This application brought electrospray into mainstream scientific and industrial usage.

Subsequent decades saw growing interest in the fundamental fluid mechanics, electrodynamics, and material science underlying the electrospray process. Research diversified into applications such as nanoparticle synthesis, drug delivery, micro-thrusters in space propulsion, and environmental monitoring. Modern electrospray systems explore operational parameters including flow rate, applied voltage, fluid conductivity, and ambient conditions (Cloupeau and Prunet-Foch, 1994; Fernandez de la Mora and Barrios-Collado, 2017).

Recent research has extended into the influence of physical and electrical parameters on Taylor cone formation and stability. Parameters such as fluid density, viscosity, electrical conductivity, dielectric constant, and geometry of the ionisation ring or emitter have been shown to significantly affect spray modes and cone stability (Dubey et al., 2021; Duby et al., 2006). Innovations such as using ring electrodes, needleless sprays, and multi-electrode systems have been developed to enhance electrospray efficiency and broaden its application scope. Studies now focus on optimizing geometric and operational parameters for specific applications such as fine droplet production, controlled deposition, and precision spray control.

In particular, the Taylor cone formation's sensitivity to external factors has made it a prime subject for parametric studies. Investigations into the effect of density and ionisation ring parameters contribute to a deeper understanding of jet breakup, spray angle, and droplet size distribution essential for tailoring electrospray systems for industrial and scientific use. The growing body of research reflects a transition from empirical approaches to more refined, simulation-based and experimentally validated studies, including computational fluid dynamics (CFD) and electrohydrodynamic (EHD) modelling (Higuera, 2003; Nekrasov et al., 2017).

The citation map shown in Figure 2.1 represent the research made up started knowing the advantages of electrospray. Researchers such as (Loo et al., 1989) have made significant advances in electrospray technology, enhancing precision and efficiency. The citations also demonstrate how electrospray technology progressed from fundamental research to practical applications, with researchers such as (Rauschenbach et al., 2006) and (Wang and Yin, 2018;

Wang et al., 2018) developing electrospray systems to improve flame stability and combustion performance.

The second reference map Figure 2.1, referencing (Rafie-Zinedine et al., 2024), emphasizes recent improvements in electrospray technology, notably its application in combustion systems. Over the last decade, researchers have improved our understanding of spray pattern production, charge-induced fuel atomization, and flame stabilization techniques. (Duby et al., 2006) and (Pongrác et al., 2014) discovered that the thermophysical properties of electrospray fuels are increasingly significant in multi-component systems. (Marty, 2020) propose real-time control for electrospray-assisted combustion using experimental and computational models. Recent efforts by (Huang et al., 2022) and (Dong et al., 2023; Mosa et al., 2023) show attempts to improve electrospray efficiency using voltage control methods, ionisation techniques, and nozzle design optimization.

The reference map finishes with Rafie *et al.* (2024) who presents a comprehensive framework that includes sustainable combustion techniques, renewable energy applications, electrospray technology, and machine learning (Rafie-Zinedine et al., 2024).

Furthermore in Figure 2.2, recent research mostly citation network highlights the scholarly development and influence of Huang (2022), a pivotal study within the electrospray technique domain (Huang et al., 2022). This research consolidates foundational knowledge while contributing significantly to the evolution of electrospray applications. Among the earliest cited works is (Lambropo_Ulos, 1995; Yamashita, 1984), who pioneered the electrospray ionisation (ESI) technique, providing the theoretical basis for many subsequent developments. Further foundational insights into fluid dynamics and electrohydrodynamic (EHD) behavior can be traced through the works of (Barreto and Hernandez-Rivera, 2022a). Building upon these, mid-stage contributions by (Magnusson et al., 2020; Rovelli et al., 2020; Zhu and Chiarot, 2020) advanced the field through experimental studies and modeling efforts on cone-jet stability, electric field control, and flow characteristics.

Surrounding Huang (2022) are several contemporary studies, including (Jia et al., 2021; Yang et al., 2021; Zhou and Biswas, 2021), which explore related methodological approaches such as multi-nozzle designs, Taylor cone behavior, and electrospray-enhanced combustion or material deposition. These works signify a thematic convergence in the literature during this period. Moreover, the influence of Huang (2022) extends forward to more recent publications by (Chen et al., 2023; Khan et al., 2019; Nashee and Hmood, 2023; Silva et al., 2024), indicating its growing relevance in cutting-edge applications such as bioelectrospray, nanoparticle synthesis, and microscale flame stabilization. The temporal aggregation of significant studies from 2019 to 2024 indicates a heightened interest, perhaps stimulated by advancements in microfluidic devices, precise droplet manipulation, and computational modeling.

While the majority of referenced publications are interrelated, exceptions like (Gan et al., 2019b; Jiang et al., 2019; Zhang et al., 2019) despite their limited network linkages, indicate ancillary or multidisciplinary significance. Huang (2022) functions as a key integrative point in the advancing domain of electrospray research, adeptly connecting traditional electrospray theory with novel advancements across several technological sectors.

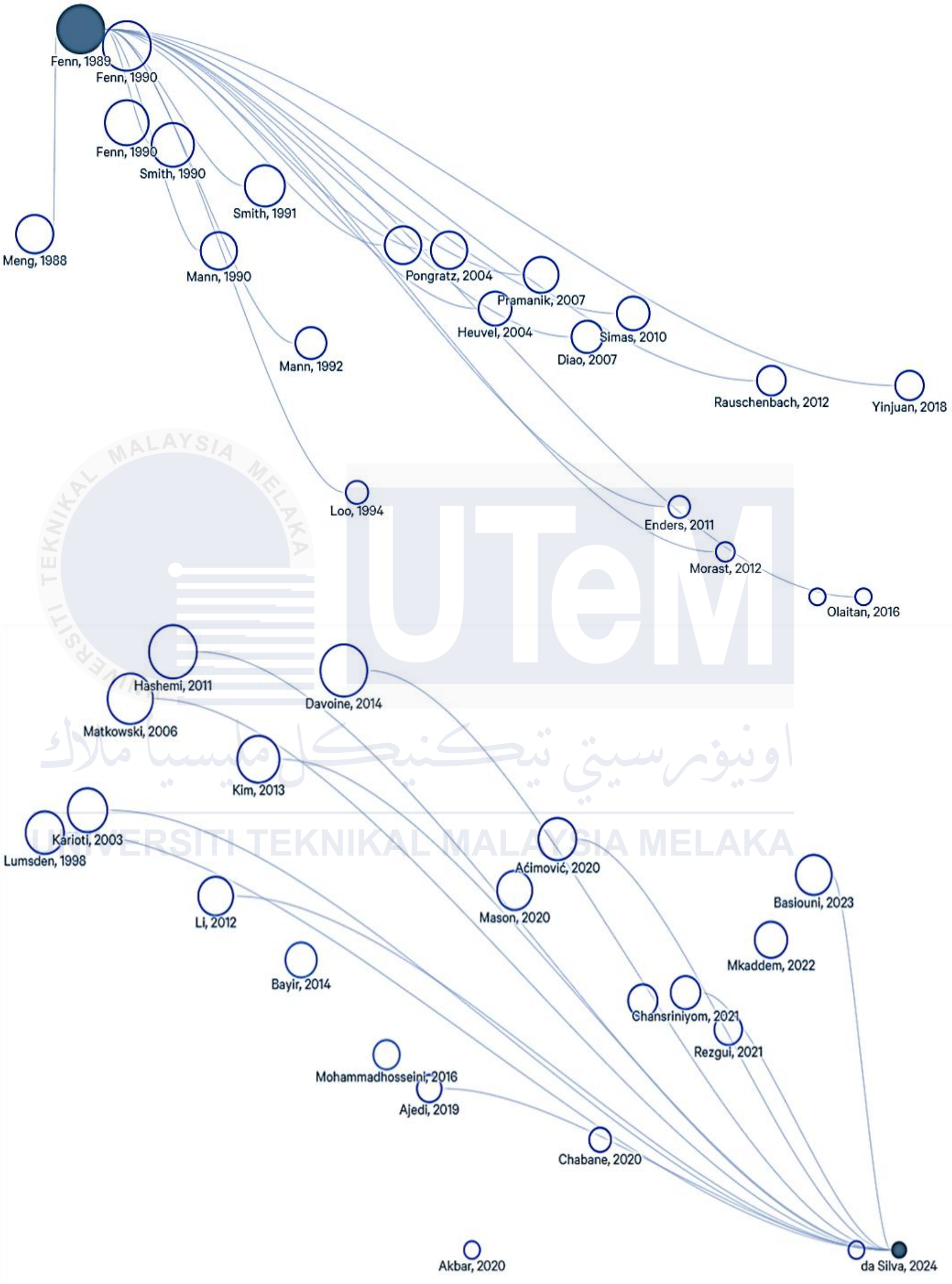

Figure 2.1 Electrospray Foundation Maps (Giusti and Fredrich, 2024a)

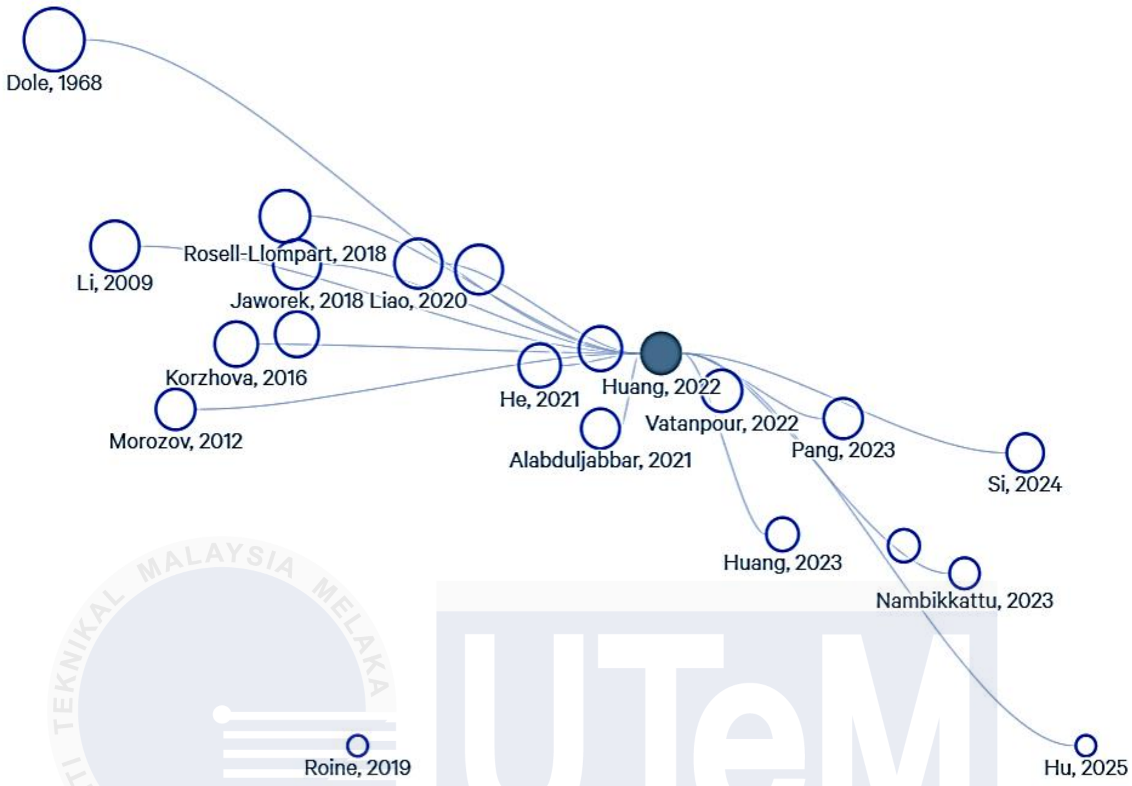

Figure 2.2 Networking citation in recent research(Huang et al., 2022)

2.3.2 Overview of Previous Project Objectives and Implementation Summary of Prior Setup

The earlier phase of the research and development initiative laid a crucial foundation for the current investigation into electrospray-based. The main goal of the earlier research was to create and test a basic setup that could produce a stable Taylor cone using the electrospray technique in air (Gañán-Calvo et al., 2018; Thuppul et al., 2020). This program aimed to explore the key features of electrospray processes, focusing on how the cone-jet forms, how stable the flow is, and how things like voltage, nozzle shape, and fluid properties affect it.

One of the core goals was to achieve a repeatable and observable Taylor cone structure for various liquid fuels namely ethanol, n-heptane, and their binary mixtures while systematically documenting the onset voltage required for stable emission (Munir and Mikami, 2015). The initial setup incorporated a high-voltage power supply connected to a metallic capillary nozzle, with the counter-electrode positioned at a controlled distance to induce the electric field necessary for electrospray formation. The fuel reservoir was gravity-fed or assisted by a low-flow rate syringe pump to ensure steady delivery of the liquid to the nozzle tip (Hery Soegiharto et al., 2017). Observations were captured using a high-resolution digital microscope or high-speed camera to study the behavior of the cone under different operating conditions (Kim et al., 2011).

Additionally, the project explored the visual and thermal interaction of the electrospray fuel with a small ignition flame placed downstream of the spray zone (Saputro et al., 2022; 2021). This preliminary combustion setup served to determine whether the electrospray enhanced fuel atomization and flame anchoring compared to conventional injection methods. Although not optimized for quantitative combustion analysis, the experiment successfully demonstrated that electrospray droplets exhibited a finer dispersion and better mixing, leading to a more consistent flame presence at lower fuel flow rates (Abdul Munir et al., 2018a).

Throughout the implementation of the initial system, several technical challenges were addressed, including voltage instability, corona discharge suppression, and dielectric breakdown of surrounding air (Gan et al., 2015; Lim et al., 2017). These issues were mitigated by fine-tuning the distance between electrodes, optimizing nozzle-tip diameter, and introducing a grounded shield ring to stabilize the electric field lines (Pongrác et al., 2014). Furthermore, the project provided valuable insights into the role of fluid conductivity, surface tension, and viscosity on the cone formation threshold and spray morphology.

In summary, the prior setup established a functional electrospray platform with sufficient control over key parameters, thereby validating the feasibility of using electrospray as a means of improving spray quality. The foundational knowledge and experimental techniques developed during this phase serve as the foundation for the present study, which aims to enhance flame stability through refined control of electrospray parameters and advanced diagnostics. The lessons learned, particularly with respect to fluid-electric interactions and initial flame response, have directly influenced the design improvements and research focus in the current project phase.

2.3.3 Experimental Setup and Configuration from the Previous Project

Over the years 2018 to 2025, various research initiatives exploring electrospray technology have contributed valuable insights into the design and performance of the system, particularly focusing on flame stabilization, spray pattern control, and fine droplet generation.

a) Ionisation Ring Placement and Voltage Strategy

The ionisation ring, called the charging electrode, was placed around the spray channel to keep the electric field steady, following earlier electrospray research (Thuppul et al., 2020). This arrangement was essential for stabilizing the Taylor cone and reducing asymmetric droplet deflection. The distance from the nozzle tip to the ionisation ring was adjusted between 3 mm and 15 mm, with closer proximity 3 to 5 mm augmenting the electric field intensity at the liquid meniscus, thereby facilitating the early development of the cone (He and Jokerst, 2020; Soares et al., 2018). Excessive closeness, however, posed a danger of electrical breakdown at elevated voltages, especially for low-density fluids such as n-heptane (Chen et al., 2017; Yao et al., 2014). Optimal cone-jet stability in ethanol-based electrosprays was seen at intermediate distances 5 to 10 mm, but greater distances over to 10 mm often resulted in unstable phenomena such as dripping or spindle formation, particularly in high-viscosity fluids (Jahan et al., 2021a; Jiang et al., 2023; Xian et al., 2022).

The voltage provided to the ionisation ring was modified according to the fluid's conductivity and the intended spray configuration. For low-conductivity fluids like n-heptane, higher voltages between positive polarities 8 kV and 10 kV were needed to help move charges, while for high-conductivity fluids like ethanol, lower voltages of positive polarities 2 kV to 5 kV were sufficient because they naturally allow ions to move more easily. Negative voltages between negative polarities 2 kV and 5 kV were sometimes applied to help spread out the droplets or change the direction of the spray, particularly when accurate placement was needed. Adjusting the voltage facilitated transitions among dripping, spindle, cone-jet, and multi-jet modes, with the stability of the cone-jet being acutely responsive to the interaction of voltage, fluid characteristics, and nozzle configuration (Jweeg et al., 2024; Namoos and Jasim, 2024; S. Wang et al., 2024).

b) Nozzle Design and Fluid-Specific Adaptations

Multiple nozzle designs were used, including stainless steel capillary nozzles, nozzle-type emitters, and glass capillaries, with internal diameters varying from 50 µm to 300 µm. Nozzle lengths and wall thicknesses were determined according to desired spray performance and suitability for high-voltage operation. The distance between the nozzle and the substrate or collector was a crucial element, varying significantly from 10 mm to 50 mm depending on the application.

The selection of nozzle geometry and material substantially affected the performance of the electrospray. Tapered stainless steel nozzles with inner diameters from 0.1 mm to 0.5 mm were often used for their capacity to concentrate electric field lines, thereby promoting cone-jet initiation (Fernandez de la Mora and Barrios-Collado, 2017). Sharp-edged nozzles were especially efficacious for low-surface-tension fluids such as n-heptane, whereas glass capillaries were favored for electrically insulating applications due to their ability to reduce parasitic currents (Pan et al., 2014).

The nozzle-to-ring distance (NRD) was empirically tuned, with 5 mm being optimal for ethanol to reduce satellite droplet formation, but 8–10 mm was preferable for n-heptane owing to its reduced surface tension and vulnerability to charge saturation (Hartman et al., 2000). The nozzle-to-collector distance (NTCD) was adjusted from 10 mm to 50 mm to examine its influence on droplet flight duration and deposition uniformity. Reduced distances below 20 mm correlated with increased collecting efficiency but posed a danger of electrical arcing, whereas wider distances over than 30 mm facilitated enhanced droplet evaporation and dispersion (Kang et al., 2021; 2023).

c) Fluid Properties and Their Electrospray Response

It was found that the density, conductivity, and surface tension of the working fluid had a significant impact on the behavior of the electrospray. In contrast to ethanol, which displayed greater operational stability at voltages ranging from 4 kV to 6 kV, n-heptane, which has a density of 684 kg/m³, required higher ionisation ring voltages, ranging from 7 kV to 9 kV, to accomplish stable cone-jet formation. This information is summarized in Table 2.1. According to Pan et al. (2014), high-density fluids, such as water with a density of 998 kg/m³, exhibited shallow charge penetration, which required the positioning of proximal rings between three and five millimeters in order to achieve successful droplet charging.

Table 2.1 Fluid properties and their corresponding electrospray (Pan et al., 2014)

Parameter	n-heptane	Ethanol	Water
Density (kg/m³)	684	789	998
Conductivity (S/m)	~10^{-6}	~1.3×10^{-3}	~5×10^{-6} (with 0.1M NaCl)
Surface Tension (mN/m)	20.1	22.1	72
Optimal Voltage Range	+7 to +9 kV	+4 to +6 kV	+10 to +12 kV (pulsating mode only)
Stability Window	±0.5 kV	±2 kV	Unstable
Charge/Mass Ratio (Q/m)	~1.5×10^{4}	~0.7×10^{4}	~2×10^{4}

Higher voltages were required to ensure steady jetting, even though lower-density fluids often showed higher charge-to-mass ratios (Q/m) due to their reduced droplet mass (Johari et al., 2022). Conversely, viscous resistance was more likely to occur in high-density fluids, which might compromise cone-jet stability at low flow rates (Hartman et al., 1999). Even though they produced more monodisperse droplets at lower flow rates, the same conclusion was reached.

d) Synergistic Effects of Density and Ionisation Parameters

The relationship between fluid density and ionisation ring parameters was crucial in determining electrospray efficacy. The low density of n-heptane necessitated elevated voltages and reduced ring spacing to counteract its weak inertial forces, while ethanol's intermediate density allowed for greater operational flexibility (Thakkar and Misra, 2021; Yu et al., 2021). Additionally, applying a negative charge was shown to help control the spray direction in thick fluids by preventing droplets from clumping together. Future research could explore multi-ring electrode configurations to distinguish between primary and secondary charging effects, as well as pulsed voltage techniques to reduce corona discharge in low-density sprays (Gan et al., 2019a; Laimer et al., 2019; Wang et al., 2015). CFD simulations could help explain how fluid behavior changes with density and how the electric field is spread out.

e) Overview of Parameters Used and Controlled

Throughout the body of study from 2018 to 2025, the following electrospray parameters were mostly altered and observed as shown in Table 2.2. Somehow, in several tests, supplementary factors like nozzle tilt angle, ambient gas flow, and substrate temperature were investigated to assess their impact on droplet dispersion and flame morphology.

Table 2.2 Overview parameters from previous research (Bošković and Bugarski, 2018)

Parameter	Typical Range	Purpose
Applied Voltage (V)	2–10 kV (DC)	Initiates and stabilizes electrospray cone-jet
Flow Rate (µL/min)	1–50 µL/min	Controls droplet size, jet stability
Nozzle-Collector Gap	10–50 mm	Defines electric field strength and deposition area
Electrode Position	3–15 mm from nozzle	Modulates ionisation efficiency and charge distribution
Fluid Conductivity	$10^{-8} - 10^{-4}$ S/m	Impacts electrospray mode and droplet breakup

2.3.4 Performance Evaluation in the Previous System Observations

Electrospray ionisation (ESI) is a prevalent method in mass spectrometry for analyzing biomolecules, nanoparticles, and other chemical substances. Assessing the efficacy of electrospray systems is essential for enhancing ionisation efficiency, stability, and repeatability. Prior research has examined several factors affecting electrospray efficacy, such as voltage configurations, flow rates, solvent composition, and emitter design (Jowkar et al., 2019; Zeng et al., 2020).

In other hand, influence of voltage and flow rate is a very important. The voltage used is very important for how well electrospray works because it controls the shape of the Taylor cone, which is a cone of liquid at the tip of the emitter. Research shows that using the right voltage keeps the Taylor cone stable, which helps create small, even droplets that are good for ionisation (Zhong et al., 2018). Excessive voltage may result in electrical discharge or erratic spraying, thereby diminishing signal stability (Laimer et al., 2019). The speed at which the liquid flows is important, slower flow rates, usually in the nL/min range, create smaller droplets, which helps with desolations and increases ion yield. On the other hand, higher flow rates create bigger droplets that might not fully dry out, leading to lower sensitivity and more background noise. The findings emphasize the necessity of accurate voltage and flow rate regulation to sustain optimal ESI performance (Nekrasov et al., 2017; Uhlmann et al., 2025; Z. Wang et al., 2024).

Moreover, role of solvent composition and conductivity is the choice of solvent significantly impacts electrospray efficiency. Polar solvents such as methanol and acetonitrile are commonly used due to their ability to dissolve analytes and facilitate charge separation (Fu et al., 2020; Tian et al., 2022). The addition of volatile modifiers like formic acid further enhances ion desolation and signal intensity in positive-ion mode. However, solvent conductivity must also be considered as highly conductive solutions can alter the electrospray mechanism, sometimes leading to multiple spraying modes or unstable ion currents (Giusti and Fredrich, 2024b; Takeno et al., 2024). Therefore, optimizing solvent composition is essential for achieving consistent and sensitive ESI performance.

Without further ado, the impact of emitter design and nozzle geometry from the physical design of the electrospray emitter is another critical factor influencing performance (Arai, 2012). Traditional blunt-tip needles frequently demonstrate inconsistent spraying behavior, while tapered capillaries and microfabricated emitters offer enhanced stability and uniformity in electrospray, attributed to improved electric field distribution (Jahan et al., 2021b; Mosa et al., 2023). The emitter material influences both durability and electrochemical reactions at the liquid-metal interface. Stainless steel emitters exhibit robustness but can trigger redox reactions, whereas fused silica emitters reduce undesirable chemical interactions (Chen et al., 2021; Thirukumaran et al., 2021). Advances in emitter technology, such as modular integrated emitters and porous materials, increase the stability and sensitivity of ESI for many applications.

External factors such as temperature, humidity, and gas velocity can significantly impact the effectiveness of electrospray. Variations in the environment have an impact on the pace at which droplets evaporate, which alters the efficiency of ion production (Qian and Liu, 2022; Rovelli et al., 2020; Zhang et al., 2022). Therefore, to ensure repeatability, controlled settings are often used in quantitative research. Long-term operational stability is a challenge, as emitter clogging, solvent depletion, and voltage drift may eventually reduce performance (Gan et al., 2015; Huang et al., 2023; Lin et al., 2015). Automated technologies, like self-cleaning processes and real-time monitoring, are addressing these issues, especially in high-throughput facilities. A complicated combination of electrical, mechanical, and chemical factors determines how effective electrospray ionisation devices are.

According to earlier research, achieving stable and effective ionisation requires modifying the voltage, flow rate, solvent composition, and emitter design. Furthermore, long-term dependability depends on environmental management and system resilience. Future improvements that aim at smart electrospray systems, like adjusting settings automatically and increasing durability, could make ESI better for analytical research.

2.4 Limitations of Electrospray Observed in Previous Work

Electrospray systems have been extensively investigated for their applications in propulsion, thin-film deposition, and analytical chemistry (Namoos and Jasim, 2024). Prior research has identified several significant limitations that impact their stability and performance. The challenges include unpredictable jet behavior at high densities, problems keeping the cone stable with different dielectric fluids, and poor control over the external electrostatic field.

a) Inconsistent Jet Behavior at Higher Densities

The operation of electrospray systems faces significant challenges, notably the instability of jet formation, especially at higher fluid densities. As fluid density increases, it gets harder to keep a stable balance between the different forces, like electrostatic, viscous, and surface tension (Gan et al., 2018, 2016; Zhang et al., 2015). This delicate equilibrium is critical to preserving a consistent and continuous Taylor cone and jet. When the system is disturbed, it causes the jet to break up in an uneven way, leading to droplets of different sizes that affect the accuracy of the spray (Agrawal, 2013; Banerjee and Mazumdar, 2012).

Thicker fluids cause smaller, extra droplets to form next to the main spray, which makes it harder to get an even spray pattern. Increased fluid density leads to unpredictable mode transitions. The spray may transition from the preferred cone-jet mode to spindle or multi-jet configurations, resulting in additional inconsistencies in system performance (Chang and Urban, 2024). Instabilities are particularly harmful in high-precision applications like electric propulsion, where precise control of droplet size and velocity is essential for optimal performance and efficiency (Johari et al., 2022; Zuo et al., 2022).

b) Difficulty Maintaining Cone Stability Across Different Dielectric Fluids

The dielectric properties of the working fluid, including conductivity, viscosity, and surface tension, significantly influence the efficiency and reliability of electrospray systems. The properties directly impact how stable and shaped the Taylor cone is, which is essential for creating a steady jet in electrospray processes (Divvela and Joo, 2020; Franco et al., 2021). Fluids exhibiting low electrical conductivity present considerable challenges, necessitating disproportionately high applied voltages to initiate cone-jet formation. The elevated voltage raises operational energy requirements and increases the risk of electrical breakdown, which may harm the system and present safety issues (Ju and Maruta, 2011; Sosnowski and Hopfgartner, 2020; Zakaria et al., 2020). On the other hand, fluids that conduct electricity well quickly lose their charge, which disrupts the electric field at the surface of the fluid and causes the Taylor cones to collapse, making the spray less consistent (Wan and Zhao, 2020). Fluid thickness greatly affects how jets behave thick liquids resist changing shape when an electric force is applied, causing a slow start to the jet and a breakup pattern with thick strands instead of small droplets (Faraji et al., 2017). This phenomenon markedly decreases atomization efficiency and precision (Nekrasov et al., 2017; Oh and Kim, 2007; Yamaguchi, 2013).

The limitation of a single electrospray configuration to handle diverse fluid properties presents a major obstacle to broadening the technique's applicability across various fields. (Kavadiya and Biswas, 2018; Shimokuri et al., 2017; Xie and Zhu, 2020) point out that because electrospray doesn't work the same way for all types of fluids, it can't easily be used in systems that need to handle different fluids for things like medical delivery, making materials, or checking the environment. Addressing these limitations related to fluid properties is essential for improving the versatility and adaptability of electrospray systems.

c) Requirement for Enhanced Regulation of External Electrostatic Field

The stability and performance of electrospray emission are greatly affected by how the electrostatic field is set up, particularly the placement and design of the extractor electrode, also known as the ion ring. The electrostatic field affects the forces on the fluid at the tip of the emitter, which in turn affects how stable the Taylor cone is and how evenly the jet is emitted (Takeno et al., 2024; Yang et al., 2020). A small misalignment of the ion ring or extractor electrode can cause an uneven electric field around the fluid's surface. This results in the jet bending, emitting in an incorrect direction, and distributing droplets unevenly, potentially compromising applications that require high precision (Agrawal, 2013).

Furthermore, a non-uniform electric field might induce irregular charge buildup on the liquid's surface, disturbing the balance required for sustaining a stable cone-jet mode. This instability results in inconsistent droplet production, influencing both the size distribution and the directionality of the spray (Abdul Munir et al., 2018b; Jweeg et al., 2024; Pennisi, 2012). A further drawback is the absence of dynamic flexibility in several conventional electrospray configurations. Users cannot easily change the spray settings to match changing conditions or fluid properties because they can't actively move the electrodes or adjust the voltages as needed.

Research by Kang et al. (2023) and Qian and Liu (2022) highlights how important it is to position the ion ring correctly, showing that even small mistakes in alignment can completely disrupt the cone-jet mode. This sensitivity highlights the necessity for robust mechanical designs and possibly adaptive control techniques that ensure electrode placement remains within critical limits. Optimizing the electrostatic field design, particularly by meticulous and changeable positioning of the ion ring, is crucial for attaining stable, repeatable, and controlled electrospray functioning.

2.4.1 Ideology and Conceptual Framework for Improvement

Recent improvements in electrospray systems have significantly emphasized the refinement of fluid density ranges to enhance operational stability. The fluid density directly affects the equilibrium between electrostatic forces and surface tension at the emission location, which determines the stability of the Taylor cone and the resulting jet. Researchers have reduced jet instability by controlling the density range of the working fluid, particularly in situations where small changes in fluid properties could otherwise cause erratic spray patterns (Li et al., 2014; Ouyang and Cooks, 2009; Zhou and Biswas, 2021). A new ionisation ring shape has been added to enhance the homogeneity of the electrostatic field, complementing this method. Modifications in the curvature and spatial orientation of the ring around the emitter nozzle have shown the ability to enhance symmetrical field distribution, hence stabilizing cone formation and lowering the threshold voltage necessary for commencing electrospray (S. Wang et al., 2024; Zeng et al., 2020).

In parallel with material and structural optimizations, significant progress has also been made in the realm of diagnostics and measurement techniques for electrospray systems. High-speed imaging technologies now allow researchers to observe jet formation and cone dynamics with high temporal resolution, enabling the detection of transient instabilities and droplet ejection patterns in real time (Kim et al., 2011). Additionally, the integration of phase Doppler anemometry provides quantitative data on droplet size distribution and velocity, which are critical for assessing spray quality (Uhlmann et al., 2025; Yamaguchi, 2013). These diagnostic tools are further enhanced by real-time monitoring systems that support adaptive feedback control. Such systems dynamically modulate operational parameters in response to spray behavior, thereby ensuring consistent droplet emission even under fluctuating environmental or fluid conditions (Huang et al., 2023).

Further improvements in electrospray stability have been realized through the refinement of nozzle and ionisation ring configurations. A newly designed nozzle-ring assembly enables precise spatial alignment and adjustable electrode positioning, which contributes to more accurate control over the electric field gradient across the emission region (Yu et al., 2021). This precise alignment is essential for achieving stable Taylor cone formation, particularly in systems that operate with highly viscous or low-conductivity fluids (Jiang et al., 2023). Moreover, researchers have developed active voltage modulation techniques that adapt the electrical potential applied to the emitter in real time. This approach allows for compensation of fluid property variations such as changes in viscosity or permittivity thereby extending the system's operational range and enhancing its adaptability to a wider range of dielectric liquids (Parhizkar et al., 2017).

Collectively, these advancements have significantly improved the controllability and reliability of electrospray systems. The convergence of optimized fluid parameters, enhanced electrode design, and advanced diagnostics has facilitated the development of more robust emission platforms capable of operating under diverse conditions. As a result, electrospray technology is becoming increasingly viable for high-precision applications across fields such as micro propulsion, nanotechnology, and biomedical engineering, where stable and controllable droplet generation is essential (Caballero-Pérez et al., 2025).

2.4.2 Research Gap and Motivation Current Research

Despite the extensive development in electrospray technology over recent decades, significant gaps remain in the understanding and optimization of Taylor cone behavior, particularly under variable fluid properties and non-uniform electrostatic conditions. Existing studies have primarily focused on conventional symmetrical configurations, assuming ideal field distributions and homogeneous dielectric properties of working fluids (Dong et al., 2023; Kim et al., 2022; Yu et al., 2021). While these assumptions hold under tightly controlled laboratory environments, real-world applications often involve fluctuating fluid densities, changing dielectric constants, and nonlinear electrostatic field effects factors that have been inadequately explored in current literature.

One critical gap lies in the insufficient characterization of how fluid density variation affects Taylor cone stability and jet dynamics across a broader range of operating conditions. Although researchers such as Liu, Cheng and Tang (2023) have proposed improved nozzle and ionisation ring configurations to enhance alignment and field distribution, the interplay between fluid density, surface tension, and electrostatic focusing remains only partially understood (Chiu et al., 2023). Furthermore, the lack of consensus on optimal ionisation ring geometries for diverse electrospray modes (e.g., cone-jet, pulsating, or microdripping) limits the ability to generalize existing models across different engineering applications.

Another overlooked area is the real-time adaptability of electrospray systems under dynamic fluidic or electrical conditions. While advancements in high-speed imaging and diagnostic tools have enabled better visualization of cone-jet transitions (Zuo et al., 2022), relatively few studies have incorporated active control mechanisms such as voltage modulation and feedback systems to adaptively stabilize the spray process (Chen et al., 2021; Chiu et al., 2023). Moreover, the integration of these systems with optimized hardware configurations particularly redesigned ionisation rings that can generate tunable field gradients is still at a preliminary stage, creating a gap between theoretical modelling and practical implementation.

From an application standpoint, there is also a need to explore electrospray performance across various dielectric fluids beyond standard test liquids like ethanol or glycerol. Many industrial applications, such as targeted drug delivery, nanoparticle synthesis, and micro propulsion, involve complex or proprietary fluid mixtures whose properties deviate significantly from those studied in academic experiments (Caballero-Pérez et al., 2025). This mismatch highlights the need for a more robust electrospray system capable of compensating for diverse fluid characteristics while maintaining stability and efficiency.

Motivated by these limitations, the present study aims to systematically investigate the effect of fluid density and ionisation ring geometry on the electrospray process, particularly focusing on the stability and characteristics of Taylor cone formation. This research proposes a novel ionisation ring configuration with adjustable parameters, alongside controlled variation of fluid density, to evaluate their combined effects on cone shape, onset voltage, and jet stability. By incorporating real-time monitoring and active voltage modulation, this study also seeks to establish a more adaptive electrospray model that can function reliably across a range of non-ideal conditions.

Ultimately, the motivation for this research lies in addressing the disconnect between idealized laboratory studies and real-world requirements. The expected outcome is a set of design guidelines and empirical data that enhance our understanding of electrospray performance under varied operating conditions and all these gaps more seen from Table 2.3. These insights are intended to support future developments in high-precision applications where electrospray technology serves as a core component, such as in biomedical engineering, aerospace propulsion, and nanomaterial fabrication.

Table 2.3 Summary of Identified Research Gaps in Electrospray Studies

No	Research gap	Description	Supporting references	Addressed in current study
1. 1	Limited study on fluid density variation	Most electrospray studies assume constant fluid properties, lacking data on how varying density affects cone stability and jet behavior.	Kim, Lee and Park (2022); Martínez-Sánchez et al. (2023)	Investigates cone performance across controlled fluid density ranges.
2.	Inadequate optimization of ionisation ring geometry	Existing designs do not fully explore how ring diameter, curvature, and spacing affect field uniformity and cone formation.	Wang and Feng (2023); Liu, Cheng and Tang (2023)	Proposes a novel ring geometry with adjustable parameters.
3.	Lack of integrated real-time control mechanisms	Few studies integrate high-speed diagnostics with adaptive feedback or voltage modulation to stabilize emission.	Zhao, Chen and Mei (2023); Deng, Zhao and Huang (2023)	Implements active voltage control and real-time feedback using imaging.
4.	Narrow focus on idealized working fluids	Most electrospray work relies on standard test fluids, with little analysis of performance with real-world or complex dielectric liquids.	Martínez-Sánchez, Gamero-Castaño and Lozano (2023)	Tests system performance using fluids of varying dielectric properties.
5.	Disconnection between laboratory results and applied field requirements	Existing models often fail to translate well to real-world electrospray systems used in propulsion, nanotech, or biomedical fields.	Yang, Zhao and Lin (2022); Liu, Cheng and Tang (2023)	Aims to bridge experimental data with practical application scenarios.
6.	Lack of systematic correlation between ring-field configuration and cone dynamics	Few studies quantify the impact of electric field distribution, shaped by electrode geometry, on Taylor cone stability.	Wang and Feng (2023); Kim, Lee and Park (2022)	Quantifies field effects on cone shape and onset voltage systematically.

2.4.3 Summary of Design Evolution and Key Learnings

Early electrospray systems predominantly used single-capillary emitters, which limited throughput and scale. The shift towards multi-nozzle arrays was a major advancement that allowed for higher spray currents, increased deposition rates, and broader applicability in industrial and biomedical domains. These multi-nozzle designs addressed challenges of charge repulsion and droplet uniformity through careful spatial arrangement and voltage control, leading to better spray stability and efficiency (Tang et al., 2021).

A pivotal learning was the control of Taylor cone geometry, which is crucial for achieving stable electrospray. Researchers found that precise modulation of electric field strength, flow rate, and liquid conductivity allowed better predictability and repeatability of cone-jet mode formation. This directly improved spray monodispersed and reduced operational instability in electrospray-based applications such as mass spectrometry and thin film deposition (Li et al., 2014).

Recent studies demonstrated that ring electrode configuration significantly influences electric field focusing and cone stability. The introduction of conical or stepped ring geometries was shown to enhance field uniformity around the spray tip, thereby lowering the voltage required to initiate spraying and improving the electrospray's energy efficiency (Dong et al., 2023).

Key learnings also include the role of dielectric material in preventing electrical breakdown and corona discharge. High-performance materials such as polyether ether ketone (PEEK) and Teflon were adopted to improve safety and longevity of electrospray devices, especially in prolonged operations under high voltage conditions (Kang et al., 2021).

Design evolution moved toward miniaturization, enabling integration of electrospray systems into lab-on-chip and portable devices. Microelectromechanical systems (MEMS)-

based emitters were developed to facilitate compact and low-power configurations suitable for point-of-care diagnostics and atmospheric aerosol research (Zhang et al., 2015).

A recent advancement involved embedding real-time sensing and feedback control mechanisms in electrospray setups. This enabled dynamic tuning of operational parameters such as voltage and flow rate based on live feedback from optical or electrical sensors, which significantly enhanced precision in particle size and spray directionality (Gonzalez-Ramirez et al., 2024).

Understanding mode transitions from dripping to cone-jet to multi-jet modes was crucial for optimizing process windows. Studies mapped these transitions using high-speed imaging and current-voltage characterization, establishing clearer guidelines for desired spray regimes under different fluid and environmental conditions (Jia et al., 2021).

Lastly, the sustainability of electrospray systems has been examined, especially regarding solvent selection and energy usage. Green solvents and bio-based materials are increasingly being used to reduce ecological impact, and innovations in low-voltage operation continue to lower power consumption without compromising spray quality (Uhlmann et al., 2025).

2.5 Spray Pattern Characteristics in Fuel Mixtures

In curtain condition, how spray designs are made greatly affects how well fuel mixes and burns (Franco et al., 2021). The size of the drops, their charge, and how the spray spreads all greatly affect how stable the flame is in electrospray-assisted burning. Research shows that changing the features of an electrospray can alter how it looks, which can then influence how well it burns.

The chemical interactions and varying evaporation rates of water and ethanol in a mixture can lead to several issues. The variations in spray patterns lead to inconsistencies that affect the rate of flame initiation and spread, as indicated by the research. Parameters of the electrospray process, including tip-to-target distance, ring-ionisation size, and applied voltage, can be adjusted to achieve a more uniform distribution of fuel.

A few researchers, found that spray pattern characteristics in fuel mixtures during electrospray processes are determined by factors such as fuel composition, nozzle design, and operational conditions (Gamero-Castaño and Cisquella-Serra, 2021; Huang et al., 2012; Ramshani et al., 2016). Studies demonstrate that incorporating oxygenated fuels, including ethanol and butanol, modifies spray morphology and stability, resulting in unique patterns that can be adjusted for enhanced performance. The Table 2.4 the essential features of spray pattern characteristics in electrospray.

Table 2.4 Past finding for spray pattern

Researcher	Finding	Method Used	Year
Zhen Huang, Jin Xiao, Xinqi Qiao	CO2 improves atomization and creates parabolic-shaped spray. Various factors significantly influence spray characteristics of CO2 fuel.	Instantaneous shadowgraphy and high-speed photography Phase Doppler anemometry (PDA) and LDSA	2012
Zeinab Ramshani, Michael J. Johnson, Massood Z. Atashbar	Broad area spray generated from piezoelectric transformer surface. Spray current non-linear with solution conductivity, minimal surface tension dependence.	High voltage applied to piezoelectric transformer surface. Paper wick delivers liquid to generate spray.	2016
Zhuoying Jiang, Xiong Yu	Effects of controllable parameters on deposition area not reported. Limited studies on droplet dynamics in electrospraying process.	Simplified two-dimensional modeling of droplet dynamics. Experimental validation of simulation results.	2018
Hywel O. Davies, Midhat Talibi, Martin Hyde	GSV technique effectively measures droplet concentration and diameters. Ethanol blends show larger droplet diameters than gasoline.	TSI Global Sizing Velocimetry (GSV) interferometric technique Nd:YAG laser and 4 MP camera for imaging system	2019
Yun Ouedraogo, Erion Gjonaj, Herbert De Gersem	Charge-radius correlations differ from classical scaling law.	Numerical simulation of electrohydrodynamic	2020

Researcher	Finding	Method Used	Year
	Space-charge field builds up during electrospray transients.	atomization in conductive liquids. Coupled multiphase flow equations with electroquasistatic problem.	
Manuel Gamero-Castaño, Albert Cisquella-Serra	Electrosprays produce charged nanodroplets and molecular ions. Time-of-flight and retarding potential techniques measure jet velocity and potential.	Time-of-flight analysis for measuring jet velocity. Retarding potential analysis for assessing jet potential.	2021
Sarah Park, Lin Lei, Darrel D'Souza, Alex Liu, Emran Lallow	Architecting charge landscape improves ESD deposition efficiency. Achieves near 100% efficiency on small targets.	Electrospray deposition (ESD) for coating surfaces. Architecting local "charge landscape" for efficiency.	2022
Yiyu Lu, Yijing Li, Wenchuan Liu	Ethanol addition affects spray deviation under various conditions. High latent heat of evaporation influences droplet behavior and spray dynamics.	Diffused Back Illumination and Phase Doppler Anemometry Internal flow simulations for in-nozzle flow information	2023
Mahdi Bagherian Dehaghi, Mehrzad Shams, Fatemeh Sohan	Stable region for 70% ethanol exceeds 99.9% by 17703%. Stability differences among ethanol-water mixtures are significant.	High-speed imaging to assess electrospray stability. Examination of onset and end voltages across flow rates.	2023
Huidong Zhang, Wenchuan Liu, Yiyu Lu	Oxygenated fuels cause spray pattern shifts and variations. Critical width correlates with ambient pressure and spray characteristics	Diffuse backlight illumination method Phase Doppler anemometry method	2024

2.6 Summary

This chapter reviewed the fundamental principles and recent developments in electrospray technology, with emphasis on Taylor cone formation and the parameters influencing its stability and performance. The Taylor cone, a conical meniscus formed under an electric field, is central to producing uniform, fine droplets in electrospray systems. Its stability depends on a complex interplay between the working fluid's physical properties and the surrounding electric field, which can be shaped by electrode geometry.

Three key parameters were identified for detailed investigation which is ionisation ring diameter (IDIR), ionisation ring position, and fluid density. The ionisation ring is acting as a counter electrode for directly affects the electric field distribution around the Taylor cone. Its diameter determines how concentrated or dispersed the field lines are either smaller diameters can intensify the field, producing sharper cone angles, or larger diameters promote broader and potentially more stable spray patterns. The position of the ring relative to the nozzle tip controls how the electric field interacts with the emerging liquid jet, influencing the transition between electrospray modes and the stability of the cone-jet. Fine-tuning both parameters is essential for optimising spray uniformity, and cone stability.

Density is equally important because it governs the inertial and viscous forces within the fluid, affecting the onset voltage required for cone formation and the stability of the jet. This study focuses on three representative fluids which is water, a high-density, high-surface-tension liquid, represents challenging conditions for cone stability due to its resistance to deformation. Meanwhile, for the ethanol, with intermediate density and low surface tension, is easier to ionise and forms cones at lower voltages, making it a widely studied reference fluid and n-Heptane, a low-density, low-conductivity hydrocarbon, presents unique challenges for stable spraying but is relevant for related applications. By selecting fluids with contrasting densities and physical properties, the study aims to capture a broad spread of electrospray behaviours. This approach allows the combined effects of density and ionisation ring configuration to be systematically explored, filling a notable gap in existing research that often treats these factors in isolation.

In conclusion, the literature demonstrates that while many studies have examined either fluid properties or electrode geometry independently, few have addressed their combined influence on Taylor cone stability particularly for fluids of varied densities relevant to practical applications. This gap forms the central motivation for the current research, which seeks to optimise electrospray performance through controlled variation of ionisation ring geometry and fluid density.

CHAPTER 3

METHODOLOGY

3.1 Introduction

This chapter presents the detailed description of the experimental setup and the step-by-step procedures undertaken to achieve the objective of the study. The study focuses on investigating the influence of electrospray parameters on the formation and behaviour of the cone jet. Specifically, the study seeks to determine the optimal parameter for generating a stable cone jet from working fluid of water, ethanol and mixtures of ethanol and heptane. The findings are expected to provide valuable insights for vast applications that need precision in droplet size and distribution.

The outline of this chapter is set as follows; Section 3.2 presents the project flowcharts are described beginning with the identifications of the problem statement and continuing through to the conclusion of the study. Section 3.3 describe the experimental setup along with the equipment used in the experiment that is listed down along with its descriptions. Here the details about the electrospray parameters, namely the size, distance and position of the ionization ring (IR) will be explained and discussed in detail. Section 3.4 further elaborates on the equipment, their specifications, and the parameters utilized for the electrospray setup. Section 3.5 describes the working fluid that furnishes supplementary information on other equipment specifications that bolster the overall electrospray setup. Section 3.6 focuses on the analysis of the experimental results.

3.2 Project Flow Chart

Figure 3.1 shown flow chart of the development of a project from conception to completion. To achieve all of the research goals, from literature review to hardware preparation of the experiment, data collection and finally the results are being analyse.

Based on the flowchart in Figure 3.1, the flowchart outlines a systematic approach for analyzing and improving the electrospray technology, highlighting the achievement of a stable Taylor cone, the study involves much of research from its inception to the present. A comprehensive analysis of recent research is conducted in order to understand electrospray ionization, the impact of charged droplets, and the significance of factors such as voltage, charge distribution, and fuel atomization. The procedure starts with an analysis of the development of the electrospray technology, followed by the formulation of the problem description and research objectives. It then analyzes suitable parameters that enhance electrospray stability, researchers are looking at key factors such as the size of the ionization ring, the distance from the tip to the target, and the flow rate of the fuel to understand their impact on Taylor cone formations. In this stage the identification of the crucial and significant parameters to the formations of the Taylor cone is identified. Followed by the design and execution of an experimental equipment to assess the method. Initial studies focus on investigating the impact of diverse parameters on the characteristics of the Taylor cone, namely the cone angle and jet stability. Based on the parameter identified for the electrospray, a test rig is developed and an experimental setup is prepared for the electrospray based on the identified parameters. The setup involves careful placing of the electrodes, control of the voltage, and improving the spray pattern to make sure the droplets spread evenly. By improving the design of the electrospray nozzle and fine-tuning the voltage used, the experiment makes sure that the spray pattern of the electrospray can be achieved. Before the experimental setup is run a through checks is done on the electrospray device's functionality.

This involves testing the camera, flowrates, voltage, and positioning the nozzle. If the technique doesn't work as expected, changes are made by looking back at the experiment setup and adjusting the electrospray details. This step-by-step method helps make ongoing changes by fixing any problems with how droplets spread, charge buildup, or even burning.

Following successful functional testing, the next step involves the data collection to achieved objectives 1 which is the parameter that influences the Taylor cone characteristics. This involves, finding the best positions for the electrodes and ionization rings, and making sure that electrospray works well with current solution utilized. Now that the basic structure is set, we make improvements by changing electrospray settings to better distribute charge, speed up droplet evaporation, and improve burning efficiency. The almost similar step is repeated second time for the density variations of the liquid to achieved the objective 2.

Informed by these findings, appropriate working fluids such as water, ethanol, and ethanol and n-heptane mixtures are chosen for further testing. Subsequent studies investigate the impact of fluid density modifications and ionization ring parameters on cone formation and jet dynamics. The findings are then analyzed to discern patterns and correlations among density, ring configuration, and cone properties. The study ultimately closes by identifying the ideal fluid density and ionization ring parameters required for the formation of a stable Taylor cone, thus achieving the research purpose.

.

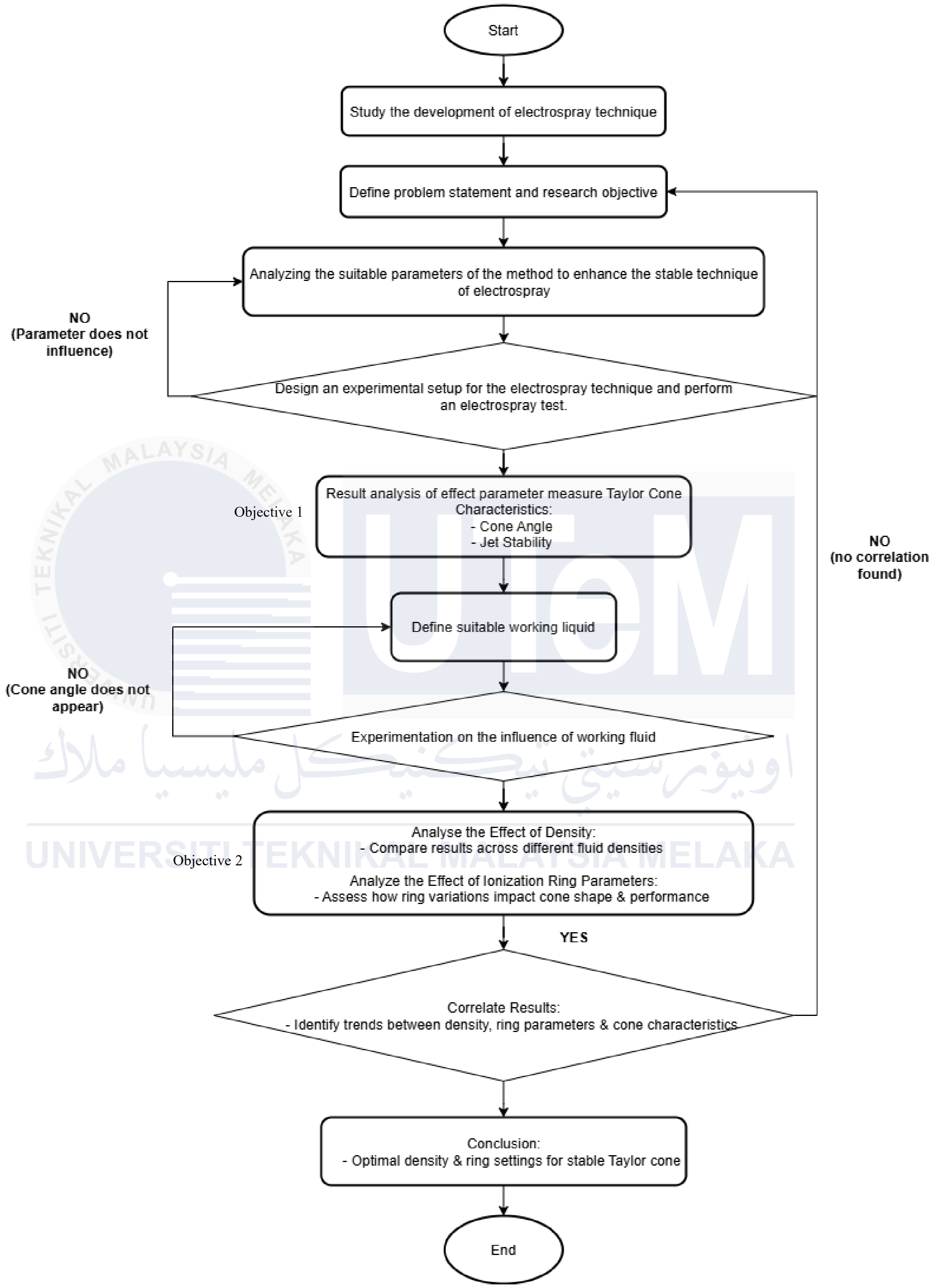

Figure 3.1 Project flow chart

3.3 Experimental Setup

The electrospray system is a specialized device that generates a fine spray of charged droplets, commonly used in mass spectrometry, nanoparticle generation, and fuel atomization. The basic setup of an electrospray device consists of a nozzle, a high-voltage source, and electrodes strategically positioned to control the spray.

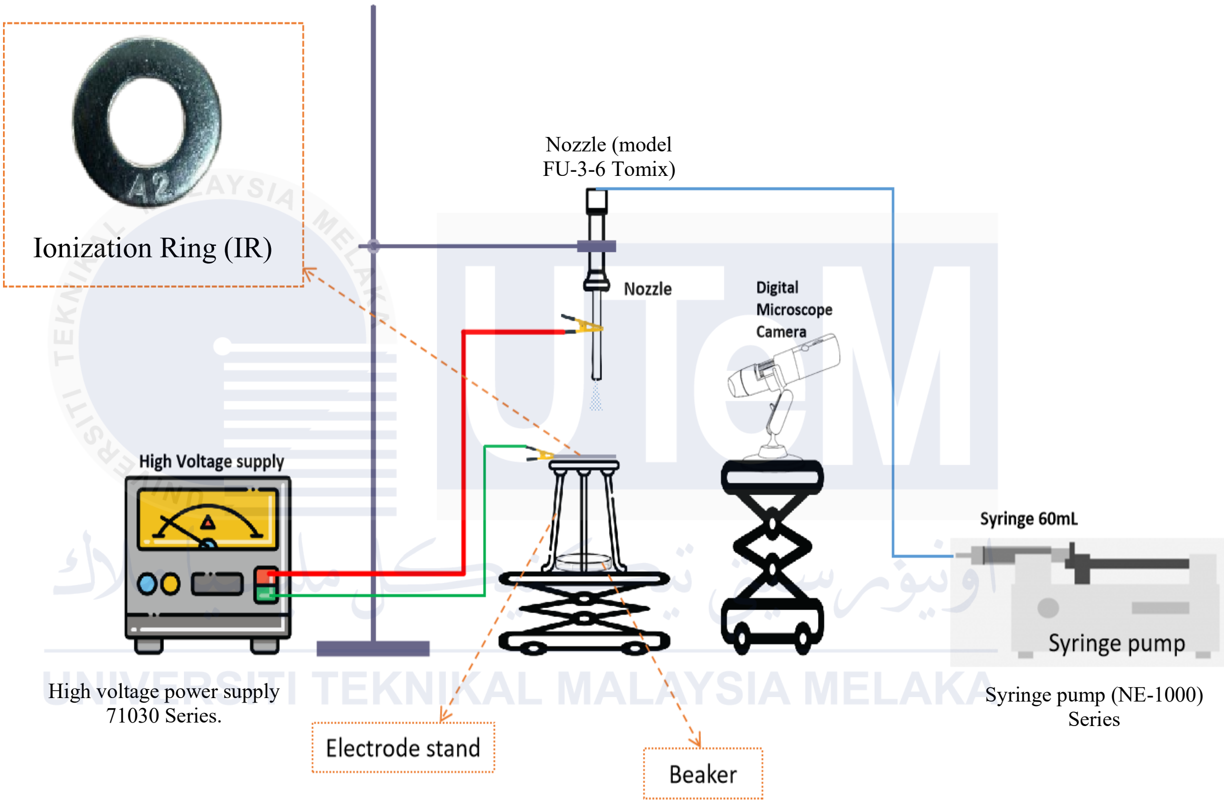

Figure 3.2 Schematic experimental setup

A schematic diagram of the experimental setup is illustrated in Figure 3.2. The apparatus features a high-voltage power supply (71030 Series), capable of generating a direct current (DC) electric field with output voltages ranging from 0 to 10 kV and a maximum output current of 3.0 mA, developed by Genvolt. In this setup, a syringe pump (NE-1000 Series) is utilized to regulate the flow rates of the liquid being sprayed. To prepare the system, the desired solution is loaded into a 60 mL syringe with an inside diameter of 29.7 mm. The syringe pump is designed to operate with a 12 VDC power supply and can achieve infusion rates up to a maximum of 35.33 mL/min. A standard nozzle (model FU-3-6 Tomix) is connected at the output of the syringe. This nozzle has a gauge size of 20 G, with an outer diameter of 0.88 mm and an inner diameter of 0.55 mm, along with a nozzle length of 80 mm. The positioning of the ionisation ring (IR) detector is crucial, it is set downstream from the nozzle tip at a carefully defined distance to allow efficient droplet desolation and ionisation processes to occur.

Additionally, the experimental design includes a ring electrode referred as ionisation ring that is linked to the ground terminal of the power supply, thus establishing the essential electric field required for effective electrospray ionisation. This arrangement facilitates the controlled generation of charged droplets, which are pivotal for subsequent analysis and experimentation.

Electrospray is a technique that utilizes a high voltage applied to a liquid flowing through a capillary. The high voltage applied to the liquid is thus charges the liquid into negative charge. As widely known to be discharge, the liquid with a negative charge is eager to be grounded or jump to positive charge electrode. This kind of phenomenon experience by the liquid generate a cone line shape at the tip of the nozzle which known as the Taylor cone. At the end of the Taylor cone, a spray pattern is observed which is a fine aerosol is observed. When the electric field overcomes the liquid's surface tension, a Taylor cone forms at the capillary tip, ejecting a jet that breaks into small, charged droplets. As the solvent evaporates, the droplets shrink and undergo Coulombic fission, eventually producing gas-phase ions

3.4 Hardware Equipment

The hardware equipment for the technique is made up of the following components, which are measured the angle using AutoCAD software. Furthermore, this design to monitors the effect of various ionisation ring and the effect of fluid density. This section contains a list of the hardware that was used to measure the parameter.

3.4.1 High-Voltage DC Power Supply

The 71030 Series High Voltage Power Supply from Genvolt. It is designed for applications that require accurate voltage management and reliable power delivery. This material is widely used in scientific research, industrial applications, medical equipment, and electrospray systems due to its excellent voltage stability, efficiency, and dependability.

Superior voltage control technology gives the 71030 Series change high-voltage output from kV to hundreds of kV. Appendix D (I) tabulated the specification of the 71030 Series High Voltage Power Supply from Genvolt. For sensitive electronics, the low ripple and noise architecture provides clean, steady power. Precision digital controls, over-voltage safety, current limitations, and overheating shutoff are included. These safeguard operations and equipment.

3.4.2 Syringe Pump System

The NE-1000 Syringe Pump functions as a high-precision fluid delivery system, suitable for use in laboratory and industrial environments. The system accommodates multiple syringe sizes, with a maximum capacity of 60 mL, thereby providing flexibility for managing various fluid volumes in accordance with experimental or process specifications. This programmable single-syringe pump delivers a steady and continuous liquid flow, which is critical for maintaining stable spray properties during the electrospray process.

The pump can accommodate syringes with capacities up to 60 mL and flow rates ranging from minimum flow rates of 0.73 µL/hr with using a 1 mL syringe and a maximum flow rates of 2120 mL/hr with using a 60 mL syringe. The extensive operational range enables utilization in applications that necessitate very slow and precise fluid delivery, in addition to those that require a relatively high-speed infusion or withdrawal. The details specifications of the syringe pump are tabulated in Appendix D (II). This wide range of flow rate control is critical for maintaining stable electrospray conditions since fluctuations in liquid supply can have a considerable impact on spray properties, Taylor cone formation, and overall flame stability. The current investigation adjusted the syringe pump to a consistent flow rate of ±0.1 mL/min to ensure consistent liquid dispersion via the G20 needle throughout the electrospray procedure. Additionally, RS-232 interface included in the NE-1000 also enables external control and automation, hence improving uniformity in electrospray research.

Furthermore, its non-volatile memory stores important operating parameters, decreasing any inconsistencies between trials. The fine control given by this syringe pump was critical in the study of electrospray modes, notably in determining the effects of voltage and ionisation ring location on Taylor cone stability and spray pattern dynamics. The syringe pump reduced experimental variability by supplying a consistent and controlled flow, allowing for a more precise investigation of the electrospray-assisted combustion process and its implications for flame stabilization in microscale energy systems.

3.4.3 Metallic Capillary Nozzles - Nozzle spray gun with nozzle FU-3-6

The FU-3-6 nozzle spray as shown in Figure 3.3 cannon features a precision-engineered spraying mechanism for regulated fluid atomization, making it perfect for uses such as fuel injection, electrospray-assisted combustion, industrial coating, and biomedical misting systems (Emi Corporation, 2025). This nozzle is great at producing fine mist drops that spread evenly with the right droplet size, helping to mix fuel and air effectively. FU-3-6 sprays are directed by a precision nozzle valve. This ensures consistent drops and sprays. Stainless steel or rust-proof elements make the construction sturdy and chemical- and heat-resistant. Different industries can use the nozzle's cone, fan, and jet spray patterns.

The FU-3-6 nozzle spray gun controls liquid flow using a nozzle valve. This valve controls droplet size and speed. The pressure forces liquid into the opening chamber. The nozzle valve is carefully adjusted to vary flow rate and spray pattern. In the schematic of the nozzle spray gun, the valve responsible for controlling droplet size and spray speed is located at the top central section of the assembly, where the adjustment knob is positioned. This valve regulates the flow of liquid by varying the pressure within the opening chamber, thereby determining the rate at which the liquid exits through the nozzle. By carefully adjusting this nozzle valve, the operator can fine-tune the liquid flow rate and consequently modify the spray pattern, enabling precise control over droplet formation and distribution to achieve the desired atomisation effect. Shear forces separate the liquid into small, even drops as it travels through the tiny orifice, which spreads out regulated. This technology improves how medicine is delivered in aerosol form, provides better coating uses, and helps fuel burn more effectively by breaking liquids into fine droplets. Appendix D (III) tabulated the specification of the nozzle.

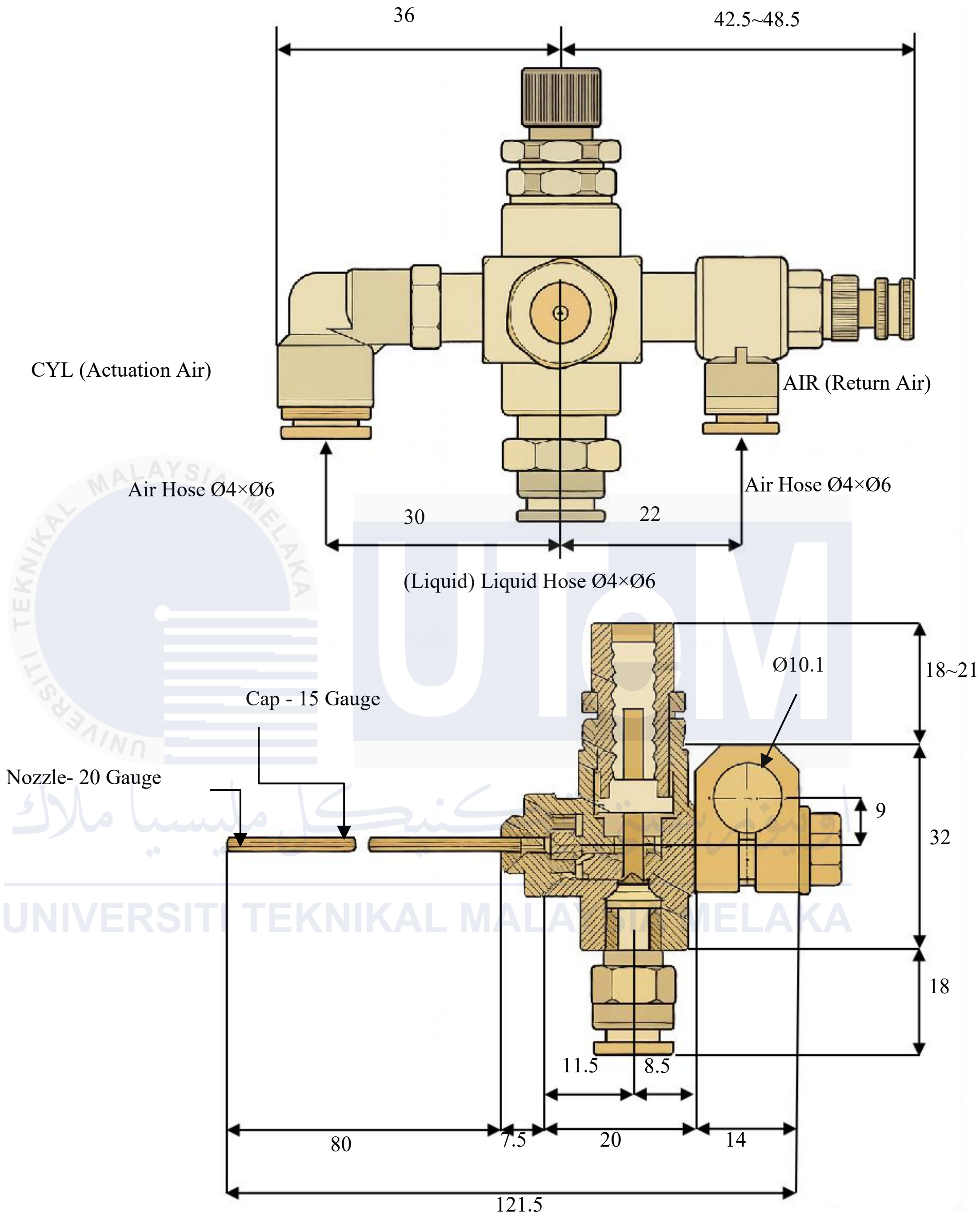

Figure 3.3 Schematic of Nozzle spray gun (Emi Corporation, 2025)

3.4.4 Imaging System

To record the creation of the Taylor cone, the U500X type digital microscope camera is used as shown in Figure 3.4. Both the video and picture resolutions of the microscope camera are rather high, measuring in at 0.3 Megapixels and 640 x 480 pixels per inch, respectively. These cameras have high-resolution sensors that can show the electrospray production and the movement of the Taylor cone. in addition. The camera's 15 mm to 40 mm focal range allows for good recording of bead shapes and spread sizes. In addition, the brightness, which is defined as the number of picture flashes on the screen per second to create the appearance of genuine movement, is 600 lux, and the frame rate is 30 fps. The electrospray needle and the region where the Taylor cone emerges are good examples of where it needs to focus.

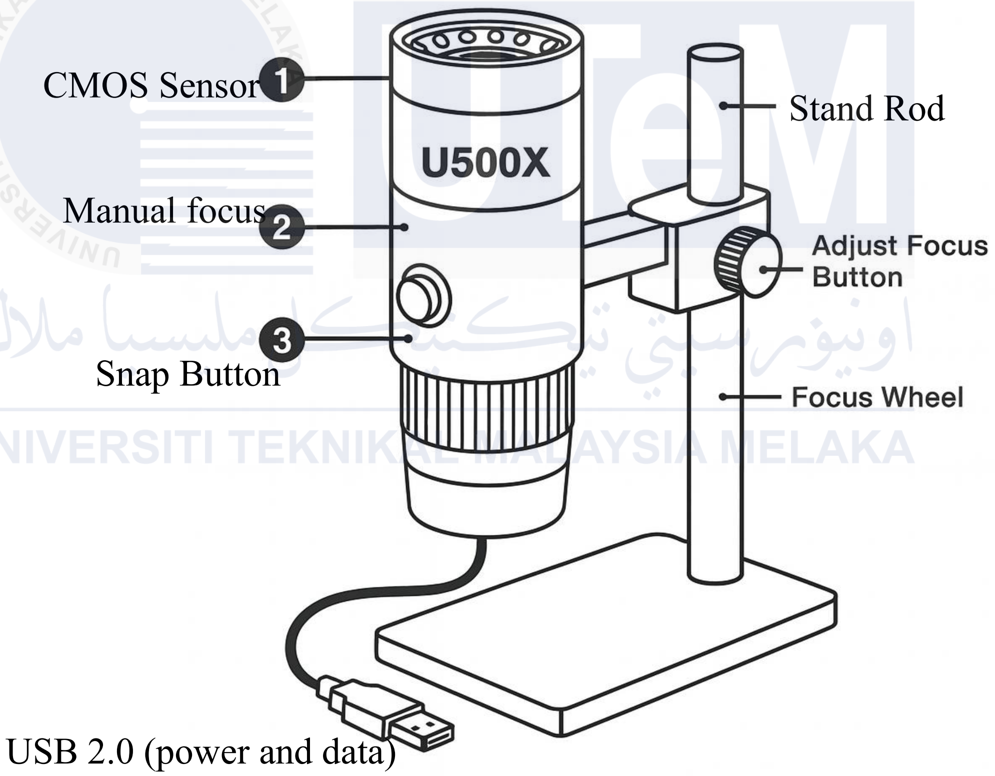

Figure 3.4 Schematic diagram digital microscope camera

As the camera captures delayed images and videos under various experimental settings, tracking its development becomes easy. Prior to the start of the trial, a thorough positioning and calibration process is required to ensure accurate imaging and evaluation. In order to provide the best possible data gathering during the alignment operation, it is necessary to know both the cardinal location of the electrospray needle and the visible zone in the camera's field of vision.

3.4.5 Parameters: Voltage Influence and Charge Generation

Ground of the power source is linked to a vital component of the electrospray system, the ring electrode. This arrangement produces the required electric field, which helps liquid droplets to be under control ionized. Direct behind the needle tip, the infrared (IR) helps charge transfer and improves droplets drying efficiency.

Starting the electrospray process, the power source has turned on; the voltage is adjusted between 0 kV and 10 kV. Initiated to run a consistent 0.10 mL per minute via the needle, the syringe pump. The ionization ring can be adjusted in both position and size, facilitating the understanding of its effects on spray stability and the formation of the Taylor cone.

During the study, the power source settings, the ionization ring's size, and the needle's position were changed. The interplay of these components regarding the homogeneity of the spray, is observed in this work.

3.4.6 Parameters: Influence of Ionisation Ring (IR)

The ionization ring (IR) plays a critical role in the operation of the electrospray setup during the spray's motion. The primary function is to regulate and enhance the distribution of the electric field during the discharge process. The proximity of the Taylor cone to the aperture or needle is critical for ensuring an even liquid flow and maintaining the stability of the cone. This configuration enhances the uniformity and intensity of the electric field. This improved field design enhances the stability and accuracy of the spray, facilitating better control over the landing and movement of collectors and particles.

Ionization ring (IR)s with internal diameters (ID) of 10.3, 15.3, and 21.2 millimetres (mm) and the thickness diameter is 1.9 millimetres (mm) were used to investigate the impact of the opening size on the strength of the electric field, the behaviours of the jet, and the discharge pattern as shown in the Figure 3.5. The dimensions of the ionization ring (IR) influence the convergence of the electric field surrounding the orifice, subsequently impacting the movement of the particle. The ionization ring (IR) plays a critical role in electrospray technology, enabling precise control over various components.

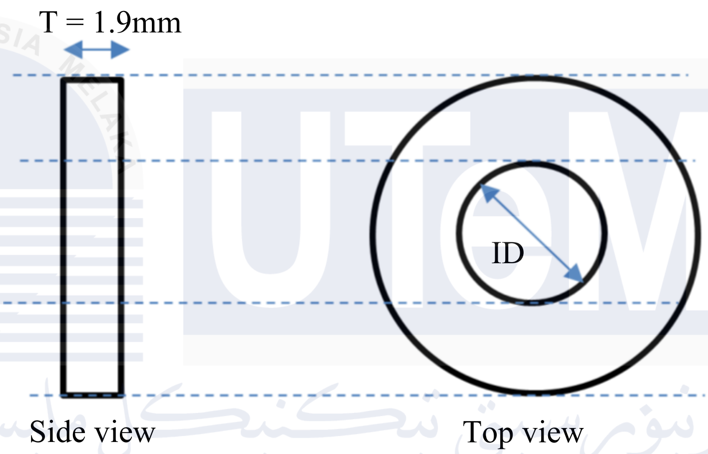

Figure 3.5 Ionisation Ring (IR)

3.4.7 Effect of Nozzle Position on Electrospray Stability

Another crucial consideration investigated in this study is the precise location of the needle tip concerning the ionisation ring (IR). Taylor cone formation, durability, and stability depend mostly on the position of the needle. Based on literature it is found that the position of ionisation rings influence significantly the spray characteristics of the Taylor cone (Barreto and Hernandez-Rivera, 2022b; Faraji et al., 2017). Thus, in these investigations two position of needle are being consider which represented as position A and position B. Figure 3.6 shows that two different needle tip locations are being studied:

- Position A: The tip of the needle is located above the ionisation ring (IR).
- Position B: The needle tip is located beyond the ionisation ring (IR).

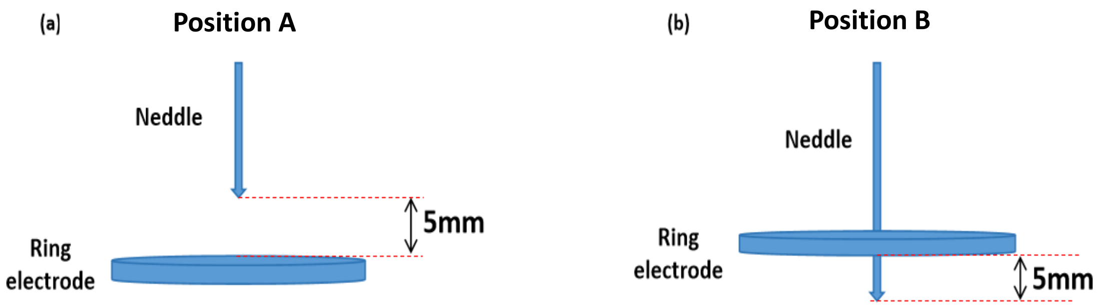

Figure 3.6 Schematic positioning needle tip to ionisation ring (a) position A - above ionisation ring (b) position B - passes ionisation ring

This study indicates Position A as the primary configuration for experimental investigations related to second objective for this research, which aims to establish the fundamental relationship between working fluid density and Taylor cone characteristics. The justification for selecting Position A, with the needle tip located 5 mm above the ionisation ring, lies in its ability to ensure a more uniform and stable electric field distribution at the nozzle outlet. This configuration reduces the direct disturbance of the liquid meniscus by the ionisation ring, allowing the Taylor cone to develop under regulated electrohydrodynamic forces instead of being excessively affected by geometric limitations. The stability of the system is essential when analysing fluids with differing densities, such as water, ethanol, and ethanol and n-heptane mixtures. This stability guarantees that variations in cone angle, jet initiation, or discharge behaviour are primarily due to the inherent physical properties of the fluid, rather than external artifacts related to the electrode configuration. Position A provides the most dependable experimental framework for fulfilling the aims of this research.

In contrast, Position B, where the needle tip protrudes beyond the plane of the ionisation ring, results in a heightened concentration of the localised field and increased distortion at the needle–ring interface. This arrangement may improve charge injection and accelerate jet initiation; however, it also raises the risk of unstable spray modes and premature jet disruption. In this investigation, such effects are undesirable as they complicate the systematic evaluation of fluid density's role. Position B was included in the preliminary analysis to serve as a comparative reference and to illustrate the impact of needle–electrode alignment on spray behaviour. The comparison of these two positions draws attention to the importance of electrode geometry in electrospray stability and establishes a solid framework for isolating the effects of working fluid density on Taylor cone formation.

3.5 Working Fluid

3.5.1 Specification of Liquid

The experimental work in this study involved the use of three primary liquid components which are ultrapure deionized water, absolute ethanol, and n-heptane. These liquids were selected based on their relevance to droplet formation, spray characteristics, and homogeneity behaviours commonly studied in electrospray and fluid atomization research. Absolute ethanol (C_2H_5OH) of ≥ 99.8% purity, while n-heptane (C_7H_{16}) of ≥ 99% purity.

The selection of ethanol and n-heptane allowed for investigation of a wide polarity spread, given ethanol’s polar protic nature and n-heptane’s non-polar hydrocarbon characteristics. Water was included as a control substance due to its unique polar properties and high surface tension. The properties of each fluid such as volatility, polarity, and viscosity are play a critical role in determining the behaviour of the electrospray jet and were therefore considered during experimental design.

3.5.2 Mixing Ratios and Composition

Electrospray Ionisation (ESI) involves a relationship between a liquid’s density and the required charge current, which is influenced by physical properties including viscosity, surface tension, and electrical conductivity. Low-density liquids with high electrical conductivity, low surface tension, and low viscosity require a lower charge current, as droplets are smaller and more easily charged. Conversely, low-density liquids with low electrical conductivity or high surface tension require a higher charge current to promote ionisation and sustain the spray. This relationship is based on the natural physical properties of the liquid. While water and ethanol can each produce a stable cone-jet independently, n-heptane cannot due to its very low electrical conductivity, non-polar nature, and weak inertial forces, which make it inherently unsuitable for electrospray. Since electrospray requires a conductive medium to generate ions effectively, pure n-heptane demands a much higher charge current for ionisation, and in many cases, may fail to form a stable spray or produce a detectable signal. In laboratory practice, non-polar, non-conductive liquids such as n-heptane are rarely used alone in ESI, instead, they are commonly mixed with polar solvents for example with methanol, acetonitrile, or water to enhance conductivity and spray stability.

To examine the effects of fluid composition on spray characteristics and fluid properties, a series of binary and pure liquid samples were prepared. The binary mixtures consisted of ethanol and n-heptane in three volumetric ratios:

- 30% ethanol: 70% n-heptane
- 20% ethanol: 80% n-heptane
- 10% ethanol: 90% n-heptane

In addition, pure ethanol (100%) and pure water (100%) were tested as reference samples. These specific ratios were selected to provide a gradient of decreasing ethanol concentration while increasing the proportion of n-heptane. This systematic variation enabled the analysis of how ethanol's polar nature influences key parameters such as density, surface tension, and viscosity when diluted in a non-polar medium. The use of pure water served as a comparative benchmark due to its distinctly different physicochemical characteristics, including high density, high surface tension, and strong conductivity. By introducing ethanol into n-heptane, the mixture's conductivity is improved while retaining n-heptane's high energy content, enabling stable cone-jet formation and making the fuel blend more suitable for electrospray-based combustion applications.

3.6 Data Collection and Analysis

The angle of the Taylor cones is one of the most crucial parameters in determining whether an electrospray experiment is successful. During this experiment, the angles of the Taylor cone that are produced by the setup will be documented and analysed using the reliable computer-aided design program known as AutoCAD. The electrospray Taylor cones are first taken using a digital microscope camera. After the images have been taken, they must be uploaded to the AutoCAD program. The bead angles that are investigated in depth utilizing AutoCAD's rich measurement and annotation tools are shown in Figure 3.7.

A line is drawn approximately on both sides of the needle moving toward the tip of the needle. Then, the end of the line becomes the reference point to draw straight lines along the electrospray Taylor cone. To guarantee accurate measurement of the orientation of each bead, these lines are precisely aligned with its longitudinal axis. Next, an angle measurement tool in AutoCAD is used to figure out the angle between the line drawn along the Taylor cone's as shown in Figure 3.7. This capability allows you to precisely estimate bead angles, which is critical when analysing the stability and direction of the electrospray jet. The peak angle in this context refers to the measured angular divergence formed at the apex of the Taylor cone, which is the sharpest point where the liquid meniscus transitions into a jet.

This angle is taken from the reference point at the tip of the needle, extending symmetrically along both sides of the cone, as illustrated in Figure 3.7. By clearly defining the peak angle, the measurement provides an objective parameter to evaluate the sharpness and stability of the Taylor cone, which directly influences the onset of jet emission and spray uniformity. A smaller peak angle typically signifies a more stable cone-jet mode, while a larger angle indicates weaker confinement of the electrostatic forces, potentially leading to instability in the electrospray process. Thus, clarifying this measurement ensures that the relationship between applied parameters and cone formation can be interpreted with higher precision, which directly supports the study's objective of establishing the fundamental relationship between working fluid density and Taylor cone characteristics.

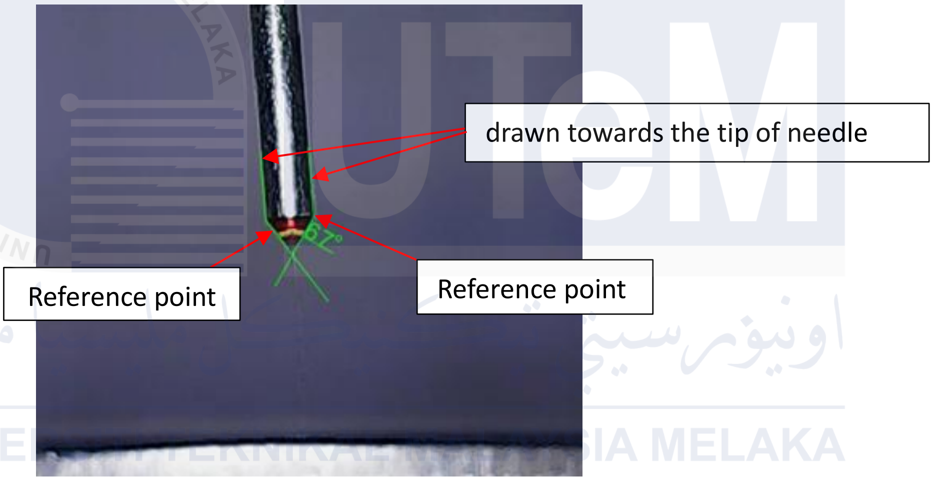

Figure 3.7 Positioning of angle that has been measured

CHAPTER 4

RESULT AND DISCUSSION

4.1 Introduction

This chapter presents the experimental and analytical data about the characteristics of Taylor cone under variations in electrospray parameters. The size, axial position, and applied voltage of the Ionisation Diameter Ring (IDIR) are examined to determine their influence on the formation and stability of the cone-jet mode. In electrospray, these parameters govern the electric field distribution, which influences atomization and jet dynamics.

This study highlights the significance of fluidic physical parameters, especially fluid density, in the formation of Taylor cones, alongside geometric and electrical considerations. The secondary objective of this study is to examine the relationship between fluid density and Taylor cone characteristics to comprehend the influence of fluid inertia on electrospray dynamics. This chapter analyses Taylor cones across various parameters and fluid densities via visual observation. The visual observations, measurement data, and theoretical analyses to ascertain the ideal operating parameters for stable cone-jet formation and enhanced atomization.

The chapter is organized as follows: Section 4.2 examines electrospray parameters, and the spray patterns observed. Section 4.3 Elaborates on liquid variations effects towards Taylor cone behaviour. Finally, Section 4.4 summarizes the important results and discusses the implications for electrospray technique.

4.2 Analysis of Electrospray Parameters and Spray Pattern (Objective 1)

4.2.1 The Electrospray Mode

The result of electrospray modes is the observation of the Taylor cones developed at the tip of the needle which is generated by the variable supplied of voltage and flow rate. It is found out from the observations of the Taylor cone that the electrospray modes can be divided into five basic modes as shown in Figure 4.1. The electrospray modes are referred to as (1) Dripping mode, (2) Spindle mode, (3) Cone-Jet Mode, (4) Tilted Jet Mode and (5) Flying Current. The same kind of electrospray modes of Taylor cone are also observed in past studies as in reference (Kim et al., 2022).

All of these electrospray modes are found in all of our experimental results regardless of the working fluid utilized and position of the needle (refer to position A and position B in the methodology section). The details regarding each electrospray mode are explained as follows: -

a) Dripping Mode (DM): At low voltages, the electric field has little impact on the liquid, thus droplets form mostly owing to gravity forces. This mode is distinguished by a steady drop size that corresponds to the nozzle diameter.

b) Spindle Mode (SM): As the voltage rises, a partial cone formation occurs, with a jet emerging from the nozzle and creating uniform droplets at regular intervals. More constant droplet generation follows from the more ordered spindle mode than from the dripping mode.

c) Cone Jet Mode (CJ): A stable Taylor cone forms at a crucial voltage threshold to generate a fine liquid jet in Taylor Cone or Cone Jet Mode (CJ). Offering continuous droplet dispersion, this is the steadiest electrospray mode.

d) Tilted Jet (TJ): Beyond the stable Taylor cone regime, the jet deviates to one side owing to the electric field, producing an unstable and asymmetrical spray pattern.

e) Flying Current (FC): At extremely high voltages (about 10 kV), the electric field is strong enough to cause corona discharge. This produces ionisation in the surrounding medium, producing a flying stream of charged particles rather than a structured liquid spray.

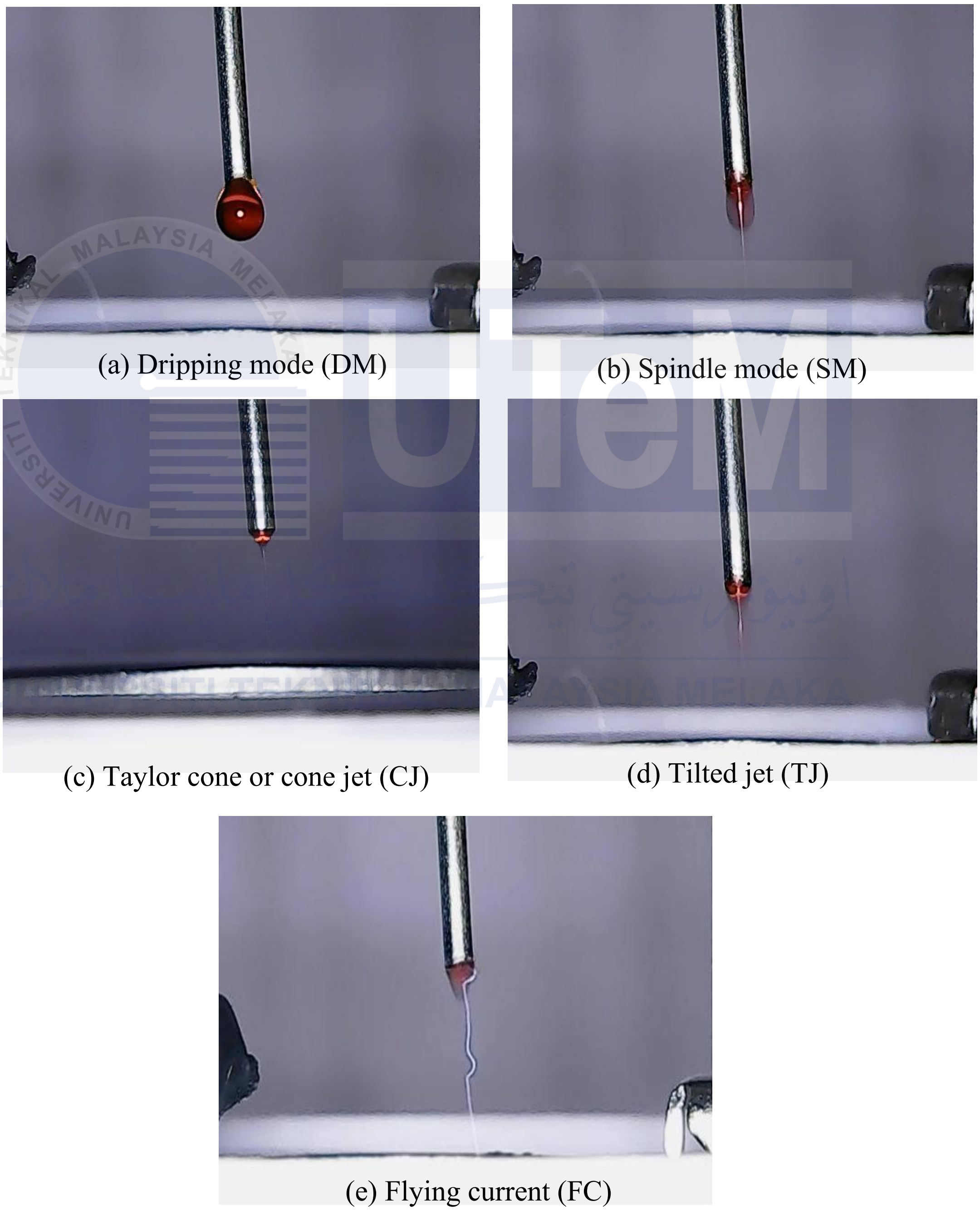

(a) Dripping mode (DM)

(b) Spindle mode (SM)

(c) Taylor cone or cone jet (CJ)

(d) Tilted jet (TJ)

(e) Flying current (FC)

Figure 4.1 Modes of Electrospray

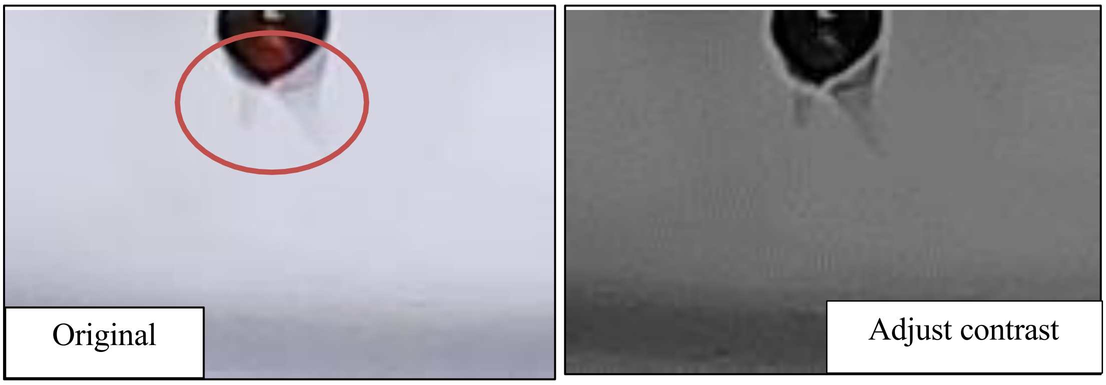

(a) Pulsed jet (PJ)

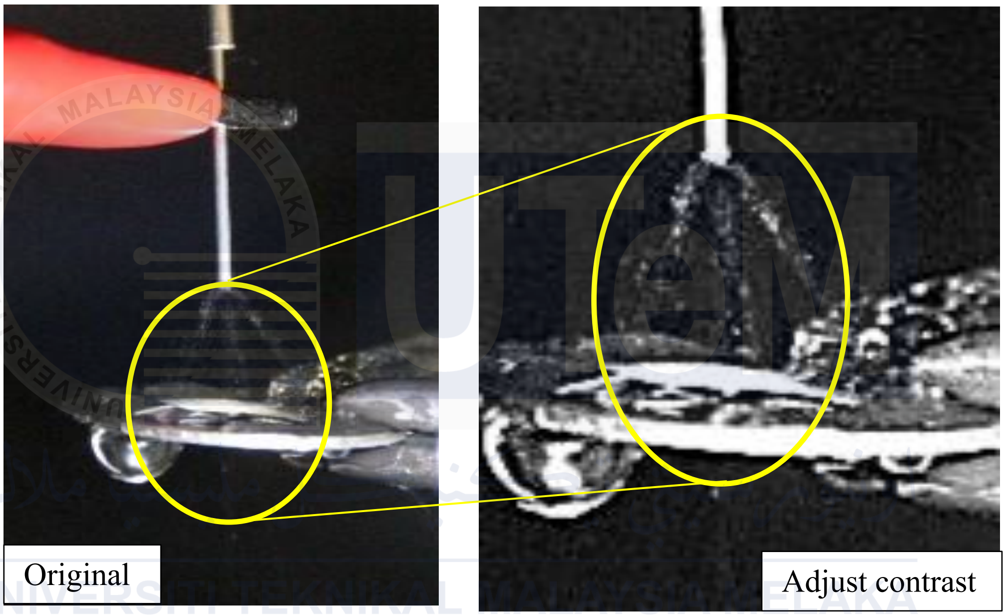

(b) Multi-jet (MT)

Figure 4.2 Difference mode electrospray based on flow rate

Additionally, from observations of the results, it is found out that apart from the five electrospray modes, there are two additional electrospray modes, namely are Multi-Jet (MT) and Pulsed Jet (PT) Modes as depicted in Figure 4.2. These kinds of behaviour were seen particularly at certain flow rates which are also observed in past refs (Kim et al., 2022) in their electrospray setup. For this study the MT and PT are observed at low flow rates (0.01–0.05 mL/min), with sporadic liquid emission. On the other hand, the MT activity was seen at higher flow rates (0.5–1.0 mL/min). These kinds of behaviour only occur for the needle setup of position A. For the case of position B, these kind observations are not consistent and easily turn into flying current.

4.2.2 Effect of Voltage and IDIR size

Table 4.1 and Table 4.2, tabulated the results obtained from the experimentation of the electrospray for position A and position B, respectively. The table presents the voltage applied in kV, the size of the IDIR, electrospray mode, and the angle produced from the cone formed at the tip of the nozzle. In general, it is observed that, for both scenarios of position A and position B, the electric current begins to exert an effect at an applied voltage of 4.5 kV to the water. As the voltage increases, the Taylor cone starts to appear and finally at a higher voltage flying current or the corona discharge starts to occur. It is also observed that larger size of IDIR allows for a broader voltage range to generate electrospray modes.

The results are explained by categorizing the collected voltage data into low voltage, mid-voltage, and high voltage groups. Low voltage is defined as ranging from 3.0 kV to 4.0 kV, mid-range voltage spans from 4.5 kV to 6.0 kV, and high voltage is categorized as exceeding 6.0 kV. At the lower voltages of 3.0 kV and 3.5 kV, both setups at position A and position B consistently generates DM, irrespective of the IDIR sizes (10.3 mm, 15.3 mm, and 21.2 mm). At 4.0 kV, the mode primarily remains DM, with the exception of position A setup and the application of 10.3 mm for IDIR, where a transition to SM occurs. As voltage exceeds 4.0 kV, increasingly complex behaviours are observed. The transition from DM to CJ occurs at approximately 4.5 kV for both position A and position B setups, indicating a consistent voltage threshold for this transformation. The development of TJ, MT, and intermittent CJ modes within the voltage range of 5.5 to 6.0 kV indicates a threshold where electrospray behaviour transitions to a more intermittent and jet- like form.

The electrospray mode and the applied voltage showed an obvious association according to the experimental data. It was discovered that certain voltage thresholds corresponded to the change between many modes:

- Low voltage (3.0–4.0 kV): Mostly DM, with sporadic upper end of this range shift to SM.
- Mid-voltage (4.5–6.0 kV) formation of a stable Taylor cone and subsequent CJ mode transition indicates ideal electrospray conditions.
- TJ, MT, and FC show appearance of instability resulting from too strong electrostatic forces upsetting the spray pattern at high voltage (>6.0 kV).

The experimental findings show that as it generates tiny and homogeneous droplets while preserving spray consistency, a voltage range of 4.5 kV to 6.0 kV is ideal for stable electrospray-assisted applications. In the datasets provided, intermittent CJ appears at different voltages for different IDIRs: 5.5 kV and 6.0 kV for the 10.3 mm ionisation ring, 6.0 kV, 6.5 kV, and higher voltages for the 15.3 mm ionisation ring, and 6.0 kV for the 21.2 mm ionisation ring, indicating that both voltage and electrode geometry influence this mode.

Overall, a consistent pattern of mode transitions as voltage increases. The IDIR determines the angle of the Taylor cone. To summarize, rising voltage consistently causes a transition from DM to more difficult modes such as CJ, TJ, and MT, with the IDIR having a significance influence on the angle of the Taylor cone.

Table 4.1 Data collection based on spray pattern and angle due nozzle above the ionisation ring (Position A)

IDIR (mm)	10.3		15.3		21.2	
Voltage (kV)	Mode	Angle (°)	Mode	Angle (°)	Mode	Angle (°)
3.0	DM	0	DM	0	DM	0
3.5	DM	0	DM	0	DM	0
4.0	SM	0	DM	0	DM	0
4.5	CJ	64	CJ	38	CJ	38
5.0	CJ	68	CJ	37	CJ	61
5.5	Intermittent CJ	70	CJ	37	CJ	61
6.0	TJ	77	Intermittent CJ	42	Intermittent CJ	65
6.5	FC	0	Spray	42	Intermittent CJ	65
7.0			Intermittent CJ	43	CJ	67
7.5			Intermittent CJ	43	CJ	71
8.0			Spray	43	Intermittent CJ	65
8.5			Intermittent CJ	43	Intermittent CJ	65
9.0			CJ	43	CJ	71
9.5			FC	0	CJ	71
10.0					FC	0

Table 4.2 Data collection based on spray pattern and angle due nozzle passes the ionisation ring (Position B)

IDIR (mm)	10.3		15.3		21.2	
Voltage (kV)	Mode	Angle (°)	Mode	Angle (°)	Mode	Angle (°)
3.0	DM	0	DM	0	DM	0
3.5	DM	0	DM	0	DM	0
4.0	DM	0	DM	0	DM	0
4.5	CJ	62	CJ	47	DM	0
5.0	CJ	84	CJ	46	DM	0
5.5	MT	80	MT	38	CJ	25

IDIR (mm)	10.3		15.3		21.2	
Voltage (kV)	Mode	Angle (°)	Mode	Angle (°)	Mode	Angle (°)
6.0	Intermittent CJ	65	CJ	50	MT	27
6.5	FC	0	CJ	54	MT	27
7.0			CJ	54	Intermittent CJ	30
7.5			CJ	54	CJ	31
8.0			CJ	54	CJ	35
8.5			CJ	54	CJ	35
9.0			FC	0	CJ	35
9.5					CJ	35
10.0					CJ	35

4.2.3 Position A and position B of Nozzle

To further comprehend the features of the electrospray modes, Figure 4.3 and Figure 4.4 depict the voltage versus angle of the Taylor cone for position A and position B, respectively. In Position A, as shown in Figure 4.3, the 10.3 mm IDIR has a strong connection with rising voltage and spray angle, which ranges from around 60° at 4.5 kV to about 80° at 9.5 kV. This constant trend means that greater voltages promote broader spray angles, which indicate more spread Taylor cone forms. The 15.3 mm IDIR has a steady spray angle, with modest changes of approximately 40° up to 10 kV, starting at around 38° at 4.5 kV and to about 43° at 5.5 kV. For this IDIR, the relative stability of the spray angle indicates that voltage fluctuations have a less apparent influence on Taylor cone dispersion. The spray angle for the 21.2 mm IDIR initially climbs from about 42° at 4.5 kV to roughly 60° at 5.5 kV, then gradually rises, stabilizing at around 65-70° between 6 kV and 10 kV.

This pattern implies that voltage has a significant early influence on Taylor cone dispersion, which becomes more stable as voltage increases. The spray angle for the 21.2 mm IDIR rapidly increases from roughly 42° at 4.5 kV to around 60° at 5.5 kV. Following that, it steadily increases and stabilizes at 65-70° between 6 kV and 10 kV. This pattern indicates that voltage initially has a substantial influence on Taylor cone dispersion before stabilizing at higher levels.

In contrast, the 10.3 mm IR in Position B, as shown in Figure 4.4, has a peak spray angle that increases substantially from about 65° at 4.5 kV to 85° at 5 kV, then declines to around 60° at 6.5 kV before stabilizing at 10 kV. Triangle symbols represent a slanted jet phenomena at 5 kV, as seen by the drop that follows this peak. This phenomenon indicates an imbalance in the electrostatic forces impacting the Taylor cone's stability. The spray angle of the 15.3 mm IR is consistent, commencing about 50° at 4.5 kV, then decreasing to around 45° at 5.5 kV, and remaining around 50° until 10 kV. Taylor cone production is continuous owing to stability, which is less susceptible to voltage changes.

The spray angle for the 21.2 mm IR gradually increases from about 35° at 4.5 kV to around 45° at 6 kV before stabilizing at 10 kV. Similar to Position A, this trend exhibits a constant Taylor cone growth as voltage increases. The data points with circles represent the intermittent spray behaviour that occurs at particular voltages for the 10.3 mm and 21.2 mm diameters of IDIR. The 10.3 mm IR exhibited MT behaviour at 5 kV and 5.5 kV. This suggests instability in Taylor cone formation at these voltages, most likely due to transitional spray regimes.

Overall, the data indicate that the Taylor cone began to emerge at a voltage of 4 kV. Increasing the voltage helps to stabilize the Taylor cone. However, at a certain voltage point, FC occur and the Taylor cone is destroyed since the current is automatically turned off as a safety mechanism. The findings for both needle locations indicate that the Taylor cone will become constant after a certain voltage. And it is reasonable to say that the position A arrangement produces a more stable Taylor cone and has a larger voltage range than position B.

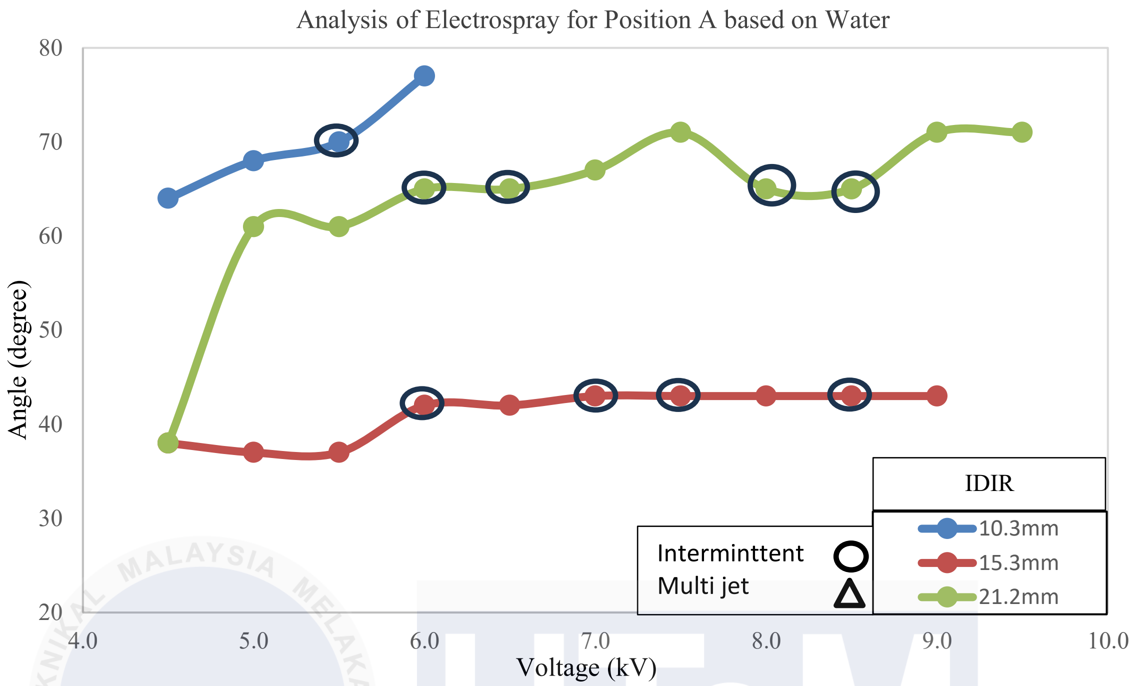

Figure 4.3 Analysis of Taylor cone patterns through the ionisation ring (Position A)

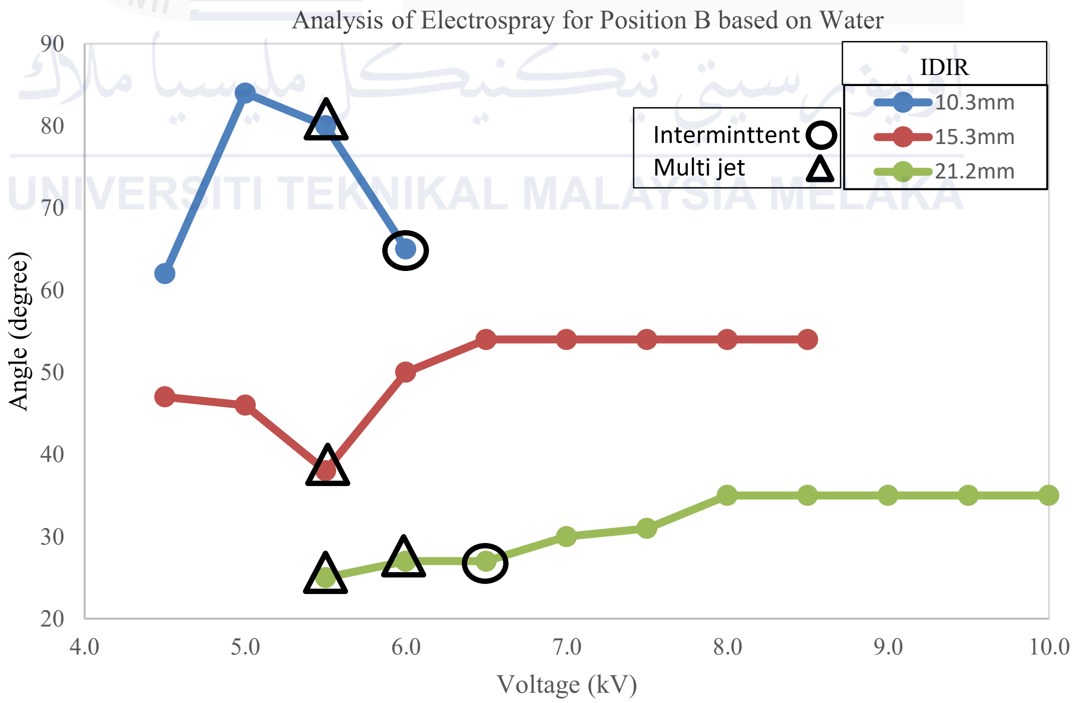

Figure 4.4 Analysis of Taylor cone patterns through the ionisation ring (Position B)

4.3 Working Fluid Density on Taylor Cone Characteristics (Objective 2)

This part examines the influence of working fluid density on Taylor cone characteristics the result is tabulated in Figure 4.5, Figure 4.6, Figure 4.7, Figure 4.8 and Figure 4.9, respectively for water, pure ethanol, mixture of ethanol and n-heptane with three different ratio which are 10% of ethanol mix with 90% of n-heptane, 20% of ethanol mix with 80% of n-heptane and 30% of ethanol mix with 70% of n-heptane, using a constant flow rate of 0.10 mL/min and fixed emitter at position A. Water is used as the reference fluid due to its high density, high surface tension, and strong conductivity. Table 4.3 shows the density, thermal conductivity and surface tension of all the liquid tested under the electrospray setup (Tycova et al., 2021; Zhang et al., 2020; Zou et al., 2024).

Table 4.3 Density, Thermal Conductivity and Surface Tension

Fluid	**Density (g/cm^3)**	**Thermal conductivity (W/m-K)**	**Surface Tension (mN/m)**	**Researcher**
Water	0.997 (≈1.00)	0.6065	71.99	(Pejman Sereshkeh et al., 2024; Pongrác et al., 2014; Wu et al., 2020)
Ethanol	0.789	0.171	22.39	(Cao et al., 2022; Gan et al., 2018; Jiang et al., 2019)
n-Heptane	0.68	~0.14	≈ 20.14	(Pielecha et al., 2021; Tycova et al., 2021; Yao et al., 2014)
Mixture (ethanol – n-heptane) 10% ethanol + 90% n-heptane 20% ethanol + 80% n-heptane 30% ethanol + 70% n-heptane	Intermediate (assume based on the ratio)	estimated between components	likely intermediate	(Zhang et al., 2020; Zou et al., 2024)

4.3.1 Influence of Voltage

It suggests that, water required higher onset voltage to initiate the cone-jet mode compared to other liquids as can be seen in Figure 4.5 to Figure 4.9. It is observed that regardless the IDIR size, the voltage to generates Taylor cone in within the range of 4.0 kV to 10.0 kV for water, for ethanol the voltages is between 2.0 kV and 7.0 kV in Figure 4.6, while a mixture of ethanol and n-heptane begins to form a jet cone at voltages from 1.0 kV to 7.0 kV. Thus, from this observation, the results suggest that, the higher of percentage of ethanol in the mixture of ethanol with n-heptane will reduce the voltage required to generate the Taylor cone.

4.3.2 Influence of IDIR

The experimental results demonstrate that the inner diameter of the ionisation ring (IDIR) and the liquid properties strongly influence Taylor cone behaviour. In general, a smaller IDIR (10.3 mm) produces larger cone angles due to higher electric field concentration, but this condition is less stable. In contrast, a larger IDIR (21.2 mm) generates smaller cone angles with more consistent behaviour.

For water that can be seen in Figure 4.5, cone angles were highest (up to 90°) with noticeable differences between IDIR values, reflecting the effect of its high surface tension and permittivity. Ethanol (Figure 4.6), with lower surface tension, produced smaller cone angles (20–50°) and showed minimal variation across IDIR, indicating reduced sensitivity to geometry. In the case of ethanol and n-heptane mixtures, stability improved with increasing ethanol concentration. At 10% ethanol, cone angles were high but plateaued after 4 kV. At 20% ethanol, cone angles stabilised around 60–80° with smaller IDIR variations, while at 30% ethanol, the cone behaviour was the most consistent across all IDIRs (Figure 4.7 to Figure 4.9).

Overall, the most stable condition was observed with 20–30% ethanol–n-heptane mixtures using 15.3 mm IDIR, where cone angles remained moderate and steady with increasing voltage. This confirms that both the geometry of the ionisation ring and the fluid's physicochemical properties jointly determine the stability and shape of the Taylor cone.

4.3.3 Taylor Cone Shape Character

The experimental findings reveal that both liquid properties and the ionisation ring inner diameter (IDIR) exert a significant influence on Taylor cone formation. Water, owing to its high surface tension and permittivity, produces the largest cone angles (up to ~90°), yet its response is unstable across different IDIR values. Ethanol, in contrast, forms smaller cone angles (20–50°) with minimal variation between IDIRs, reflecting its lower surface tension and reduced sensitivity to field geometry. Ethanol–n-heptane mixtures demonstrate a more progressive stabilisation, where 10% ethanol yields wide but fluctuating cones, while 20–30% ethanol produces moderate and steady cone angles (60–80°), indicating improved balance between polarity and surface tension.

A consistent trend is observed across all liquids: the cone angle decreases as IDIR increases. A smaller IDIR (10.3 mm) intensifies the electric field at the emitter tip, producing wider cone angles but also greater instability, especially at higher voltages. Conversely, a larger IDIR (21.2 mm) spreads the electric field, resulting in smaller but more stable cone angles. Water requires a stronger and more concentrated electric field to overcome its density and surface tension, leading to pronounced cone angles at smaller IDIRs but instability at elevated voltages. Larger IDIRs reduce field intensity, producing narrower yet steadier cones.

Taken together, the comparative findings establish a clear and fundamental relationship between working fluid density and Taylor cone behaviour.

- High-density fluids (water): Require higher voltages and shorter IDIRs to form cones, producing sharper but less stable angles.
- Low-density fluids (ethanol): Form cones at lower voltages, with wider and smoother angle transitions, demonstrating greater responsiveness to the applied electric field.
- Intermediate-density fluids (ethanol and n-heptane mixtures): Exhibit balanced performance, combining reasonable cone sharpness with enhanced stability across varying IDIRs.

The most stable condition is achieved with 20–30% ethanol–n-heptane mixtures at 15.3 mm IDIR, which consistently maintains moderate cone angles under increasing voltage. This demonstrates that both the fluid's physicochemical properties and the geometrical configuration of the ionisation ring are crucial in determining Taylor cone stability and effectiveness. Overall, the results confirm that both ionisation ring geometry and working fluid density are fundamental parameters governing Taylor cone characteristics. Larger IR diameters promote earlier cone-jet formation, while higher density fluids favour wider and more stable cone angles. Once the system enters the stable cone-jet regime, the cone angle becomes largely independent of further voltage increases, reflecting the balance between electrostatic and capillary forces. The results confirm that as fluid density decreases, Taylor cones become easier to initiate, more responsive to applied voltage, and generally more stable across different ionization ring positions.

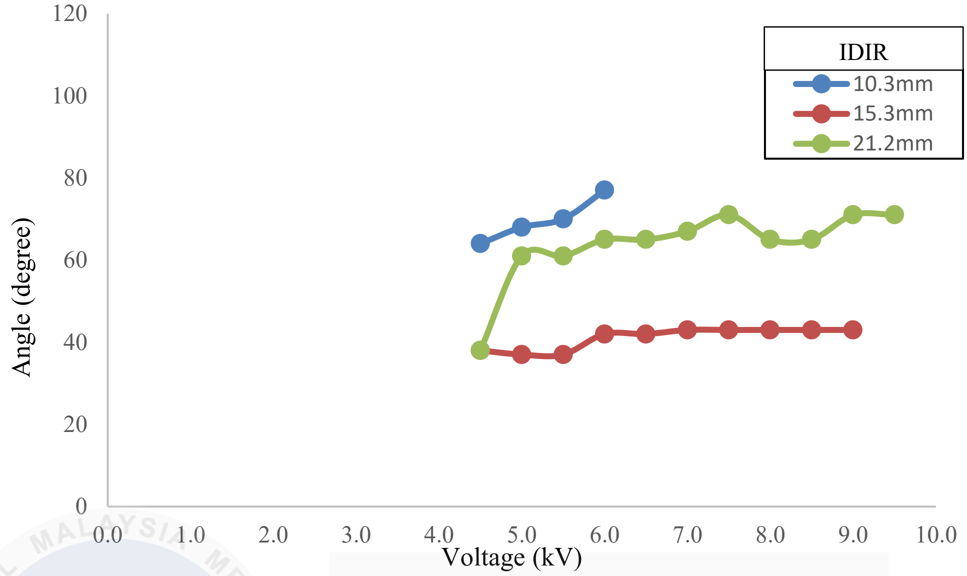

Figure 4.5 Analysis of Taylor cone patterns through the voltage (Position A - Water)

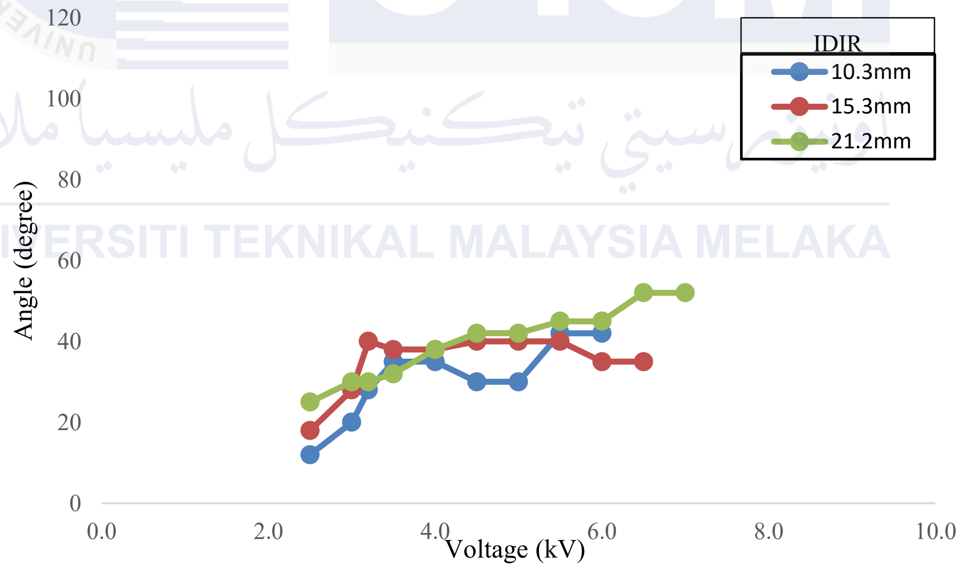

Figure 4.6 Analysis of Taylor cone patterns through the voltage (Position A - Ethanol)

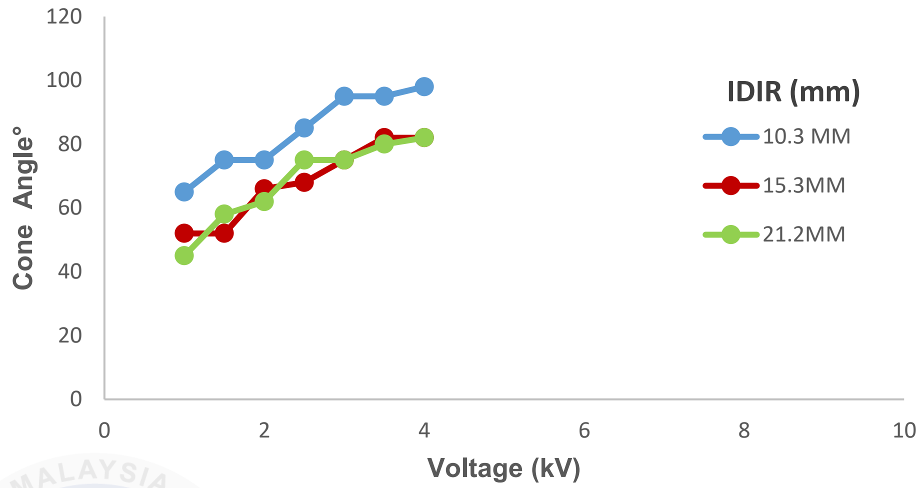

Figure 4.7 Analysis of Taylor cone patterns through the ionisation ring in position with mixture liquid (Ethanol 10%: n-Heptane 90%)

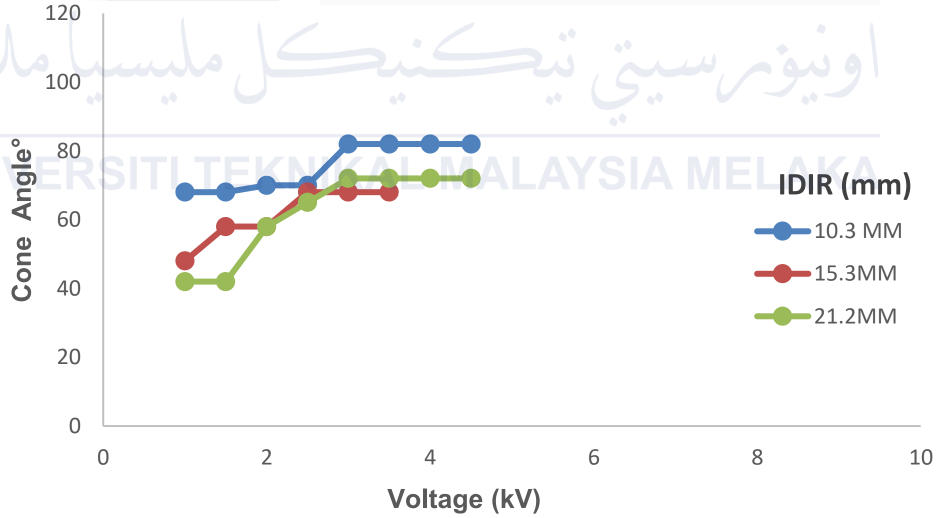

Figure 4.8 Analysis of Taylor cone patterns through the ionisation ring in position with mixture liquid (Ethanol 20%: n-Heptane 80%)

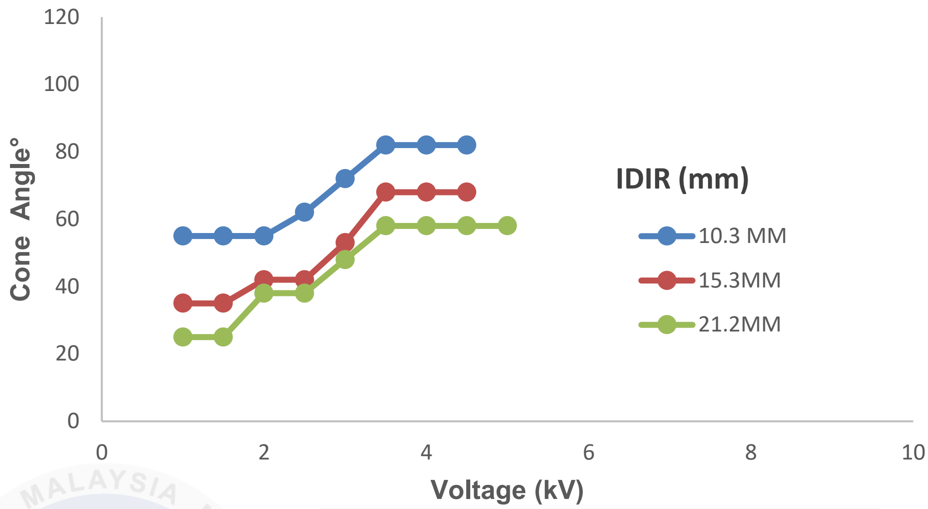

Figure 4.9 Analysis of Taylor cone patterns through the ionisation ring in position with mixture liquid (Ethanol 30%: n-Heptane 70%)

4.3.4 Summary

The results indicate that both spray cone angle and jet stability are strongly influenced by the physical properties of the working fluid, particularly its density, and the applied voltage as shown in Table 4.4. At an IDIR of 10.3 mm, water required a relatively high operating voltage of 4.5 kV to achieve a stable Taylor cone, producing a cone angle of 64°. While water could generate larger cone angles of up to 77°, these were typically observed at higher voltages and were accompanied by noticeable jet instability.

Ethanol, having a lower density than water, formed stable Taylor cones more efficiently, achieving stability at the same voltage of 4.5 kV with a cone angle of 64°. Furthermore, ethanol was capable of producing wider cone angles up to 82° approximately at lower voltages compared to water, with less instability observed.

For ethanol and n-heptane mixtures, jet stability was maintained at lower voltages. A 10%:90% ethanol-to-n-heptane ratio achieved the widest stable cone angle of 75° at 3.0 kV to 3.5 kV. Increasing the ethanol content to 20%:80% produced a slightly narrower stable cone of 70° at the same voltage range. At 30%:70%, stability was observed at 3.5 kV with a cone angle of 72°. These results suggest that fluids with moderate to low density can maintain wider and more stable jets at reduced operating voltages, improving electrospray precision and control. Experiments were also conducted for IDIR values of 15.3 mm and 21.2 mm, with corresponding results provided in

Appendix E.

Table 4.4 Taylor cone formation, voltage range, stable cone angles, and jet stability for various fluids at IDIR = 10.3 mm.

Fluid type	**Water**	**Ethanol**	**Mixture Fluid (Ethanol and n-heptane)**		
			10%:90%	**20%:80%**	**30%:70%**
Taylor Cone formation	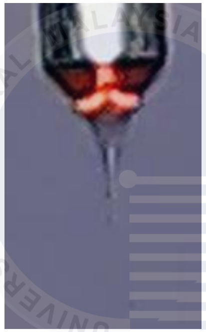				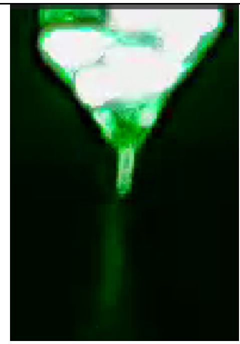
Voltage (kV)	4.5 – 5.0 kV	4.5 – 5.0 kV	3.0 – 3.5 kV	3.0 – 3.5 kV	3.5 - 4.0 kV
Stable Cone Angle (°)	64° - 68°	64° - 77°	75° - 85°	70°	62° - 72°

CHAPTER 5

CONCLUSION AND RECOMMENDATIONS FOR FUTURE RESEARCH

5.1 Conclusion

The electrospray technology, especially in the spray pattern and air-fuel mixture, is investigated in this work. This work aimed to elucidate the effects of liquid density and electrospray parameters on Taylor cone characteristics. In the present study, the characteristics of the Taylor cone were observed based on the changes in the electrospray parameters, namely the voltage, distance of the ionisation ring (IR), inner diameter of the ionisation ring (IDIR), and density of the working fluid. The work examined cone-jet formation and how liquid density affected Taylor cone characteristics. An imaging technique and observations analysis were employed to assess the influence of electrospray settings on Taylor cone characteristics.

Based on the first objective, in an electrospray system, the position and size of the inner diameter of the ionisation ring (IR) and the voltage applied significantly influence the stability of the Taylor cone. The inner diameter of the ionisation ring (IDIR) is crucial for generating an electric field around the needle tip; the smaller the diameter of the IDIR, the greater the strength of the electric field, making it easier to construct a stable and finer Taylor cone. However, a larger diameter of the IDIR may result in a weaker formation but limits the creation of flying current. The voltage supplied directly affects the electrospray mode, with ideal limits being between 4.5 and 7.5 kV for water and 3.0 and 4.5 kV for ethanol. Voltages below these limits often result in jet behaviour due to dripping or pulsing, while voltages above these thresholds cause jet breakup due to repulsive forces among charged particles.

For the second objective, liquid density also plays a significant role in determining the behaviour of the Taylor cone. Liquids with lower density, such as ethanol and n-heptane, are more sensitive to electrostatic forces, requiring lower voltages to create and maintain a stable Taylor cone and producing wider spray angles at lower voltages, especially with smaller IDIRs. However, higher amounts of ethanol led to early instability and spray breakdown at higher voltages, showing a trade-off between quick atomisation and lasting jet stability.

According to the findings of the research, ionisation ring widths that were bigger contributed to the maintaining of electrospray stability at high voltages, while diameters that were smaller led to rapid spray dispersion. The spray angle was broadened, and the density of the solution was decreased when the applied voltage was increased. Because it has a lower density than other substances, ethanol exhibited the steadiest electrospray performance. A further finding of the research was that it is necessary to determine the optimal voltage range, which is between 4.5 and 6.0 kV.

5.2 Recommendation of Future Works

Based on this study's findings about how density and ionisation ring (IR) factors influence Taylor cone features using the electrospray method, several suggestions for future research are made to better understand electrospray behaviour and expand its possible uses.

Firstly, future studies should explore a wider variety of fuel compositions, particularly focusing on biofuels, fuel blends, and industrial solvents. While the current study used ethanol, n-heptane, and water to show different fluid densities and electrical properties, adding fuels with more complicated structures, like biodiesel, butanol, or mixed fuels, would help researchers see how thicker liquids and different behaviours affect the formation and stability of the cone-jet. This expansion is crucial for translating electrospray technology into real-world energy systems and combustion applications, where fuel variability is a common challenge.

Secondly, more systematic investigations into the design and optimisation of the ionisation ring (IR) are recommended. This study primarily focused on varying the IR size, position, and applied voltage; however, future works should consider the geometric profile and material properties of the ring, as well as the integration of multi-electrode configurations. Such improvements could allow for better control of the electric field, which would help stabilise the Taylor cone, make droplet sizes more consistent, and increase the overall efficiency of atomisation. Additionally, researchers could explore the development of adaptive IR systems that self-tune the field strength in response to dynamic flow conditions.

Thirdly, a comprehensive parametric study on the interplay between liquid density and IR characteristics is necessary. While some early patterns have been noticed, a deeper understanding of how changing the liquid density affects the threshold voltage, cone angle, and jet breakup mode can help create models that predict how well the electrospray will work. These models will be particularly valuable in optimising the electrospray process for different operating regimes and environmental conditions.

Lastly, the incorporation of advanced diagnostic and computational tools should be prioritised in future investigations. Techniques that use lasers, like shadowgraphy, schlieren imaging, and laser-induced fluorescence (LIF), can be used to take clear pictures of the Taylor cone and how droplets spread out. At the same time, using computational fluid dynamics (CFD) simulations along with electrohydrodynamic modelling can provide a clearer understanding of how fluids behave inside and how they interact with electric fields, which will enhance the results from the experiments. Combining these methods will help create a strong theoretical understanding of electrospray processes, which will aid in the design of advanced atomisation systems for use in combustion, medical delivery, and making nanomaterials.

5.3 Summary

The electrospray was found to be stable at high voltages when the ionisation ring widths were larger, whereas the spray spread out rapidly when the widths were smaller, according to this research. The density of the solution decreased as the applied voltage was increased, and the discharge angle was widened. Ethanol demonstrated the most consistent electrospray performance due to its lower density than other substances. Another important finding of the investigation was the need to identify the optimal voltage range, which lies between 4.5 and 6.0 kV. Conversely, the results were limited to controlled laboratory conditions and only examined specific fuel combinations. Additional research is necessary to evaluate a broader range of hydrocarbon and biofuel compositions, as well as to improve the design of electrospray nozzles and charge distribution methods. The research contributes to a more comprehensive understanding of the objective of electrospray technology in the improvement of energy efficiency and pollution reduction techniques.

REFERENCES

Abdul Munir, F., Ikhwan Muazzam, M., Gader, A., Mikami, M., Saputro, H., Fitriana, L., Melaka, M., Tuah Jaya Melaka, H., 2018a. Effects of Wall Thickness on Flame Stabilization Limits for Combustors with Wire Mesh. Journal of Advanced Research in Fluid Mechanics and Thermal Sciences Journal homepage 49, 11–17.

Abdul Munir, F., Ikhwan Muazzam, M., Gader, A., Mikami, M., Saputro, H., Fitriana, L., Melaka, M., Tuah Jaya Melaka, H., 2018b. Effects of Wall Thickness on Flame Stabilization Limits for Combustors with Wire Mesh. Journal of Advanced Research in Fluid Mechanics and Thermal Sciences Journal homepage 49, 11–17.

Agrawal, K.S., 2013. International Association of Scientific Innovation and Research (IASIR) International Journal of Emerging Technologies in Computational and Applied Sciences (IJETCAS) www.iasir.net Breakup of Liquid Jets.

Alfatama, M., Shahzad, Y., Choukaife, H., 2024. Recent advances of electrospray technique for multiparticulate preparation: Drug delivery applications. Adv Colloid Interface Sci. https://doi.org/10.1016/j.cis.2024.103098

Arai, M., 2012. Physics behind Diesel Sprays.

Banerjee, S., Mazumdar, S., 2012. Electrospray Ionization Mass Spectrometry: A Technique to Access the Information beyond the Molecular Weight of the Analyte. Int J Anal Chem 2012, 1–40. https://doi.org/10.1155/2012/282574

Barreto, M.A., Hernandez-Rivera, S., 2022a. Depositing Sample using the ESI Needle Spray Deposition Technique.

Barreto, M.A., Hernandez-Rivera, S., 2022b. Depositing Sample using the ESI Needle Spray Deposition Technique.

Bošković, S., Bugarski, B., 2018. Review of electrospray observations and theory. Journal of Engineering & Processing Management 10, 41–53. https://doi.org/10.7251/jepm181002041b

Bruins, A.P., 1998. Mechanistic aspects of electrospray ionization, Journal of Chromatography A.

Caballero-Pérez, M., Galobardes-Esteban, M., Gamero-Castaño, M., 2025. High specific impulse electrospray propulsion with small capillary emitters.

Camelot, D.M.A., Hartman, R.P.A., Marijnissen, J.C.M., Scarlett, B., Brunnerr, D., 2018. Experimental Study Of The Jet Break Up For EHDA Of Liquids In The Cone-Jet Mode.

Cao, Q., Xie, D., Wang, K., Wang, N., Shi, B., 2022. A technique to establish liquid ethanol tubular combustion by dual swirl. Fuel 316. https://doi.org/10.1016/j.fuel.2022.123443

Chang, C.H., Urban, P.L., 2024. Does the Formation of a Taylor Cone in a Pulsating Electrospray Directly Impact Mass Spectrometry Signals? ACS Omega 9, 43211–43218. https://doi.org/10.1021/acsomega.4c07653

Chen, J., Song, W., Xu, D., 2017. Optimal combustor dimensions for the catalytic combustion of methane-air mixtures in micro-channels. Energy Convers Manag 134, 197–207. https://doi.org/10.1016/j.enconman.2016.12.028

Chen, L., Ru, C., Zhang, H., Zhang, Y., Chi, Z., Wang, H., Li, G., 2021. Assembling Hybrid Energetic Materials with Controllable Interfacial Microstructures by Electrospray. ACS Omega 6, 16816–16825. https://doi.org/10.1021/acsomega.1c01371

Chen, N., Gan, Y., Luo, Y., Jiang, Z., 2022. A review on the technology development and fundamental research of electrospray combustion of liquid fuel at small-scale. Fuel Processing Technology. https://doi.org/10.1016/j.fuproc.2022.107342

Chen, N., Gan, Y., Shi, D., Luo, Y., Jiang, Z., 2023. Experimental investigation on the electrospray counterflow flame in a small combustor with a porous media as the grounding electrode. Energy 284. https://doi.org/10.1016/j.energy.2023.128611

Chiu, T.K.F., Xia, Q., Zhou, X., Chai, C.S., Cheng, M., 2023. Systematic literature review on opportunities, challenges, and future research recommendations of artificial intelligence in education. Computers and Education: Artificial Intelligence. https://doi.org/10.1016/j.caeai.2022.100118

Cloupeau, M., Prunet-Foch, B., 1994. Pergamon ELECTROHYDRODYNAMIC SPRAYING FUNCTIONING MODES: A CRITICAL REVIEW, J. Aerosol Sci.

Crotti, S., Seraglia, R., Traldi, P., 2011. Some thoughts on electrospray ionization mechanisms. European Journal of Mass Spectrometry. https://doi.org/10.1255/ejms.1129

Di Natale, F., Parisi, A., Carotenuto, C., Lancia, A., 2023. A model for the absorption rate in electrically charged droplets. Chem Eng Sci 280. https://doi.org/10.1016/j.ces.2023.118964

Divvela, M.J., Joo, Y.L., 2020. Design principles in continuous inkjet electrohydrodynamic printing from discretized modeling and image analysis. J Manuf Process 54, 413–419. https://doi.org/10.1016/j.jmapro.2020.03.064

Dong, T., Wang, J.X., Wang, Y., Tang, G.H., Cheng, Y., Yan, W.C., 2023. Development of machine learning based droplet diameter prediction model for electrohydrodynamic atomization systems. Chem Eng Sci 268. https://doi.org/10.1016/j.ces.2022.118398

Dubey, P., Gopinath, P., Craig, D.Q.M., Takiar, V., 2021. Applications of electrospraying in tissue engineering and beyond, in: Biomedical Applications of Electrospinning and Electrospraying. Elsevier, pp. 229–243. https://doi.org/10.1016/B978-0-12-822476-2.00009-1

Duby, M.H., Deng, W., Kim, K., Gomez, T., Gomez, A., 2006. Stabilization of monodisperse electrosprays in the multi-jet mode via electric field enhancement. J Aerosol Sci 37, 306–322. https://doi.org/10.1016/j.jaerosci.2005.05.013

Emi Corporation, 2025. Contact Us – Emi Trade Online Store [WWW Document]. URL https://emi-trade.store/pages/contact-us (accessed 8.26.25).

Faraji, S., Sadri, B., Vajdi Hokmabad, B., Jadidoleslam, N., Esmaeilzadeh, E., 2017. Experimental study on the role of electrical conductivity in pulsating modes of electrospraying. Exp Therm Fluid Sci 81, 327–335. https://doi.org/10.1016/j.expthermflusci.2016.10.030

Fenn, J.B., Mann, M., Meng, C.K., Wong, S.F., Whitehouse, C.M., 1989. Electrospray Ionization for Mass Spectrometry of Large Biomolecules.

Fernandez de la Mora, J., Barrios-Collado, C., 2017. A bipolar electrospray source of singly charged salt clusters of precisely controlled composition. Aerosol Science and Technology 51, 778–786. https://doi.org/10.1080/02786826.2017.1302070

Franco, M.C., Rocha, R.C., Costa, M., Yehia, M., 2021. Characteristics of NH3/H2/air flames in a combustor fired by a swirl and bluff-body stabilized burner. Proceedings of the Combustion Institute 38, 5129–5138. https://doi.org/10.1016/j.proci.2020.06.141

Fu, Z., Gao, H., Zeng, Z., Liu, J., Zhu, Q., 2020. Generation characteristics of thermal NOx in a double-swirler annular combustor under various inlet conditions. Energy 200. https://doi.org/10.1016/j.energy.2020.117487

Gafian-Calvo, A.M., Davila, J., Barrero, A., 1997. CURRENT AND DROPLET SIZE IN THE ELECTROSPRAYING OF LIQUIDS. SCALING LAWS, I Aerowl Ser.

Gamero-Castaño, M., Cisquella-Serra, A., 2021. Electrosprays of highly conducting liquids: A study of droplet and ion emission based on retarding potential and time-of-flight spectrometry. Phys Rev Fluids 6. https://doi.org/10.1103/PhysRevFluids.6.013701

Gan, Y., Chen, X., Tong, Y., Zhang, X., Zhang, Y., 2018. Thermal performance of a meso-scale combustor with electrospray technique using liquid ethanol as fuel. Appl Therm Eng 128, 274–281. https://doi.org/10.1016/j.applthermaleng.2017.09.016

Gan, Y., Jiang, Z., Li, H., Luo, Y., Chen, X., Shi, Y., Yan, Yuying, Yan, Yunfei, 2019a. A comparative study on droplet characteristics and specific charge of ethanol in two small-scale electrospray systems. Sci Rep 9. https://doi.org/10.1038/s41598-019-55223-6

Gan, Y., Li, H., Jiang, Z., Chen, X., Luo, Y., Tong, Y., Shi, Y., Jiang, X., 2019b. An experimental investigation on the electrospray characteristics in a meso-scale system at different modes. Exp Therm Fluid Sci 106, 130–137. https://doi.org/10.1016/j.expthermflusci.2019.04.029

Gan, Y., Luo, Z., Cheng, Y., Xu, J., 2015. The electro-spraying characteristics of ethanol for application in a small-scale combustor under combined electric field. Appl Therm Eng 87, 595–604. https://doi.org/10.1016/j.applthermaleng.2015.05.046

Gan, Y., Wang, M., Luo, Y., Chen, X., Xu, J., 2016. Effects of direct-current electric fields on flame shape and combustion characteristics of ethanol in small scale. Advances in Mechanical Engineering 8. https://doi.org/10.1177/1687814015624846

Gañán-Calvo, A.M., López-Herrera, J.M., Herrada, M.A., Ramos, A., Montanero, J.M., 2018. Review on the physics of electrospray: From electrokinetics to the operating conditions of single and coaxial Taylor cone-jets, and AC electrospray. J Aerosol Sci. https://doi.org/10.1016/j.jaerosci.2018.05.002

Gañán-Calvo, A.M., Montanero, J.M., 2009. Revision of capillary cone-jet physics: Electrospray and flow focusing. Phys Rev E Stat Nonlin Soft Matter Phys 79. https://doi.org/10.1103/PhysRevE.79.066305

Geoffrey Taylor, 1964. Disintegration of water drops in an electric field. Proc R Soc Lond A Math Phys Sci 280, 383–397. https://doi.org/10.1098/rspa.1964.0151

Giusti, A., Fredrich, D., 2024a. Fuel effects on the electrostatic control of charged droplet trajectories. Fuel 366. https://doi.org/10.1016/j.fuel.2024.131009

Giusti, A., Fredrich, D., 2024b. Fuel effects on the electrostatic control of charged droplet trajectories. Fuel 366. https://doi.org/10.1016/j.fuel.2024.131009

Gonzalez-Ramirez, M., Cerezo, A.B., Valero, E., Troncoso, A.M., Garcia-Parrilla, M.C., 2024. From tyrosine to hydroxytyrosol: a pathway involving biologically active compounds and their determination in wines by ultra performance liquid chromatography with mass spectrometry. J Sci Food Agric 104, 9399–9409. https://doi.org/10.1002/jsfa.13762

Hartman, R.P.A., Brunner, D.J., Camelot, D.M.A., Marijnissen, J.C.M., Scarlett, B., 2000. Jet Break-Up In Electrohydrodynamic Atomization In The Cone-Jet Mode, J. Aerosol Sci.

Hartman, R.P.A., Brunner, D.J., Camelot, D.M.A., Marijnissen, J.C.M., Scarlett, B., 1999. Electrohydrodynamic Atomization In The Cone}Jet Mode Physical Modeling Of The Liquid Cone And Jet, J. Aerosol Sci.

He, T., Jokerst, J. V., 2020. Structured micro/nano materials synthesized: Via electrospray: A review. Biomater Sci. https://doi.org/10.1039/d0bm01313g

Hery Soegiharto, A.F., Wardana, I.N.G., Yuliati, L., Nursasongko, M., 2017. The Role of Liquid Fuels Channel Configuration on the Combustion inside Cylindrical Mesoscale Combustor. Journal of Combustion 2017. https://doi.org/10.1155/2017/3679679

Higuera, F.J., 2003. Flow rate and electric current emitted by a Taylor cone. J Fluid Mech 484, 303–327. https://doi.org/10.1017/S0022112003004385

Huang, B., Xie, H., Li, Z., 2023. Microfluidic Methods for Generation of Submicron Droplets: A Review. Micromachines (Basel). https://doi.org/10.3390/mi14030638

Huang, K.H., Ghosh, J., Xu, S., Cooks, R.G., 2022. Late-Stage Functionalization and Characterization of Drugs by High-Throughput Desorption Electrospray Ionization Mass Spectrometry. Chempluschem 87. https://doi.org/10.1002/cplu.202100449

Huang, Z., Xiao, J., Qiao, X., Jiang, G., Shao, Y., Shiga, S., Daisho, Y., 2012. Spray characteristics and controlling mechanism of fuel containing CO 2. Frontiers in Energy 6, 80–88. https://doi.org/10.1007/s11708-012-0180-3

Jahan, S., Ferdows, M., Zaimi, K., 2021a. Effects of Solar Radiation and Viscous Dissipation on Mixed Convective Non-Isothermal Hybrid Nanofluid over Moving Thin Needle. Journal of Advanced Research in Micro and Nano Engineering 3, 1–11.

Jahan, S., Ferdows, M., Zaimi, K., 2021b. Effects of Solar Radiation and Viscous Dissipation on Mixed Convective Non-Isothermal Hybrid Nanofluid over Moving Thin Needle. Journal of Advanced Research in Micro and Nano Engineering 3, 1–11.

Jaworek, A., Krupa, A., 1999. Classification Of The Modes Of Ehd Spraying, J. Aerosol Sci.

Jia, W., Kharraz, J.A., Sun, J., An, A.K., 2021. Hierarchical Janus membrane via a sequential electrospray coating method with wetting and fouling resistance for membrane distillation. Desalination 520. https://doi.org/10.1016/j.desal.2021.115313

Jiang, J., Qian, Z., Wang, X., Chen, H., Kang, G., Liu, Y., Zheng, G., Li, W., 2023. Numerical Simulation of Motion and Distribution Characteristics for Electrospray Droplets. Micromachines (Basel) 14. https://doi.org/10.3390/mi14020396

Jiang, Z., Gan, Y., Ju, Y., Liang, J., Zhou, Y., 2019. Experimental study on the electrospray and combustion characteristics of biodiesel-ethanol blends in a meso-scale combustor. Energy 179, 843–849. https://doi.org/10.1016/j.energy.2019.05.024

Johari, N.H., Hamady, M., Xu, X.Y., 2022. Fluid-Structure Interaction Study of The Effect of Stent on Local Hemodynamics Parameters at The Stented Carotid Artery Bifurcation. Journal of Advanced Research in Applied Sciences and Engineering Technology 28, 247–255. https://doi.org/10.37934/araset.28.2.247255

John Zeleny, B., 1917. THE THE ELECTRICAL DISCHARGE FROM LIQUID POINTS, AND A HYDROSTATIC METHOD OF MEASURING THE ELECTRIC INTENSITY AT THEIR SURFACES. ', Secorid Series. Febrlary.

Jowkar, S., Jafari, M., Morad, M.R., 2019. Heat transfer characteristics of high flow rate electrospray and droplet cooling. Appl Therm Eng 162. https://doi.org/10.1016/j.applthermaleng.2019.114239

Ju, Y., Maruta, K., 2011. Microscale combustion: Technology development and fundamental research. Prog Energy Combust Sci. https://doi.org/10.1016/j.pecs.2011.03.001

Jweeg, M.J., Hussein, E.Q., Rashid, F.L., Basem, A., 2024. Investigation of Two-Way Fluid-Structure Interaction of Blood Flow at Different Temperature using CFD. Journal of Advanced Research in Applied Sciences and Engineering Technology 36, 120–130. https://doi.org/10.37934/araset.36.2.120130

Kang, M.S., Park, S.H., Yoo, C.S., Park, J., Chung, S.H., 2021. Effect of core metal on flame spread and extinction for horizontal electrical wire with applied AC electric fields. Proceedings of the Combustion Institute 38, 4747–4756. https://doi.org/10.1016/j.proci.2020.05.060

Kang, Z., Shi, Z., Ye, J., Tian, X., Huang, Z., Wang, H., Wei, D., Peng, Q., Tu, Y., 2023. A Review of Micro Power System and Micro Combustion: Present Situation, Techniques and Prospects. Energies (Basel). https://doi.org/10.3390/en16073201

Kavadiya, S., Biswas, P., 2018. Electrospray deposition of biomolecules: Applications, challenges, and recommendations. J Aerosol Sci. https://doi.org/10.1016/j.jaerosci.2018.04.009

Khan, Ibrahim, Saeed, K., Khan, Idrees, 2019. Nanoparticles: Properties, applications and toxicities. Arabian Journal of Chemistry. https://doi.org/10.1016/j.arabjc.2017.05.011

Kim, H.H., Kim, J.H., Ogata, A., 2011. Time-resolved high-speed camera observation of electrospray. J Aerosol Sci 42, 249–263. https://doi.org/10.1016/j.jaerosci.2011.01.007

Kim, J.Y., Lee, S.J., Hong, J.G., 2022. Spray Mode and Monodisperse Droplet Properties of an Electrospray. ACS Omega 7, 28667–28674. https://doi.org/10.1021/acsomega.2c04002

Laimer, F., Kranabetter, L., Tiefenthaler, L., Albertini, S., Zappa, F., Ellis, A.M., Gatchell, M., Scheier, P., 2019. Highly Charged Droplets of Superfluid Helium. Phys Rev Lett 123. https://doi.org/10.1103/PhysRevLett.123.165301

Lambropo_Ulos, N., 1995. High Performance Liquid Chromatography And Electrospray Mass Spectrometry Of Zinc Dithiophosphates As Lubricating Oil Additives.

Lee, H., An, S., Kim, S., Jeon, B., Kim, M., Kim, I.S., 2018. Readily Functionalizable and Stabilizable Polymeric Particles with Controlled Size and Morphology by Electrospray. Sci Rep 8. https://doi.org/10.1038/s41598-018-34124-0

Li, L., Chen, T.C., Ren, Y., Hendricks, P.I., Cooks, R.G., Ouyang, Z., 2014. Mini 12, miniature mass spectrometer for clinical and other applications - Introduction and characterization. Anal Chem 86, 2909–2916. https://doi.org/10.1021/ac403766c

Lim, S.J., Park, S.H., Park, J., Fujita, O., Keel, S.I., Chung, S.H., 2017. Flame spread over inclined electrical wires with AC electric fields. Combust Flame 185, 82–92. https://doi.org/10.1016/j.combustflame.2017.07.010

Lin, Y.R., Chen, H., Mashuga, C., Mannan, M.S., 2015. Improved electrospray design for aerosol generation and flame propagation analysis. J Loss Prev Process Ind 38, 148–155. https://doi.org/10.1016/j.jlp.2015.09.011

Loo, J.A., Udseth, H.R., Smith', R.D., 1989. Peptide and Protein Analysis by Electrospray lonization-Mass Spectrometry and Capillary Electrophoresis-Mass Spectrometry, ANALYTICALBIOCHEMISTRY.

López-Herrera, J.M., Riesco-Chueca, P., Gañán-Calvo, A.M., 2005. Linear stability analysis of axisymmetric perturbations in imperfectly conducting liquid jets. Physics of Fluids 17. https://doi.org/10.1063/1.1863285

Magnusson, J.M., Collins, A.L., Wirz, R.E., 2020. Polyatomic ion-induced electron emission (Iiee) in electrospray thrusters. Aerospace 7, 1–21. https://doi.org/10.3390/aerospace7110153

Marty, M.T., 2020. A Universal Score for Deconvolution of Intact Protein and Native Electrospray Mass Spectra. Anal Chem 92, 4395–4401. https://doi.org/10.1021/acs.analchem.9b05272

Mosa, M.A., Bang, J., Yeop Jo, J., Lee, J.S., Kwon, K.S., 2023. Continuous ink supply and circulation system for a multi-nozzle electrospray. Jpn J Appl Phys 62. https://doi.org/10.35848/1347-4065/acac39

Munir, F.A., Mikami, M., 2015. A numerical study of propane-air combustion in meso-scale tube combustors with concentric rings. Journal of Thermal Science and Technology 10. https://doi.org/10.1299/jtst.2015jtst0008

Naderi, P., Shams, M., Ghassemi, H., 2019. Investigation on the onset voltage and stability island of electrospray in the cone-jet mode using curved counter electrode. J Electrostat 98, 1–10. https://doi.org/10.1016/j.elstat.2019.01.004

Namoos, H.A.A., Jasim, A.M., 2024. The Analytical Improvement of q-Homotopy Analysis Method for Magneto-hydrodynamic (MHD) Jeffrey Hamel Nanofluid Flow. Journal of Advanced Research in Fluid Mechanics and Thermal Sciences 119, 32–55. https://doi.org/10.37934/arfmts.119.2.3255

Nashee, S.R., Hmood, H.M., 2023. Numerical Study of Heat Transfer and Fluid Flow over Circular Cylinders in 2D Cross Flow. Journal of Advanced Research in Applied Sciences and Engineering Technology 30, 216–224. https://doi.org/10.37934/araset.30.2.216224

Nekrasov, Y.S., Ikonnikov, N.S., Borisov, Y.A., Kiselev, S.S., Kornienko, A.G., Velezheva, V.S., Lyakhovetsky, Y.I., 2017. Reactivity of N-Methylidenemalonates of 3-Arylaminoindoles and p-Dimethylamino-N-Phenylaniline in the Course of Their Analysis by Electrospray Ionization Mass Spectrometry. Int J Anal Mass Spectrom Cromatogr 05, 1–16. https://doi.org/10.4236/ijamsc.2017.51001

Oh, H., Kim, S., 2007. Synthesis of ceria nanoparticles by flame electrospray pyrolysis. J Aerosol Sci 38, 1185–1196. https://doi.org/10.1016/j.jaerosci.2007.09.007

Ondimu, O.M., Ganesan, V.A., Gatari, M.J., Marijnissen, J.C.M., Agostinho, L.L.F., 2017. Modeling simple-jet mode electrohydrodynamic-atomization droplets' trajectories and spray pattern for a single nozzle system. J Electrostat 89, 77–87. https://doi.org/10.1016/j.elstat.2017.08.001

Ouyang, Z., Cooks, R.G., 2009. Miniature mass spectrometers. Annual Review of Analytical Chemistry 2, 187–214. https://doi.org/10.1146/annurev-anchem-060908-155229

Pan, J.F., Wu, D., Liu, Y.X., Zhang, H.F., Tang, A.K., Xue, H., 2014. Hydrogen/oxygen premixed combustion characteristics in micro porous media combustor, in: Energy Procedia. Elsevier Ltd, pp. 1279–1285. https://doi.org/10.1016/j.egypro.2014.11.1081

Panahi, A., Pishevar, A.R., Tavakoli, M.R., 2020. Experimental investigation of electrohydrodynamic modes in electrospraying of viscoelastic polymeric solutions. Physics of Fluids 32. https://doi.org/10.1063/1.5132556

Parhizkar, M., Reardon, P.J.T., Knowles, J.C., Browning, R.J., Stride, E., Pedley, R.B., Grego, T., Edirisinghe, M., 2017. Performance of novel high throughput multi electrospray systems for forming of polymeric micro/nanoparticles. Mater Des 126, 73–84. https://doi.org/10.1016/j.matdes.2017.04.029

Park, N.A., Glish, G.L., Dick, J.E., 2022. Supplemental Material Investigating Electrosprayed Droplets using Particle-into-Liquid Sampling for Nanoliter Electrochemical Reactions (PILSNER).

Pejman Sereshkeh, S.R., Llumiquinga, B., Bapatla, S., Grzenda, M.J., Specca, D., Both, A.J., Singer, J.P., 2024. Staticaponics: Electrospray delivery of nutrients and water to the plant root zone. J Electrostat 128. https://doi.org/10.1016/j.elstat.2024.103902

Pennisi, M.W., 2012. Characterization Of 1-Butanol Electrospray Combustion.

Pielecha, I., Wierzbicki, S., Sidorowicz, M., Pietras, D., 2021. Combustion thermodynamics of ethanol, n-heptane, and n-butanol in a rapid compression machine with a dual direct injection (DDI) supply system. Energies (Basel) 14. https://doi.org/10.3390/en14092729

Pongrác, B., Kim, H.H., Negishi, N., Machala, Z., 2014. Influence of water conductivity on particular electrospray modes with dc corona discharge - Optical visualization approach. European Physical Journal D. https://doi.org/10.1140/epjd/e2014-50052-4

Qian, P., Liu, M., 2022. Influencing factors of wall temperature and flame stability of micro-combustors in micro-thermophotovoltaic and micro-thermoelectric systems. Fuel. https://doi.org/10.1016/j.fuel.2021.122436

Rafeq Saleman, A., Shukri Zakaria, M., Kejuruteraan Mekanikal, F., Jumaidin, R., Hazwani Mokhtar Fakulti Teknologi Kejuruteraan, N., Aslily Sarkam, N., 2022a.

Molecular Dynamics Study: Correlation of Heat Conduction Across S-L Interfaces Between Constant Heat Flux and Shear Applied to Liquid Systems, Journal of Mechanical Engineering.

Rafeq Saleman, A., Shukri Zakaria, M., Kejuruteraan Mekanikal, F., Jumaidin, R., Hazwani Mokhtar Fakulti Teknologi Kejuruteraan, N., Aslily Sarkam, N., 2022b. Molecular Dynamics Study: Correlation of Heat Conduction Across S-L Interfaces Between Constant Heat Flux and Shear Applied to Liquid Systems, Journal of Mechanical Engineering.

Rafie-Zinedine, S., Yenupuri, T.V., Worbs, L., Maia, F.R.N.C., Heymann, M., Schulz, J., Bielecki, J., 2024. Enhancing electrospray ionization efficiency for particle transmission through an aerodynamic lens stack. J Synchrotron Radiat 31, 222–232. https://doi.org/10.1107/S1600577524000158

Ramshani, Z., Johnson, M.J., Atashbar, M.Z., Go, D.B., 2016. A broad area electrospray generated by a piezoelectric transformer. Appl Phys Lett 109. https://doi.org/10.1063/1.4960153

Rauschenbach, S., Stadler, F.L., Lunedei, E., Malinowski, N., Koltsov, S., Costantini, G., Kern, K., 2006. Electrospray ion beam deposition of clusters and biomolecules. Small 2, 540–547. https://doi.org/10.1002/smll.200500479

Rovelli, G., Jacobs, M.I., Willis, M.D., Rapf, R.J., Prophet, A.M., Wilson, K.R., 2020. A critical analysis of electrospray techniques for the determination of accelerated rates and mechanisms of chemical reactions in droplets. Chem Sci 11, 13026–13043. https://doi.org/10.1039/d0sc04611f

Saleman, A.R. bin, Chilukoti, H.K., Kikugawa, G., Ohara, T., 2019. A molecular dynamics study on the thermal rectification effect at the solid–liquid interfaces between the face-centred cubic (FCC) of gold (Au) with the surfaces of (100), (110) and (111) crystal planes facing the liquid methane (CH4). Mol Simul 45, 68–79. https://doi.org/10.1080/08927022.2018.1535177

Saputro, H., Ariyanto, E.D., Wijayanto, D.S., Muslim, R., Fitriana, L., Munir, F.A., 2021. An experimental study into the effect of fuel on step micro-combustor to the flame stability characterization, in: IOP Conference Series: Earth and Environmental Science. IOP Publishing Ltd. https://doi.org/10.1088/1742-6596/1808/1/012020

Saputro, H., Fitriana, L., Purwanto, A., Munir, F.A., Wang, W.C., 2022. A Development of Meso-Scale Vortex Combustion for a Micro Power Generator Based on a Thermoelectric Generator. Fluids 7. https://doi.org/10.3390/fluids7120386

Shimokuri, D., Taomoto, Y., Matsumoto, R., 2017. Development of a powerful miniature power system with a meso-scale vortex combustor. Proceedings of the Combustion Institute 36, 4253–4260. https://doi.org/10.1016/j.proci.2016.06.180

Si, Y., Shi, S., Hu, J., 2024. Electrospinning and electrospraying synergism: Twins-tech collaboration across dimensions. Matter. https://doi.org/10.1016/j.matt.2024.01.009

Silva, A.O., Paulazzi, A.R., Andrade, K.L., Machado, R.A.F., Marangoni, C., Hotza, D., 2024. Electrospray crystallization: A review on submicrometric and nanosized crystal synthesis. Progress in Crystal Growth and Characterization of Materials. https://doi.org/10.1016/j.pcrysgrow.2024.100636

Soares, R.M.D., Siqueira, N.M., Prabhakaram, M.P., Ramakrishna, S., 2018. Electrospinning and electrospray of bio-based and natural polymers for biomaterials development. Materials Science and Engineering C. https://doi.org/10.1016/j.msec.2018.08.004

Sosnowski, P., Hopfgartner, G., 2020. Application of 3D printed tools for customized open port probe-electrospray mass spectrometry. Talanta 215. https://doi.org/10.1016/j.talanta.2020.120894

Takeno, K., Kido, H., Takeda, H., Yamamoto, S., Shentsov, V., Makarov, D., Molkov, V., 2024. Flame Stabilisation Mechanism for Under-Expanded Hydrogen Jets. Fire 7. https://doi.org/10.3390/fire7020048

Tang, C., Guo, T., Zhang, Z., Yang, P., Song, H., 2021. Rapid visualized characterization of phenolic taste compounds in tea extract by high-performance thin-layer chromatography coupled to desorption electrospray ionization mass spectrometry. Food Chem 355. https://doi.org/10.1016/j.foodchem.2021.129555

Thakkar, S., Misra, M., 2021. Electrospray particles as drug delivery systems: Concepts, strategies, and applications, in: Biomedical Applications of Electrospinning and Electrospraying. Elsevier, pp. 245–275. https://doi.org/10.1016/B978-0-12-822476-2.00013-3

Thirukumaran, M., Singh, V., Arao, Y., Fujito, Y., Nishimura, M., Ogura, T., Pawliszyn, J., 2021. Solid-phase microextraction- probe electrospray ionization devices for screening and quantitating drugs of abuse in small amounts of biofluids. Talanta 231. https://doi.org/10.1016/j.talanta.2021.122317

Thuppul, A., Wright, P.L., Collins, A.L., Ziemer, J.K., Wirz, R.E., 2020. Lifetime considerations for electrospray thrusters. Aerospace 7. https://doi.org/10.3390/AEROSPACE7080108

Tian, L., Sun, H., Xu, Y., Jiang, P., Lu, H., Hu, X., 2022. Numerical analysis on combustion flow characteristics of jet-stabilized combustor with different geometry. Case Studies in Thermal Engineering 32. https://doi.org/10.1016/j.csite.2022.101885

Tycova, A., Prikryl, J., Kotzianova, A., Datinska, V., Velebny, V., Foret, F., 2021. Electrospray: More than just an ionization source. Electrophoresis. https://doi.org/10.1002/elps.202000191

Uhlmann, E., Polte, J., Neuwald, T., Fasselt, J., Hocke, T., 2025. Additive Manufacturing of hard magnetic materials via Cold Spray Additive Manufacturing.

Wan, J., Zhao, H., 2020. Anomalous blow-off limit of methane-air premixed flame in a micro preheated combustor with a flame holder. Int J Hydrogen Energy 45, 31202–31212. https://doi.org/10.1016/j.ijhydene.2020.08.130

Wang, F., Elbadawi, M., Tsilova, S.L., Gaisford, S., Basit, A.W., Parhizkar, M., 2022. Machine learning predicts electrospray particle size. Mater Des 219. https://doi.org/10.1016/j.matdes.2022.110735

Wang, J., Yin, Z., 2018. SU-8 nano-nozzle fabrication for electrohydrodynamic jet printing using UV photolithography. Mater Sci Semicond Process 84, 144–150. https://doi.org/10.1016/j.mssp.2018.05.028

Wang, S., Yazdkhsti, A., Alizadeh, A., Basem, A., Jasim, D.J., Al-Rubaye, A.H., Salahshour, S., Toghraie, D., 2024. Calculating minimum droplet diameter in dripping, spindle, and cone-jet modes based on experimental data in the electrospray process. Exp Therm Fluid Sci. https://doi.org/10.1016/j.expthermflusci.2024.111154

Wang, Y., Zhang, W., Sun, Q., Lin, S., Sun, S., Deng, X., 2020. Facile strategy to generate charged droplets with desired polarities. ACS Omega 5, 26908–26913. https://doi.org/10.1021/acsomega.0c04140

Wang, Z., Dai, Q., Yang, S., Tian, J., Wang, Jue, Huo, Y., Wang, Junfeng, 2024. An experimental study on the role of electrical conductivity in the steady cone-jet electrospray. International Journal of Multiphase Flow 171. https://doi.org/10.1016/j.ijmultiphaseflow.2023.104696

Wang, Z., Xia, L., Tian, L., Wang, J., Zhan, S., Huo, Y., Tu, J., 2018. Natural periodicity of electrohydrodynamic spraying in ethanol. J Aerosol Sci 117, 127–138. https://doi.org/10.1016/j.jaerosci.2017.12.008

Wang, Z., Zhang, Y., Guo, T., Zhu, Z., Wang, X., Wen, J., 2015. Experimental Study on Size and Velocity of Charged Droplets, in: Procedia Engineering. Elsevier Ltd, pp. 522–526. https://doi.org/10.1016/j.proeng.2015.11.295

Wu, H., Mendel, N., van der Ham, S., Shui, L., Zhou, G., Mugele, F., 2020. Charge Trapping-Based Electricity Generator (CTEG): An Ultrarobust and High Efficiency Nanogenerator for Energy Harvesting from Water Droplets. Advanced Materials 32. https://doi.org/10.1002/adma.202001699

Xian, H.W., Saidur, R., Sidik, N.A.C., Asako, Y., 2022. Viscosity Of CuO Nanofluid Due to Nanoparticles Size and Concentration. Journal of Advanced Research in Applied Sciences and Engineering Technology 28, 161–167. https://doi.org/10.37934/araset.28.1.161167

Xie, J., Zhu, Y., 2020. Characteristics study on a modified advanced vortex combustor. Energy 193. https://doi.org/10.1016/j.energy.2019.116805

Yamaguchi, K., 2013. Cold-Spray Ionization Mass Spectrometry: Applications in Structural Coordination Chemistry. Mass Spectrometry 2, S0012–S0012. https://doi.org/10.5702/massspectrometry.s0012

Yamashita, 1984. Electrospray Ion Source Another variation on the Free-jet Theme.

Yang, D., Wang, B., Wang, Y., Liu, A., Liu, J., Zhang, M., 2024. Microbial inactivation of pressure spray combined with high-voltage electrospray and its application in honey raspberry juice. Int J Food Microbiol 413. https://doi.org/10.1016/j.ijfoodmicro.2024.110602

Yang, S., Wang, Z., Kong, Q., Li, B., Wang, J., 2022. Visualization on electrified micro-jet instability from Taylor cone in electrohydrodynamic atomization. Chin J Chem Eng 44, 456–465. https://doi.org/10.1016/j.cjche.2021.03.005

Yang, X., Yang, W., Dong, S., Tan, H., 2020. Flame stability analysis of premixed hydrogen/air mixtures in a swirl micro-combustor. Energy 209. https://doi.org/10.1016/j.energy.2020.118495

Yang, X., Yu, B., Peng, X., Zhou, H., 2021. Investigation of thermal performance and energy conversion in a novel planar micro-combustor with four-corner entrances for thermo-photovoltaic power generators. J Power Sources 515. https://doi.org/10.1016/j.jpowsour.2021.230625

Yao, R., Qiu, Z., Li, J., Huang, J., Chen, X., Wanga, N., 2014. Experimental study on n-heptane droplet combustion in a micro-T ube, in: Energy Procedia. Elsevier Ltd, pp. 2528–2531. https://doi.org/10.1016/j.egypro.2014.12.038

Yeo, L.Y., Gagnon, Z., Chang, H.C., 2005. AC electrospray biomaterials synthesis. Biomaterials 26, 6122–6128. https://doi.org/10.1016/j.biomaterials.2005.03.033

Yu, D.G., Zhou, F., Parker, G.J.M., Simaite, A., Buzgo, M., Williams, G.R., 2021. Innovations and advances in electrospraying technology, in: Biomedical Applications of Electrospinning and Electrospraying. Elsevier, pp. 207–228. https://doi.org/10.1016/B978-0-12-822476-2.00006-6

Zakaria, M.R., Md Akil, H., Omar, M.F., Abdul Kudus, M.H., Mohd Sabri, F.N.A., Abdullah, M.M.A.B., 2020. Enhancement of mechanical and thermal properties of carbon fiber epoxy composite laminates reinforced with carbon nanotubes interlayer using electrospray deposition. Composites Part C: Open Access 3. https://doi.org/10.1016/j.jcomc.2020.100075

Zeng, Z., Cheng, H., Wang, Z., 2020. Investigation of the flow and heat transfer characteristics in advanced vortex combustor. International Journal of Thermal Sciences 156. https://doi.org/10.1016/j.ijthermalsci.2020.106459

Zhang, C., Wang, X., Xiao, M., Ma, J., Qu, Y., Zou, L., Zhang, J., 2022. Nano-in-micro alginate/chitosan hydrogel via electrospray technology for orally curcumin delivery to effectively alleviate ulcerative colitis. Mater Des 221. https://doi.org/10.1016/j.matdes.2022.110894

Zhang, J., Cai, G., Liu, X., He, B., Wang, W., 2021. Molecular dynamics simulation of ionic liquid electrospray: Revealing the effects of interaction potential models. Acta Astronaut 179, 581–593. https://doi.org/10.1016/j.actaastro.2020.11.018

Zhang, P., Chan, W., Ang, I.L., Wei, R., Lam, M.M.T., Lei, K.M.K., Poon, T.C.W., 2019. Revisiting Fragmentation Reactions of Protonated α-Amino Acids by High-

Resolution Electrospray Ionization Tandem Mass Spectrometry with Collision-Induced Dissociation. Sci Rep 9. https://doi.org/10.1038/s41598-019-42777-8

Zhang, X., Duan, C., Liu, L., Li, X., Xie, H., 2015. A non-resonant fiber scanner based on an electrothermally-actuated MEMS stage. Sens Actuators A Phys 233, 239–245. https://doi.org/10.1016/j.sna.2015.07.001

Zhang, Y., Zhan, T., Chen, J., Li, X., Zhou, Q., He, M., 2020. Thermo-Acoustic Properties of (Ethanol + n-Heptane) Binary Mixtures from 293.35 to 433.89 K and up to 5.0 MPa. J Chem Eng Data 65, 3893–3905. https://doi.org/10.1021/acs.jced.0c00237

Zhao, K., Wang, W., Yang, Y., Wang, K., Yu, D.G., 2019. From Taylor cone to solid nanofiber in tri-axial electrospinning: Size relationships. Results Phys 15. https://doi.org/10.1016/j.rinp.2019.102770

Zhong, X., Qiao, L., Stauffer, G., Liu, B., Girault, H.H., 2018. On-Chip Spyhole Nanoelectrospray Ionization Mass Spectrometry for Sensitive Biomarker Detection in Small Volumes. J Am Soc Mass Spectrom 29, 1538–1545. https://doi.org/10.1007/s13361-018-1937-7

Zhou, H., Biswas, P., 2021. The prediction of size and charge of particles formed from evaporation of charged droplets generated in an electrospray system. Chem Eng Sci 231. https://doi.org/10.1016/j.ces.2020.116237

Zhu, Y., Chiarot, P.R., 2020. Directed assembly of nanomaterials using electrospray deposition and substrate-level patterning. Powder Technol 364, 845–850. https://doi.org/10.1016/j.powtec.2020.01.066

Zou, Q., Chen, Z., Ding, S., Xu, J., He, M., Liu, X., 2024. Thermal Conductivity of the Binary Mixtures of N-Heptane and Fatty Acid Esters: Measurement and Correlation. Energies (Basel) 17. https://doi.org/10.3390/en17235811

Zuo, W., Zhao, H., E, J., Li, Q., Li, D., Yang, D., Zhao, Y., 2022. Effects of injection strategies on thermal performance of a novel micro planar combustor fueled by hydrogen. Int J Hydrogen Energy 47, 9018–9029. https://doi.org/10.1016/j.ijhydene.2021.12.206

APPENDICES

Appendix A
Datasheet High Voltage 7000 Series

7000 SERIES | BENCH TYPE HIGH VOLTAGE POWER SUPPLY | GENVOLT HIGH VOLTAGE POWER SUPPLIES

High Voltage PSU

- Electrospinning, Insulation Testing, Electrophoresis
- Models From 1kV to 40kV
- 30W,60W,100W Units
- Small Footprint
- Positive or Negative Polarity Available

See 7000 Series on Website

We recommend visiting our website for any updated model information

Specification Summary

The 7000 range of high voltage power supplies are used primarily as laboratory power supplies. The power supply is equipped with digital LED display, adjustable voltage range, highly stable output, and low ripple. The unit is available in positive or negative polarity.

and one or two output connectors depending on customer requirements. Both AC and DC input units are supplied with 40kV HV output cables. AC input unit is also supplied with IEC power connector and cable, and DC input unit is supplied with 24V 5-way XLR connector (female).

Input Specifications

AC Input Voltage Range	85VAC-265VAC ,47 to 63Hz.
DC Input Voltage Range	21.6VDC-26.4VDC
DC Input Current	1.6A for 30W at full power and minimum input voltage
Efficiency at Full Load	More than 75%

Technical Specifications

Voltage Line Regulation	Less than 0.3% for an input changing from maximum input to minimum input.
Voltage Ripple	Less than 0.1% (peak to peak) of maximum output voltage at maximum load & no load
Voltage Stability	Less than 0.05% for 8 hours per day after 30minutes warmup
Temperature Drift	Less than 200ppm/°C over the specified temperature.
Circuit Protection	Overvoltage, Overload, Arcing & Short Circuit DC reverse input polarity protected Internal Overtemperature Shutdown: 65°C, Latching

30W Output Specifications

	70130	70230	71030	72030	73030	73530	74030
Output Voltage Range*	0-1kV	0-2kV	0-10kV	0-20kV	0-30kV	0-35kV	0-40kV
Maximum Output Current	30mA	15mA	3.0mA	1.5mA	1.0mA	0.85mA	0.75mA
Output Power	0 - 30W						
Output Polarity	Positive or Negative with Respective to Ground						
Voltage Load Regulation	Less than 0.01% for a load changing from no load to full load						

60W Output Specifications

	70160	70260	71060	72060	73060	73560	74060
Output Voltage Range*	0-1kV	0-2kV	0-10kV	0-20kV	0-30kV	0-35kV	0-40kV
Maximum Output Current	60mA	30mA	6.0mA	3.0mA	2.0mA	1.7mA	1.5mA
Output Power	0 - 60W						
Output Polarity	Positive or Negative with Respective to Ground						
Voltage Load Regulation	Less than 0.01% for a load changing from no load to full load						

100W Output Specifications

	701100	702100	710100	720100	730100	735100	740100
Output Voltage Range*	0-1kV	0-2kV	0-10kV	0-20kV	0-30kV	0-35kV	0-40kV
Maximum Output Current	100mA	50mA	10mA	5.0mA	3.3mA	2.85mA	2.5mA
Output Power	0 - 100W						
Output Polarity	Positive or Negative with Respective to Ground						
Voltage Load Regulation	Less than 0.01% for a load changing from no load to full load						

*For other output voltages do not hesitate to contact us. Please note that design improvements may lead to specification changes.

General High Voltage Industries Ltd. trading as Genvolt.
Registered Office: New Road, Highley, Bridgnorth, Shropshire, WV16 6NN, UK
Tel: +44 (0) 1746 862555 Fax: +44 (0) 1746 862666 E-mail: info@genvolt.co.uk

PAGE 1 of 6

7000 SERIES | BENCH TYPE HIGH VOLTAGE POWER SUPPLY | GENVOLT HIGH VOLTAGE POWER SUPPLIES

Reliability & Quality Control

Each power supply has been soak tested with full load at 40°C for no less than 24 hours.

Model Number Coding

7XXXX

Model — **Output Power**

Output Voltage

Options

- Remote interlock option available
- Dual HV output sockets
- Dual meters
- Mounting bars
- Please specify when ordering. For further information please contact us.
- Parallel PSU capability that should be done by Genvolt

Safety

This power supply contains hazardous voltages and stored energy. Contact with the output may result in fatal injury. It should only be opened and maintained by trained personnel.

- The area where the power supply is to be used should be kept clean and dry.
- Before switching the power supply on please confirm that the 10-turn potentiometer is turned fully in a counterclockwise direction.
- Keep a safe distance from the output connector and any items connected to it.
- Ensure that a secure connection is made between the Earth side of the load and the green and yellow Earth lead.

Environmental Details

Operating Temperature	-10°C to 40°C
Storage Temperature	-20°C to 60°C
Humidity	0 to 90% non-condensing

Other Applications

- Focused Ion Beam
- Gas Chromatography
- Image Intensifiers
- Microchannel Plates
- Spectroscopy

Mechanical Details

Weight	AC Input: 3.92kg (8.64lbs) DC Input: 2.8kg (8.28lbs)
Dimensions	Width 220mm, Height 120mm, Depth 275mm (excluding connectors)
Power Input Connector	AC Input: Standard IEC Connector Ì
HV Output Connector	

Important Notice
Only trained personnel should install and service this unit.

Mains voltages are present within the electronics enclosure and extreme care should be taken when servicing.

1) Do not operate the equipment uncovered.
2) Switch off and allow time for capacitors to discharge at the high voltage output before servicing.

Note: This equipment must be earthed for safe operation.

Operation

Check the following items before operation:

1. The power supply is clean and dry.

2. No unnecessary object is near the high voltage output connector or high voltage load.

3. Turn the voltage potentiometer fully anticlockwise. This will adjust the high voltage output to zero when the power supply is switched on.

4. When connecting a load ensure that the output current returns through the ground bolt or the 6mm terminal on the rear panel.

5. One switch on the front panel switches on the mains input; a second switch enables the high voltage.

Set the HV switch on. Adjust both the mA and the HV potentiometers until the desired output voltage is reached. The reading on the front panel meter shows the high voltage output measured via a resistor divider network.

Appendix B
Datasheet NE-1000 Syringe Pump

New Era Pump Systems, Inc.

Phone: 631-249-1392
SyringePump.com

NE-1000 Single Syringe Pump - $815

High Pressure Syringe Pump
NE-1010: $900

Continuous Infusion Syringe Pump System
Dual-NE-1000: $1640

Microfluidics Single Syringe Pump
NE-1002X: $1570

NE-1000 Features:

Accepts 1 syringe from the smallest size available up to 60 mL. A 140 mL syringe can be filled up to 120 mL. NE-1000 & Dual-NE-1000 pumping rate as low as 0.73 µL/hr with a 1 mL syringe or as high as 35.33 mL/min with a 60 mL syringe. NE-1010 pumping rate as low as 1.459 µL/hr with a 1 mL syringe or as high as 127.2 mL/min with a 60 mL syringe. NE-1002X pumping rate as low as .008 nL/hr with a 0.5 µL syringe or as high as 1555 µL/min with a 60 mL syringe.

The NE-1000 Family of Syringe Pumps Features

- Built for Automation
- Operates stand-alone or from a computer
- Infuses and withdraws
- Applications range from simple infusions to complex pumping programs
- Programmable preset protocols
- Program up to 41 pumping phases: change pumping rates, set dispensing volumes, insert pauses, control and respond to external signals, sound the buzzer.
- RS-232 and TTL logic control interfaces

Two pumps connected with a dual cable create a Dual Pump System allowing for continuous infusion or emulsification. Network, control, and monitor up to 100 pumps with one computer. Worldwide power supplies available. Motor stall detection. Non-volatile memory of all parameters and programming. Upgradeable to the X and X2 advanced firmware versions for gradient pumping and increased program memory. Dispensing accuracy of +/-1%. Unlimited lifetime technical support. Two year warranty. Plus many, many more features!

****Not For Clinical Use On Humans****

NE-1000 Single Syringe Pump Maximum and Minimum Flow Rates

Syringe Manufacturer (all names ™)	Syringe (mL)	Inside Diameter (mm)	Maximum Rate (mL/hr)	Minimum Rate (µL/hr)	Maximum Rate (mL/min)
B-D	1	4.699	53.07	0.73	0.884
	3	8.585	177.1	2.434	2.952
	5	11.99	345.5	4.748	5.758
	10	14.43	500.4	6.876	8.341
	20	19.05	872.2	11.99	14.53
	30	21.59	1120	15.4	18.67
	60	26.59	1699	23.35	28.32
HSW Norm-Ject	1	4.69	52.86	0.727	0.881
	3	9.65	223.8	3.076	3.73
	5	12.45	372.5	5.119	6.209
	10	15.9	607.6	8.349	10.12
	20	20.05	966.2	13.28	16.1
	30	22.9	1260	17.32	21
	50	29.2	2049	28.16	34.15
Monoject	1	5.74	79.18	1.088	1.319
	3	8.941	192.1	2.64	3.202
	6	12.7	387.6	5.326	6.46
	12	15.72	593.9	8.161	9.899
	20	20.12	972.9	13.37	16.21
	35	23.52	1329	18.27	22.15
	60	26.64	1705	23.44	28.42
	140	38	3470	47.7	57.84
Terumo	1	4.7	53.09	0.73	0.884
	3	8.95	192.5	2.646	3.208
	5	13	406.1	5.581	6.769
	10	15.8	600	8.244	10
	20	20.15	975.8	13.41	16.26
	30	23.1	1282	17.63	21.37
	60	29.7	2120	29.1	35.33
Poulten &Graf (Glass)	1	6.7	107.8	1.483	1.798
	2	8.91	190.8	2.622	3.18
	3	9.06	197.2	2.711	3.288
	5	11.75	331.8	4.559	5.53
	10	14.67	517.2	7.107	8.62
	20	19.62	925.2	12.72	15.42
	30	22.69	1237	17.01	20.62
	50	26.96	1746	24.01	29.11
Steel Syringes	1	9.538	218.6	3.005	3.644
	3	9.538	218.6	3.005	3.644
	5	12.7	387.6	5.326	6.46
	8	9.538	218.6	3.005	3.644
	20	19.13	879.5	12.09	14.65
	50	28.6	1965	27.01	32.76

	Syringe (µL)	Inside Diameter (mm)	Maximum Rate (µL/hr)	Minimum Rate (µL/hr)	Syringe (mL)	Inside Diameter (mm)	Maximum Rate (µL/hr)	Minimum Rate (µL/hr)
SGE (Glass – Gas Tight)	5	0.343	282.7	0.004	0.25	2.303	12.74	0.176
	10	0.485	565.3	0.008	0.5	3.257	25.49	0.351
	25	0.728	1273	0.018	1	4.606	50.99	0.701
	50	1.03	2549	0.036	2.5	7.284	127.5	1.752
	100	1.457	5102	0.071	5	10.3	254.9	3.504
Hamilton Microliter (Glass)	0.5	0.103	25.49	0.001	10	14.57	510.2	7.01
	1	0.146	51.23	0.001	25	23.03	1274	17.52
	2	0.206	101.9	0.002	50	27.5	1817	24.98
	5	0.326	255.4	0.004	100	34.99	2942	40.43

Specifications

Model	Style	Stall Detection	Number of Syringes	Maximum Syringe Size
NE-1000	Stand-Alone	Yes	1	60 mL; 140 mL partially filled
NE-500	OEM	No	1	60 mL; 140 mL partially filled
NE-501	OEM	No	1	60 mL; 140 mL partially filled

Mechanical

Motor type:	Step motor
Motor steps per revolution:	400
Motor to drive screw ratio:	15/28
Drive screw pitch:	20 revolutions/"
Micro-stepping:	1/8 to 1/2 depending on motor speed
Advance per step:	0.2126116 µm to 0.8504464 µm depending on motor speed
Dimensions:	8 3/4" x 5 3/4" x 4 1/2" (LxWxH) (Non-OEM versions) (22.86 cm x 14.605 cm x 11.43 cm)
Weight:	3.8 lbs. (1.63 kg)
Allen Wrench	3/32 Hex (Not all models)

Electrical

Power supply type:	External wall adapter, power source specific
Power supply output rating:	12V DC @ 1000 mA
Power connector:	2.1 mm, center positive, DC
Voltage at power connector:	12V DC at full load
Amperage:	750 mA at full load

Operational

Accuracy:	Within 1% error
Reproducibility:	Within 0.1% error
Maximum force:	45 lbs. at minimum speed, 18 lbs. at maximum speed
Syringe inside diameter range:	0.100 to 50.00 mm
Maximum speed:	5.100464828 cm/min
Minimum speed:	0.004204478 cm/hr
Maximum pumping rate:	1699 mL/hr with a B-D 60 mL syringe
Minimum pumping rate:	0.73 µL/hr with a B-D 1 mL syringe
Number of Program Phases:	41
RS-232 pump network:	100 pumps maximum
RS-232 selectable baud rates:	300, 1200, 2400, 9600, 19200

Custom Applications

For specialized and OEM applications, contact your dealer or New Era Pump Systems Inc.
Custom modifications can be made to the mechanics or the firmware.

Not For Clinical Use On Humans

Appendix C
Manual Digital Microscope

CoolingTech

Parts of Microscope

Specification

Image CMOS Sensor

Controller High Speed DSP (Driver Free available)

Focus Range 15mm ~ 40mm

Snap Shot Software and Hardware

Video Capture Resolution 0.3M.

Built-in 8 White-light LED and adjustable illumination ensure the magnified images are clear and bright

Still Image Capture Resolution 640*480

Frame Rate 30 f/s under 600 LUX Brightness

Digital Zoom 5X Sequence Mode

25/45

Brightness Control Manual adjustment

Magnification Range 25 X ~ 200X (Manually)

Power Supply USB Port (5V DC)

USB 2.0 & USB 1.1 Compatible

Operation System Windows XP, Vista, Win 7 32 bit and 64 bit.

Language: English, Chinese and other language by selection

System Requirement: Pentium Computer with 700M Hz & above,
20M HD Space CD ROM Driver, 64MB RAM, Direct X VGA Card

CD disk Driver and Micro-Measurement Tool

Product dimension 112 mm (L) X 33 mm (R)
Product net weight: 380g
Available color: Matting black, UV black; and other colors.

Notes before use

1. Don't dissemble the digital Microscope or change the interior parts, it can cause damage.
2. Don't clean the Microscope with alcohol organic solvents
3. Don't touch the lens with your fingers.
4. Avoid outdoor use if possible.
5. Storage temperature , 0°C ~ 40°C,Humidity:45%RH ~ 85RH%.
6. In case the product gets wet, leave PC connection immediately. And do not dissemble or dry by hair dryer. Send to repair center if the digit microscope was effected by liquid or other elements.
7. Measurement Data only for reference.

Product Outlook & Standard parts

1. Digital Microscope (1pcs)
2. USB 2.0 cable
3. Metal fixed Stand (1pcs)
4. CD ROM (Driver, Measurement software, User Manual)

Hardware system requirements

Windows 2000、XP、VISTA、WIN7 Pentium 1G, Celeron, AMD 1G & above, 128MB Memory, 150MB Hard Disc memory space,16-bit & above VGA ,CD-ROM, USB2.0 or USB1.1.

How to install the Driver

U500X Digital Microscope is a free Driver Product, it can be worked immediately after connected to the computer with operation system above win2000 version.

1. Connect the Portable digital microscope by USB2.0 cable to your computer, double click 'my computer' icon on your computer desktop, below interface will be shown up.

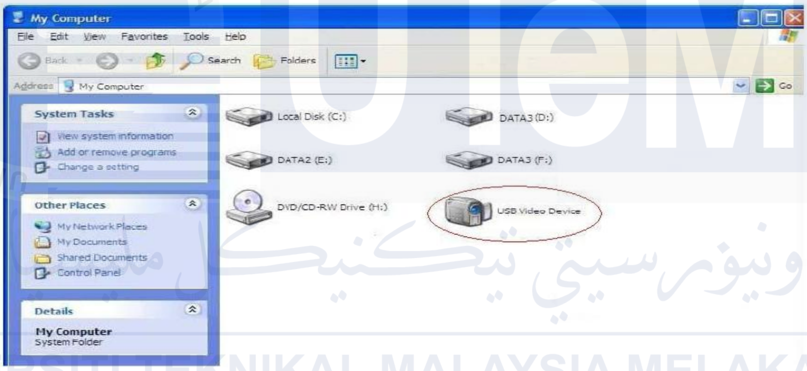

2. Double click the **Video device icon** as above red marked in your computer. Now it is ready to use.

If you can't find the Video device, or if your computer can't recognize it, please follow below steps to install the driver.

Insert the attached CD, system will auto run to the interface as below and follow the steps to complete the installation:
(NOTE: If the computer can't auto run the disc, you need to operate

manually by click "My Computer" → "DVD/CD Driver" → run"AUTORUN.EXE")

1. Driver installation

1Click 

to continue, the screen will show the installation progress.

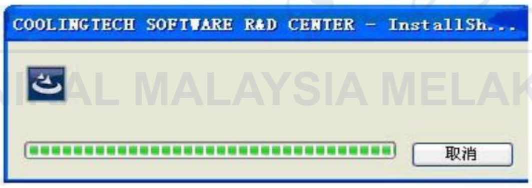

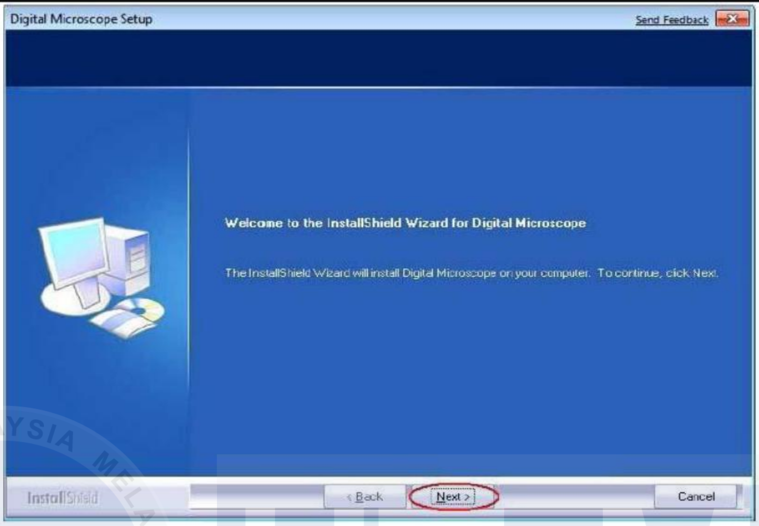

Click"next"to continue， as followings:

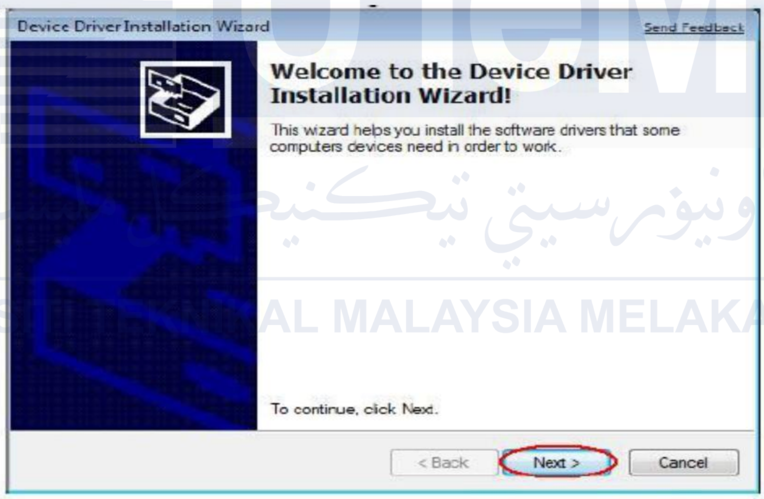

Click"next"to continue， as followings:

Click "continue Anyway",as followings:

Click"Finish"to continue, as followings

30/45

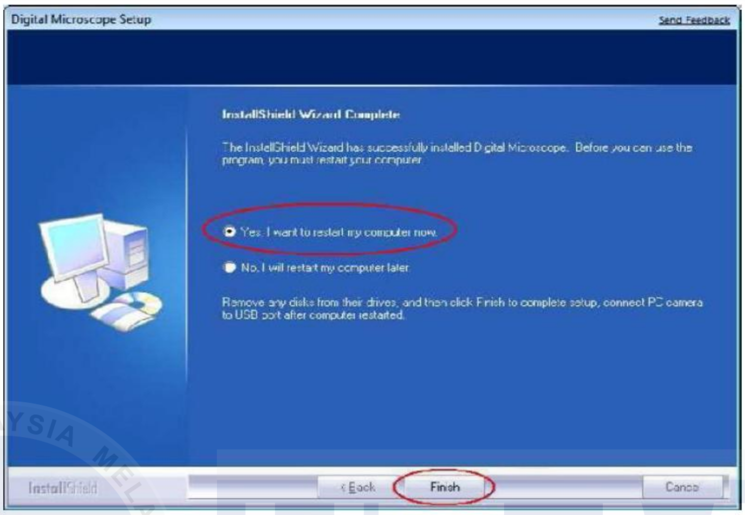

Select 'Yes, I want to restart my computer now', and click "finish".

After restart your computer, Plug-in the USB port of Digital Microscope into Computer USB port. Following the user guide by steps and complete by click "Next" -> "Continue anyway" -> "Finish".

Click “continue Anyway”,as followings:

Click“Finish”to continue， as followings

30/45

2 Measurement installations:

1 Click  to continue, as followings

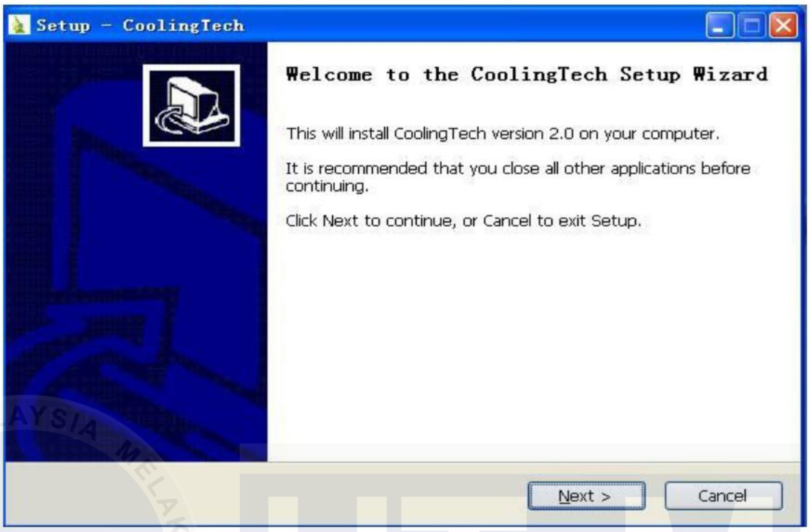

2 Click "next" to continue, as followings

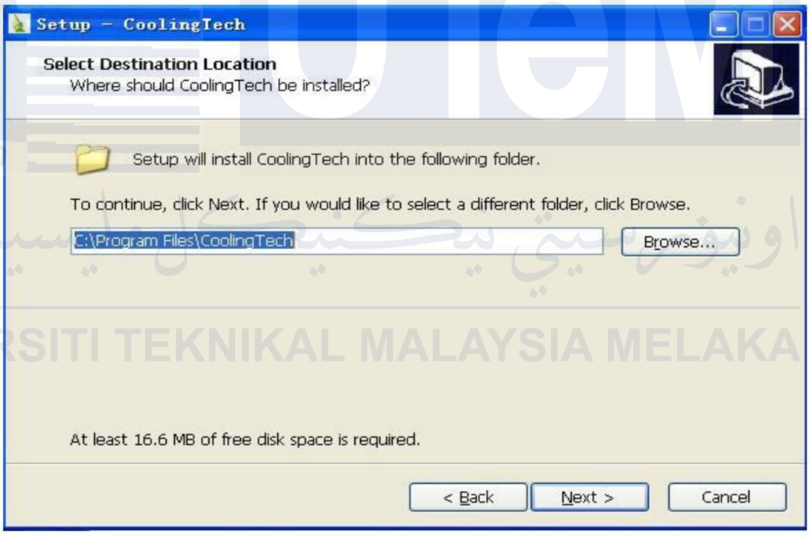

3. Click "next" to continue, as followings

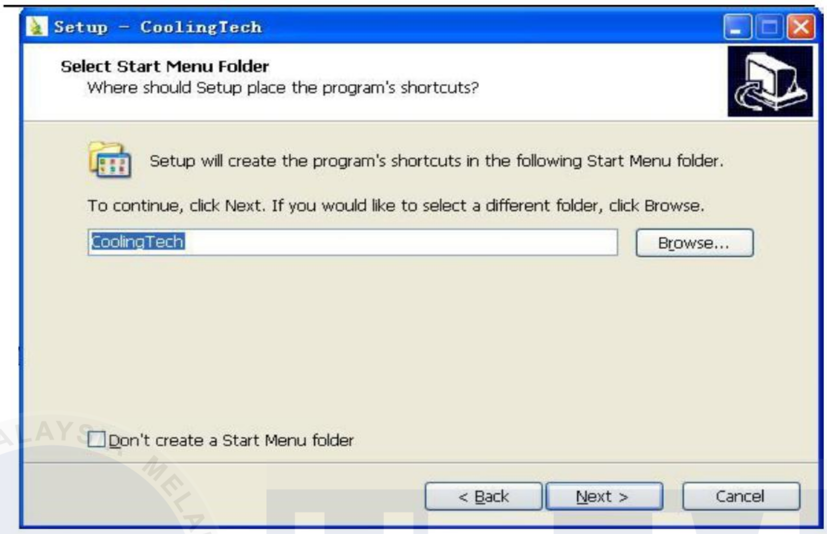

4. Click "next" to continue, as followings

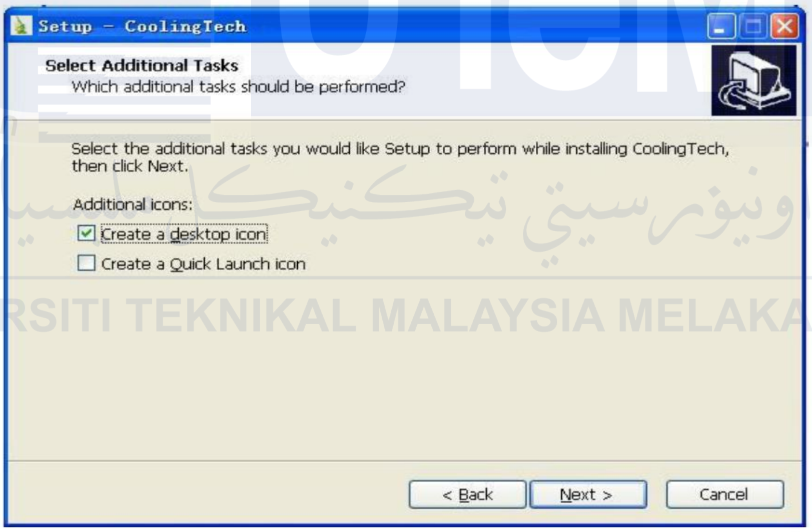

5. Click "next" to continue, as followings

34/45

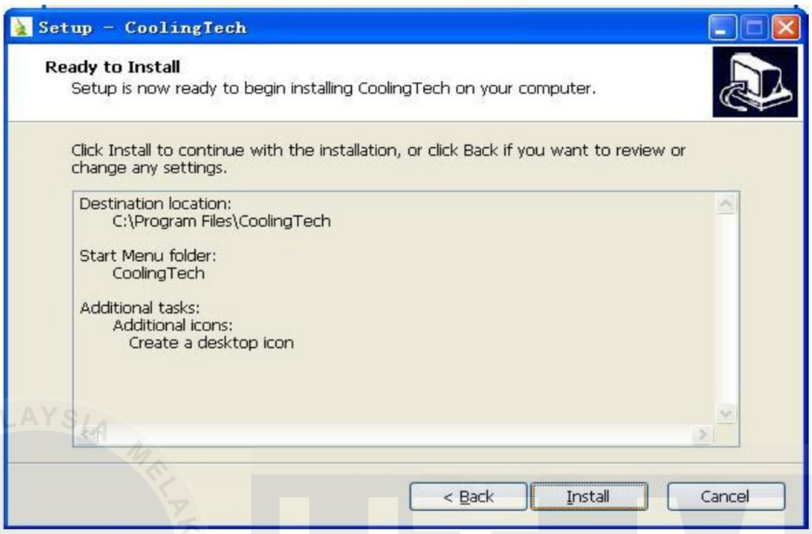

6 Click "Install" to continue, as followings

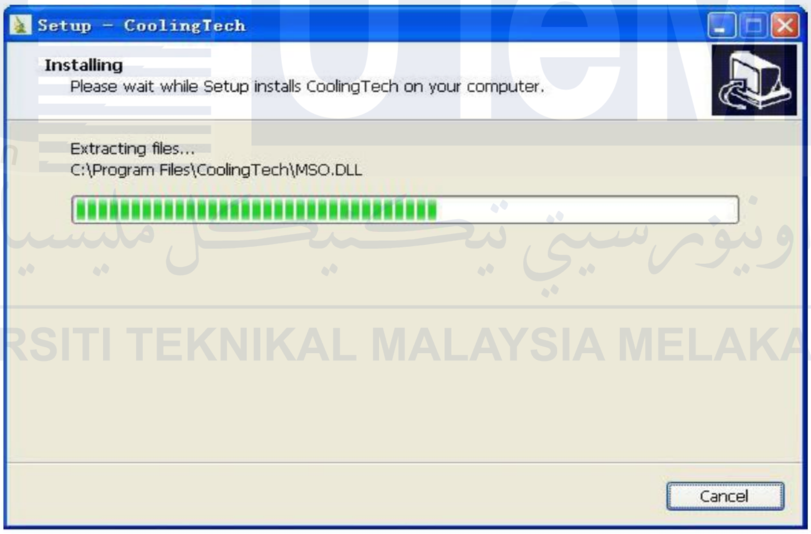

Wait a few seconds while the installation taking place.

35/45

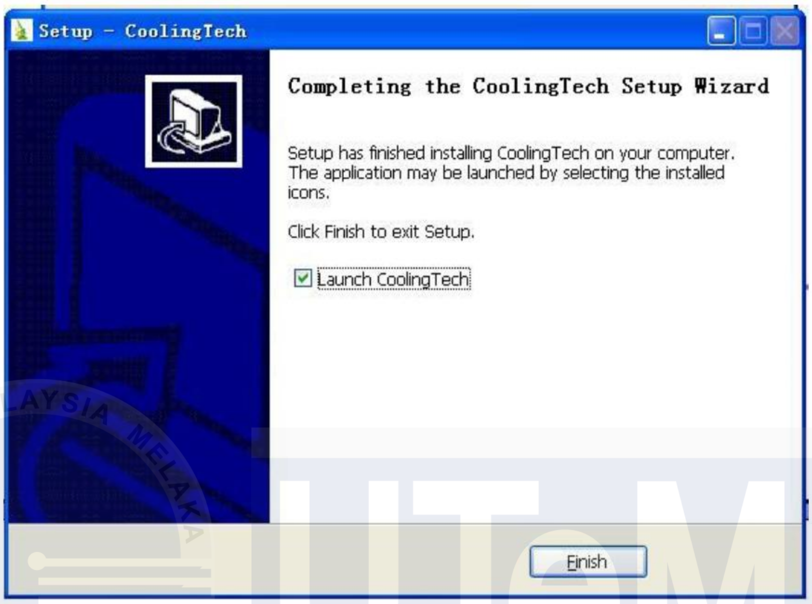

7.Click "Finish" and the installation completes.

8.After the installation completes, double click  at computer desktop to start using the software.

Plug-in the devices, Display in operation window

36/45

Appendix D
Table of Specification for Equipment

I. Specification of High Voltage Power Supply

Input voltage	90~264VAC universal AC input
Fuses	2.5A F (x2)
Efficiency	>70%
Output voltage	0-10kV DC with respect to ground
Polarity	Positive (71030P) or Negative (71030N)
Rated output current	3.0mA
Rated output power	30W
Ripple	<0.01% peak to peak at full load
Voltage regulation	<0.01% over specified load range
Temperature coefficient	<100ppm/°C
Protection	Overload and short-circuit faults will cause the unit to operate in Constant Current mode (Max. Current <= 6mA) Arcing faults will cause the unit to shut down and re-start until the fault is cleared.
Voltage adjustment	Output voltage can be adjusted by the 10-turns potentiometer on the front panel.
Voltage monitor	A 31/2 digit meter on the front panel. The display resolution is 100 volts.
Connections	-The input connection to the unit is by means of an IEC fused inlet. -The output connection is by means of a Genvolt proprietary connector: mating half and suitable high voltage cable are supplied.
Working temperature	0 - 40°C
Storage temperature	-20°C - +60°C
Humidity	<90%
Weight	2.8 kg

II. Technical Specifications of Syringe pump

Model	NE-1000 Multi-Phaser™ Syringe Pump
Control System	Microcontroller-based stepper motor drive
Syringe Compatibility	: Supports syringe sizes up to 60 mL
Flow Rate Range	Minimum: 0.73 µL/hr (with a 1 mL syringe) Maximum: 2120 mL/hr (with a 60 mL syringe)
Operation Modes	Infusion and withdrawal modes with programmable dispense volumes
Precision Control	Adjustable pumping rate with non-volatile memory for parameter storage
Power Requirements	12V DC @ 800mA regulated power supply
RS-232 Communication	Supports bi-directional control from a computer, allowing integration into automated systems

III. Specification of Nozzle Spray

Air hose	4φ × 6φ (mm)
Liquid hose	4φ × 6φ (mm)
Standard nozzle set	20G x 15G x 80L OD 0.88 OD 1.81 ID 0.58 ID 1.45
Discharge volume	Intermittent 0.001c.c./shot～ Continuous 0～2,400c.c./min
Air consumption	24Nl/min (0.3MPa)
Air pressure for piston operating	0.4～0.7MPa
Material	Nozzle/SUS304, Body/BSBM (chromium plating)

The nozzle under consideration is a precision dispensing part that can be used in a wide range of industrial and laboratory settings. It can release liquids in short bursts or all at once. It has two hose connections, each with an outer diameter (OD) of 6 mm and an inner diameter (ID) of 4 mm. This design makes sure that the flow is well controlled and that it works with standard tubing systems. There are two hoses which the air hose and the liquid hose. The standard nozzle set has a stainless-steel nozzle shape that is 20G × 15G × 80L. The 20G needles have an outer diameter of 0.88 mm and an inner diameter of 0.58 mm. The 15G needles have an outer diameter of 1.81 mm and an inner diameter of 1.45 mm. This setup lets you distribute fluids with low viscosity with great accuracy.

The system can work with both continuous and intermittent dispensing modes. The minimum amount of fluid that can be discharged at once is 0.001 c.c., and the maximum amount that can flow continuously is 0 to 2,400 c.c. per minute. Furthermore, it can be changed, it can be used for both high-volume fluid delivery and micro-dosing. At a working pressure of 0.3 MPa, the air consumption rate is 24 normal litres per minute (Nl/min). This means that pneumatic tools work well. The system needs between 0.4 and 0.7 MPa of air pressure for the pistons to work, which makes sure that the control is always responsive and consistent.

The body is made of brass (BSBM) and has a layer of chromium on top of it. This makes it more durable and resistant to chemicals and wear and tear. SUS304 stainless steel is used to make the nozzle because it is strong and doesn't rust. These features make the nozzle great for distributing fluids with high accuracy and long-lasting in tough working conditions.

Appendix E
Taylor cone formation for IDIR 15.3mm and 21.2mm

I. IDIR = 15.3 mm

Fluid type	**Water**	**Ethanol**	**Mixture Fluid (Ethanol and n-heptane)**		
			10%:90%	**20%:80%**	**30%:70%**
Taylor Cone formation					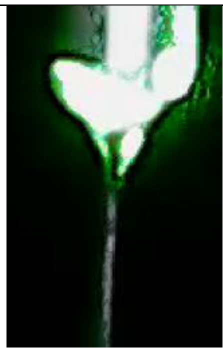
Voltage (kV)	4.5–6.0 kV	4.5–5.5 kV	3.5–4.5 kV	2.5–3.5 kV	3.5–4.5 kV
Stable Cone Angle (°)	37° - 42°	38° - 37°	66° - 75°	58° - 68°	42° - 53°

II. IDIR = 21.2mm

Fluid type	**Water**	**Ethanol**	**Mixture Fluid (Ethanol and n-heptane)**		
			10%:90%	**20%:80%**	**30%:70%**
Taylor Cone formation	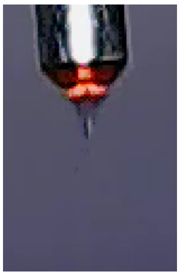				
Voltage (kV)	4.5–7.5kV	4.5–5.5 kV	3.5–4.5 kV	2.5–3.0 kV	3.5–4.5 kV
Stable Cone Angle (°)	38° - 71°	38° - 61°	58° - 75°	42° - 58°	38° - 48°